UNIVERSITÄT DUISBURG ESSEN
Open-Minded

Universität Duisburg-Essen
Fakultät für Physik

Der Fakultät für Physik der Universität Duisburg-Essen
vorgelegte Dissertation

Statistical Methods Applied to Credit Risk and Reacting Systems

von

Andreas Mühlbacher
aus Dischingen
zum Erwerb des Grades
„Dr. rer. nat.“

Datum der Disputation: 25. Oktober 2019
Erstgutachter: Prof. Dr. Thomas Guhr
Zweitgutachter: PD Dr. Hermann Kampermann

DOI: 10.17185/duepublico/70757
URN: urn:nbn:de:hbz:464-20191127-150910-9

Hiermit versichere ich, die vorliegende Dissertation selbstständig, ohne fremde Hilfe und ohne Benutzung anderer als den angegebenen Quellen angefertigt zu haben. Alle aus fremden Werken direkt oder indirekt übernommenen Stellen sind als solche gekennzeichnet. Die vorliegende Dissertation wurde in keinem anderen Promotionsverfahren eingereicht. Mit dieser Arbeit strebe ich die Erlangung des akademischen Grades "Doktor der Naturwissenschaften" (Dr. rer. nat.) an.

Ort, Datum	Andreas Mühlbacher

List of Publications

Parts of this thesis are included in the following publications:

[1] A. Mühlbacher and T. Guhr. Credit risk meets random matrices: Coping with non-stationary asset correlations. *Risks*, 6(42), 2018.

[2] A. Mühlbacher and T. Guhr. Extreme portfolio loss correlations in credit risk. *Risks*, 6(72), 2018.

[3] A. Mühlbacher and T. Guhr. WKB-type-of approximation for rare event statistics in reacting systems. *arXiv:1902.05280v2*, 2019.

Author Contributions

Here, I lay out my contributions to the publications and manuscripts mentioned above:

[1] The publication reviews recent progress of our group in modeling credit risk for correlated assets. The text was written by Thomas Guhr and me.

[2] In this article we shed light on multivariate analysis of credit risk. We analytically generalize and extend studies reviewed in [1]. The calculations and corresponding numerical evaluations are my own work. The text was mainly written by me. The project was supervised by Thomas Guhr.

[3] The paper extends a semiclassical method to calculate rare event statistics in reaction-diffusion systems put forward by Elgart and Kamenev (2004). I carried out the extension of the model and the analytical calculations. The text was mainly written by me. The project was supervised by Thomas Guhr.

Acknowledgements

I want to express my gratitude to my supervisor, Thomas Guhr, for giving me the great opportunity to work in his group and for creating an outstanding environment to conduct research. I thank him for his constant support and guidance during and in the preliminary stages of my PhD research. He broadened my knowledge in physics and economics.

Special thanks go to Sebastian Krause for his persistence in discussing various topics and for proofreading parts of this work.

I thank all current and former members of our group, especially Maram Akila, Petr Braun, Juan Camilo Henao, Felix Meier, Rudi Schäfer, Yuriy Stepanov, Daniel Waltner and Shanshan Wang for fruitful discussions. I also thank Sabine Lukas and Heinz-Rüdiger Oberhage for administrative support.

Furthermore, my thanks go to my dear friends Lynn Clark, Matthew Clark and Daniel Ullmann for proofreading parts of this thesis and providing valuable feedback.

I acknowledge financial support from the Studienstiftung des deutschen Volkes and the faculty of physics at the University of Duisburg-Essen during the years of my doctoral studies.

Last but not least, I am very grateful to Denise for standing by me and supporting me devotedly all these years.

Abstract

Statistical physics uses probability theory and statistics to provide a macroscopic description of real world systems composed of a large number of units. Its main purpose is to study the properties of complex systems, showing complicated interactions and a high degree of freedom, from the statistical behavior of their components. The central topic of the thesis is the application of methods from statistical physics on diverse complex systems. Particularly we are interested in the statistics of extreme events. These often tend to have significant consequences and hence need to be understood in detail.

The work is structured in two parts. In the first part we focus on the dynamics of financial markets and credit risk. A portfolio consisting of several credit contracts faces a high risk of large losses, especially when the underlying asset values are correlated. In order to provide a realistic model of the correlated asset values we have to take the non-stationarity of financial markets into account. This was demonstrated in a rather drastic way during the financial crisis. We introduce a random matrix approach for correlation matrices to model the non-stationarity of financial markets. Based on this approach we review recent progress in modeling credit risk for correlated assets. We discuss the effects of diversification, i.e., reducing the risk by distributing it, and investigate common risk measures for one credit portfolio. We present results of numerical simulations in which mutual dependencies between two non-overlapping credit portfolios are studied.

To obtain a comprehensive understanding of systemic credit risk we present new, analytical results for the multivariate joint loss distribution of several credit portfolios on a non-stationary market. This distribution gives us the opportunity to calculate the portfolio loss correlation of two credit portfolios. We investigate various portfolio structures, such as two non-overlapping portfolios in one market or one portfolio that operates in two on average uncorrelated markets or a subordinated debt of two creditors. This gives a quantitative understanding of the limitations of diversification.

In the second part of this work we focus on rare event statistics in reacting systems. We calculate the probabilities to find systems of reacting particles in states which largely deviate from typical behavior. We consider various systems where the interactions of particles are described by chemical reactions.

Zusammenfassung

In der Statistischen Physik werden Methoden aus der Wahrscheinlichkeitstheorie und Statistik verwendet, um eine makroskopische Beschreibung von wirklich existierenden Systemen, die aus einer Vielzahl von Einheiten bestehen, abzugeben. Ihre Hauptaufgabe besteht darin, komplexe Systeme, welche komplizierte Wechselwirkungen und eine hohe Zahl an Freiheitsgraden aufweisen, anhand des statistischen Verhaltens ihrer Komponenten zu analysieren. Das zentrale Thema dieser Dissertation ist die Anwendung von Methoden der Statistischen Physik auf verschiedenartige komplexe Systeme. Besonderes Interesse liegt uns an der Statistik extremer Ereignisse. Diese haben oftmals signifikante Auswirkungen und müssen daher im Detail verstanden werden.

Diese Arbeit ist in zwei Teile gegliedert. Im ersten Teil legen wir den Schwerpunkt auf die Dynamik von Finanzmärkten und Kreditrisiko. Ein aus Kreditverträgen bestehendes Portfolio ist besonders dann einem hohen Risiko ausgesetzt große Verluste zu erleiden, wenn die zugrundeliegenden Vermögenswerte korreliert sind. Um eine realistische Modellierung der Korrelationen der Vermögenswerte zu erreichen, muss die Nichtstationarität der Finanzmärkte mitberücksichtigt werden. Diese wurde während der Finanzkrise in verheerender Weise demonstriert. Wir erörtern einen Zufallsmatrixansatz für Korrelationsmatrizen, um die Nichtstationarität von Finanzmärkten zu beschreiben. Basierend auf diesem Ansatz rezensieren wir jüngste Forschungsergebnisse in der Modellierung von Kreditrisiko mit korrelierten Vermögenswerten. Wir diskutieren Diversifikationseffekte, d.h. Reduktion von Risiko durch Verbreiterung, und untersuchen gebräuchliche Risikomaße für ein Kreditportfolio. Wir präsentieren Ergebnisse numerischer Simulationen bei denen die wechselseitigen Abhängigkeiten zwischen zwei sich nicht überlappenden Kreditportfolios untersucht werden.

Um ein umfassendes Verständnis des systemischen Kreditrisikos zu erhalten, präsentieren wir neue, analytische Ergebnisse für die multivariate Verbundverteilung mehrerer Kreditportfolios auf einem nichtstationären Markt. Diese Verteilung ermöglicht es die Korrelationen zwischen zwei Kreditportfolios auszurechnen. Wir untersuchen zahlreiche Portfoliostrukturen, wie z.B. zwei nicht überlappende Portfolios auf einem Markt oder ein Portfolio, welches auf zwei im Mittel unkorrelierten Märkten operiert, oder ein Nachrangdarlehen zwischen zwei Gläubigern. Dies gibt ein quantitatives Verständnis über die Grenzen von Diversifikation.

Im zweiten Teil dieser Arbeit konzentrieren wir uns auf die Statistik seltener Ereignisse in Reaktions-Diffusions-Systemen. Wir berechnen die Wahrscheinlichkeiten, Systeme aus interagierenden Teilchen in Zuständen fern vom typischen Verhalten zu finden. Wir betrachten verschiedene Systeme, in denen die Interaktionen der Teilchen durch chemische Reaktionsgleichungen beschrieben werden.

Contents

1. Introduction **1**
- 1.1. Econophysics . . . 1
- 1.2. Financial Markets and Instruments . . . 2
- 1.3. Returns and Volatility . . . 5
- 1.4. Correlation and Covariance . . . 8
- 1.5. Copulae . . . 10
- 1.6. Random Nature of Prices . . . 12
- 1.7. Random Matrix Theory . . . 13
- 1.8. Risk . . . 14
- 1.9. Credit Risk . . . 16
  - 1.9.1. Phenomenology . . . 16
  - 1.9.2. Credit Ratings . . . 17
  - 1.9.3. Credit Risk Models . . . 18
- 1.10. Master Equations . . . 19
- 1.11. Outline of the Thesis . . . 20

2. Credit Risk Meets Random Matrices **21**
- 2.1. Introduction . . . 21
- 2.2. Merton Model . . . 22
- 2.3. Random Matrix Theory for Non-Stationary Asset Correlations . . . 26
  - 2.3.1. Wishart Model for Correlation and Covariance Matrices . . . 26
  - 2.3.2. New Interpretation and Application of the Wishart Model . . . 28
- 2.4. Modeling Fluctuating Asset Correlations in Credit Risk . . . 33
  - 2.4.1. Random Matrix Approach . . . 33
  - 2.4.2. Average Loss Distribution . . . 35
  - 2.4.3. Adjustability to Different Market Situations . . . 39
  - 2.4.4. Value at Risk and Expected Tail Loss . . . 42
- 2.5. Concurrent Credit Portfolio Losses . . . 43
  - 2.5.1. Simulation Setup . . . 44
  - 2.5.2. Empirical Credit Portfolios . . . 47
- 2.6. Conclusions . . . 51

3. Extreme Portfolio Loss Correlations in Credit Risk **55**
- 3.1. Introduction . . . 55

3.2. Merton Model Including Subordination 56
3.2.1. Average Loss Distribution 59
3.2.2. Homogeneous Portfolio 61
3.2.3. Non-Analytic Parts of the Loss Distribution 61
3.2.4. Infinitely Large Portfolios 64
3.3. Absence of Subordination 66
3.3.1. Absence of Subordination and Infinitely Large Portfolios . . 69
3.3.2. Several on Average Uncorrelated Markets 70
3.3.3. Absence of Subordination on Several Markets 71
3.4. Visualization of the Results 73
3.4.1. One Portfolio, Two Markets 73
3.4.2. Absence of Subordination and Disjoint Portfolios of Equal Size 74
3.4.3. Absence of Subordination and Disjoint Portfolios of Various Sizes 77
3.4.4. Subordinated Debt 79
3.5. Conclusions 80

4. WKB-Type-of Approximation for Rare Event Statistics in Reacting Systems 83
4.1. Introduction 83
4.2. Deeper Look at the Method 85
4.3. Some Examples 92
4.3.1. Binary Annihilation Revisited 92
4.3.2. Single Annihilation 97
4.3.3. Binary and Single Annihilation 99
4.3.4. Third order reaction 102
4.4. Conclusions 106

5. Summary and Outlook 109

A. Calculation of Moments 113

List of Figures 115

List of Tables 119

1. Introduction

1.1. Econophysics

Physics, economics, mathematics and computer science are examples of fields of science that have created interdisciplinary areas of research. A fine example of such an interdisciplinary area of research, which had prospered in the last two and a half decades, is econophysics [4, 5]. The term econophysics was first mentioned by H. Eugene Stanley in 1995 [6]. He claimed it to be a hybrid of the words "economics" and "physics". A popular description of econophysics is given by Rosario N. Mantegna and H. Eugene Stanley in [7, p. 355]:

> "The word econophysics describes the present attempts of a number of physicists to model financial and economic systems using paradigms and tools borrowed from theoretical and statistical physics."

In econophysics, financial markets are considered as well-defined complex systems [8]. Their macroscopic properties are generated by internal microscopic processes and interactions.

Despite the fact that econophysics, per se, is a rather young interdisciplinary research field, there are many examples throughout history where physicists and mathematicians contributed to economic sciences. One of the earliest contributions is that of Nicolaus Copernicus in the 16th century, where he investigated the behavior of inflation. Since then, many other scientists have contributed to that field. Amongst them was Daniel Bernoulli, who proposed a solution to the famous Saint Petersburg paradox, which is still in discussion today [9–11].

A direct connection between physics and economics was established in the beginning of the 20th century, when French mathematician Louis Bachelier developed a stochastic model to describe the motion of stock prices [12]. The same model was used five years later in Albert Einstein's theory of Brownian motion [13]. Later, Benoît Mandelbrot's famous work on fractals [14] was motivated by his analysis of cotton prices [15]. There are various studies which identify analogies between physical phenomena and financial markets. There are analogies in turbulence [16–19], earthquakes [20], spin systems [21–23] and many others.

Physics is driven by direct or indirect observations. This also holds for econophysics. However, the difference is that observations in econophysics can only be made on empirical data. Hence the development of econophysics is limited to the

amount of available data. About 60 years ago, Mandelbrot had only a few thousand cotton prices available for his studies. Today we live in the age of "big data" where we have massive amounts of empirical data available. This ever-increasing amount gives physicists and other researchers the opportunity to develop better and better economic models. Furthermore this progress is supplemented by the increasing processing power of modern computers. Notwithstanding, there are fields where empirical data is not only scarce but also difficult to get. This especially accounts for credit risk because the data is generally proprietary and confidential. Therefore most of the studies on credit risk are less driven by empirical data. Instead they are model- or simulation-based.

There are also some differences between physics and econophysics. In physics we are able to perform experiments in order to analyze the influence of specific features on various systems. These experiments can be repeated any number of times under the same conditions. This is not the case in econophysics. Since financial markets are highly non-stationary and change with time, we are hardly able to preserve one state. Moreover, due to limited resources and regulatory restrictions, we cannot generate significant reactions that can be observed on a stock market. Not to mention any consequences in case such an experiment would go wrong.

We already mentioned that financial markets are considered as complex systems. The anomaly towards other complex systems, which makes them particularly interesting, is their non-stationarity which is also subject to systemic changes. Put differently, the non-stationarity is not only reflected by changes in trend or changes in volatility. Fundamental changes are constantly in progress. This is exemplified by the collapse of large market-dominating companies, such as Lehman Brothers in 2008, or the introduction of new financial instruments, such as exchange-traded funds (ETFs), or new laws and regulations which may force consequences for investment strategies and risk management, such as the zero interest rate policy of the European Central Bank. The recent financial crisis drastically demonstrated the consequences.

1.2. Financial Markets and Instruments

A financial market is a place where traders meet in order to buy or sell financial instruments. On the one hand, these places exist physically, e.g., the New York Stock Exchange, and on the other hand these places are electronic systems which are linked with the internet, such as the NASDAQ. There are various kinds of different markets such as stock markets, credit markets, derivative markets and many others. In the following we give some examples of these instruments and how the price of a stock is formed.

If a company needs fresh capital it has several options. One option is to sell stocks, i.e., shares of itself, to investors who are then co-owners of the company. Depending on the type of stock, they now obtain a reward in the form of a portion of the company's profit, called a dividend, and the right to vote on strategic decisions of the company. A different option to raise capital is to search for investors that loan money to the company, i.e., the company can issue a bond. The issuer of a bond is obliged to pay back the amount of money borrowed, called principal, at a predefined time of maturity. Moreover, the issuer is under the duty to pay interest, called coupons, at predefined points in time. If the issuer faces default and is not able to pay back the outstanding debt at maturity time, he goes bankrupt. The investor loses a part or all of his money invested. In the same way as stocks are traded between investors, bonds can also be traded between investors on the bond market. These trades take place on the secondary market, whereas the fresh issue of bonds, as well as stocks, take place on the primary market. Hence, bonds are more flexible than time deposits at a bank, which usually cannot be traded. This benefit, however, is coupled with a higher chance of default, depending on the issuer of the bond. Whereas time deposits at banks are governed by deposit insurance, there is no structural uniformly regulated framework like this for bonds.

A derivative is a financial instrument whose value is determined from the value of other financial products, such as an option [24]. An option provides the right to buy or sell a specified asset, e.g., a stock, at a predefined price during a certain period in the future. A collateralized debt obligation (CDO) is a portfolio credit derivative. It is a structured financial product with a claim to the cash flow which is generated by a pool of debt securities. In a CDO this asset pool is repackaged into discrete tranches which are sold to investors. The tranches of the CDOs have different seniorities on their financial claim. In order of decreasing seniority they are called senior, mezzanine and equity tranche. If a default arises and the CDO is insufficient to pay all of its investors, the investors with the lowest seniority suffer losses first. Hence, the more senior tranches are, to a certain extent, protected against losses. In the years before the financial crisis 2007–2009 CDOs allowed the recycling of risky debt, i.e., subprime mortgage credits, into bonds that were highly-rated by rating agencies. The CDOs were packaged into more complex synthetic CDOs and sold all over the world. Starting with the rapid decrease of housing prices, many private investors were not able to pay back their debt. The crisis gathered speed when CDOs failed to reach their mezzanine and senior tranches. In 2008 the CDO market collapsed and even some highly-rated tranches lost 90% of their value [25]. The recession following the crisis had global impact.

The price of a stock is determined by its demand and supply. If the demand of a stock increases, the price of the stock will rise. Vice versa, if the demand decreases, the price will go down. The whole information on demand and supply of a stock

bid volume	price in Euro	ask volume
	114.00	1428
	113.98	1333
	113.96	798
	113.94	204
	113.92	208
374	113.86	
208	113.84	
726	113.82	
757	113.80	
1405	113.78	

Table 1.1.: An excerpt of the order book for the SAP stock on Xetra stock exchange on July 24, 2019. The spread size is 0.06 Euro.

is stored in the so called order book [26]. The order book, kept by the clearing office of a stock exchange, contains information for everyone who wants to buy or sell a stock. If a trader, due to his expectation on a certain stock, wants to buy or sell a specified amount of shares for a specified price, he places a limit order in the order book. The order book is visible for all traders at the stock exchange. An example is given in table 1.1. The order book has two sides. The "ask" side contains all the offers and the "bid" side contains all the demand for the stock. The highest bid and the lowest ask price are called best bid and best ask; their difference is called spread. Based on the placement of limit orders in the order book one can distinguish between different groups of stocks [27]. A trade takes place when the prices of best bid and best ask match. In this case the corresponding orders are removed from the order book. In many cases the volume of the orders do not match. Therefore, they are often split. The price of the stock is always the price traded last. If the spread is rather large, the price of the stock makes large jumps between best bid and best ask. To avoid this artifact, which is particularly desirable for high frequency trading, one defines the midpoint price of a stock as average of best bid and best ask. A fundamentally different order is the market order. Market orders are executed immediately; they are placed by traders willing to buy or sell a stock regardless of the price. Market orders are not stored in the order book. Instead they lead to a change in the best ask or best bid. On the order book in table 1.1 we see, for example, that if the volume of an incoming buy market order is smaller than 208 shares, it only changes the volume at the best ask. If the volume of the buy market order exceeds 208 shares, it will affect the best ask and lead to a change in the price of the stock.

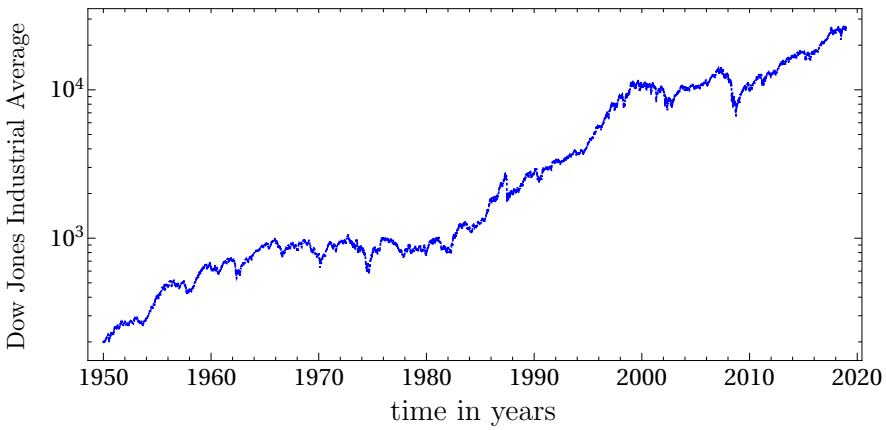

Figure 1.1.: Evolution of the Dow Jones Industrial Average from 1950 to 2019 on a logarithmic scale.

Looking at the development of a stock market on a long time horizon, we find an exponential growth. We illustrate this on the evolution of the Dow Jones Industrial Average (DJIA) in figure 1.1. The index is composed of the 30 largest companies in the USA. Besides the positive trend of the gross domestic product, the exponential growth is motivated by an equilibrium of stock markets and fixed income investments, such as time deposits in banks.

1.3. Returns and Volatility

Absolute prices $S_k(t)$ of different stocks k at time t vary widely, see figure 1.2 (a). As a consequence, for statistical analysis they are impractical especially if one wants to work with several stocks. To remedy we take the absolute price change of the stock price

$$\Delta S_k(t) = S_k(t + \Delta t) - S_k(t) \tag{1.1}$$

and divide it by the stock price, which yields a relative stock price change called return

$$r_k(t) = \frac{\Delta S_k(t)}{S_k(t)} = \frac{S_k(t + \Delta t) - S_k(t)}{S_k(t)} \,. \tag{1.2}$$

Figure 1.2 (b) exemplary shows the return time series for $\Delta t = 1$ day for the Microsoft and Goodyear stock in the period 1992–2019. The length of the return interval Δt has significant influence on the distribution of returns. For very large

return intervals the distribution becomes normally distributed [28]. However for small return intervals, like months or days or shorter, the distribution becomes leptokurtic relative to the normal distribution. In other words, the empirical return distribution shows a heavy tail that significantly differs from a normal distribution. This behavior was noted first in 1915 by Wesley C. Mitchell [29] and later on studied by Maurice Olivier [30] and Frederick C. Mills [31]. In the 1960s it was Benoît Mandelbrot [15] who drew further attention on the heavy tails of return distributions. Since then there has been ongoing research and discussion about the shape of the distribution, especially the shape of the tails [32–43].

A common opinion for the origin of heavy tails are large price shifts caused by large order volumes [37, 44–48]. More recent studies argue that gaps between limit orders in the order book are responsible for heavy tails [49–51]. Others relate the heavy tails to herding behavior [52].

The exponential growth in stock prices motivates the introduction of the logarithmic return

$$\tilde{r}_k(t) = \ln \frac{S_k(t+\Delta t)}{S_k(t)} \,, \tag{1.3}$$

which is often used for risk management purposes. For small return intervals Δt, when $\Delta S_k(t)/S_k(t) < 1$ holds, the logarithmic return can be approximated by the return (1.2)

$$\tilde{r}_k(t) = \ln\left(1 + \frac{\Delta S_k(t)}{S_k(t)}\right) \approx \frac{\Delta S_k(t)}{S_k(t)} = r_k(t). \tag{1.4}$$

The variation of stock prices over time is measured by the standard deviation

$$\sigma_k(t) = \sqrt{\langle r_k^2(t)\rangle_T - \langle r_k(t)\rangle_T^2} \,, \tag{1.5}$$

which in economics is often referred to as volatility. If we work with sampled time series we use the sample average

$$\langle r_k(t)\rangle_T = \frac{1}{T}\sum_{t=1}^{T} r_k(t) \,. \tag{1.6}$$

The volatility depends on the return interval Δt and on the estimation horizon T. Depending on the problem at hand, the estimation horizon T can be very short like hours or be rather large like weeks. Empirical studies have pointed out that the volatility is not constant over time [53, 54]. It rather is a non-stationary quantity which shows fluctuations. Especially in times of crisis the volatility rises. This exemplary can be seen in figure 1.2 (c) where the volatility is elevated for both

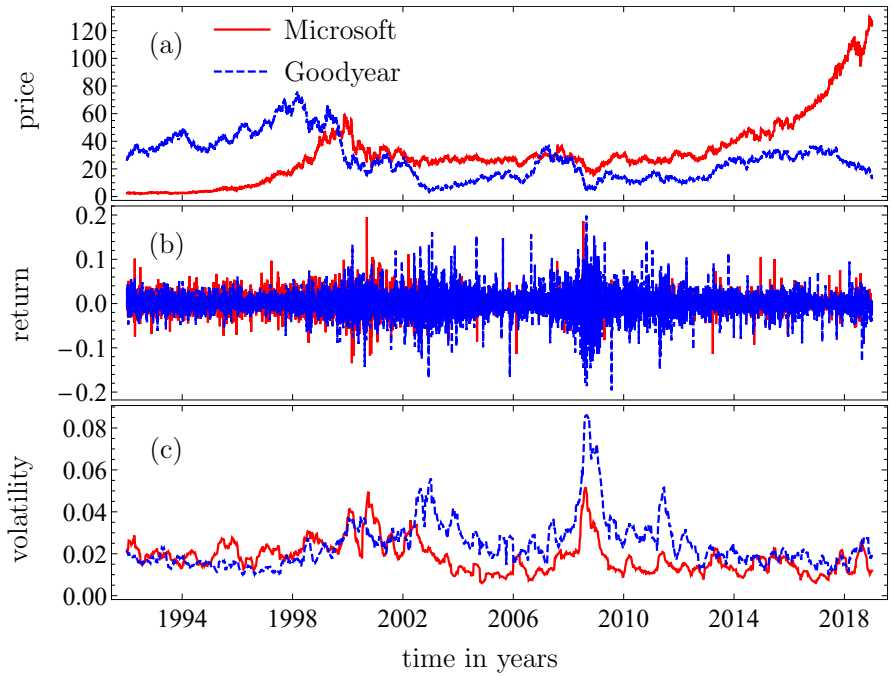

Figure 1.2.: (a) Daily closing prices in USD, (b) daily returns and (c) volatility estimated over a $T = 60$ day horizon for the Microsoft and Goodyear stock. The time period is January 1992 to June 2019.

stocks during the financial crisis 2008–2009. In contrast to the standard returns (1.2) absolute values $|r_k(t)|$ or squares $r_k^2(t)$ of returns show a slowly decaying autocorrelation function [55, 56]. This means that large returns are followed by large returns, of either sign, and small returns are most likely to be followed by small returns [15]. Thus, the volatility is clustered and also shows a slowly decaying autocorrelation function. This is a stylized fact called volatility clustering [57, 58].

A widespread belief is that the volatility quantifies the risk of a stock. Truly, dispersion or deviation measures possess many characteristics of risk measures. This holds especially for downside deviation measures like the semi-standard deviation which only accounts for negative deviations from the mean value. Overall, one has to distinguish between risk and uncertainty [59–61]. Whereas uncertainty accounts for positive and negative deviations from the current value, i.e., profits and losses, risk, from an investor's perspective, should only account for losses. This distinction is not consistently made in economics literature. Deviation measures are insensitive for certain profits [62] and hence they do not mirror the actual risk. Thus, instead of being a risk measure, the volatility $\sigma_k(t)$ is rather a measure for the market activity.

1.4. Correlation and Covariance

Different stocks sometimes behave in a similar fashion. An exemplary of this can be seen in figure 1.2 (a) in the period 2006–2014. A quantitative measure for the linkage between two stocks is the Pearson correlation coefficient. To be specific, we consider stock prices and returns, but correlations can be measured in the same way for all observables that are given as time series. We are interested in, say, K companies with stock prices $S_k(t)$, $k = 1, \ldots, K$ as functions of time t. The sampled Pearson correlation coefficients between the two companies k and l in the time window of length T are defined as

$$C_{kl} = \langle M_k(t) M_l(t) \rangle_T \tag{1.7}$$

with the time series

$$M_k(t) = \frac{r_k(t) - \langle r_k(t) \rangle_T}{\sigma_k(t)} \tag{1.8}$$

that are obtained from the return time series $r_k(t)$ by normalizing (in some communities referred to as standardizing) to zero mean and to unit variance, where the sample standard deviation $\sigma_k(t)$ is evaluated in the above-mentioned time window. Due to the normalization the correlation coefficient is bound between minus one and plus one. For a correlation of minus one the stocks are perfectly anti-correlated, i.e., they move in an opposite manner. For a correlation of one the stocks are perfectly correlated, i.e., they move identically. In that case the scatter plot of the returns of the two stocks forms a line with positive slope. If the correlation is zero, the stocks are uncorrelated and the scatter plot forms a non-ordered cloud of points.

We define the $K \times T$ rectangular data matrix M whose k-th row is the time series $M_k(t)$. The correlation matrix with entries C_{kl} is then given by

$$C = \frac{1}{T} M M^\dagger \ , \tag{1.9}$$

where † indicates the transpose. By definition, C is real symmetric and has non-negative eigenvalues. Furthermore, the correlation matrix shows a block structure. This becomes clearly visible, if we sort the stocks according to their industrial sectors. In figure 1.3 we show four consecutive correlation matrices for 481 companies listed in the S&P 500 index between January 2018 and July 2019. Each correlation matrix is sampled on a quarterly period beginning with the third quarter of 2018. Each point represents a correlation coefficient between two companies. The color indicates the strength of the correlation of the companies in the market. Hence, the diagonal is dark blue as the diagonal of a correlation matrix is one by definition.

Symbol	Industry branch
CD	Consumer Discretionary
CS	Consumer Staples
E	Energy
F	Financials
HC	Health Care
I	Industrials
IT	Information Technology
M	Materials
RE	Real Estate
TS	Telecommunications Services
U	Utilities

Table 1.2.: GICS classifications.

The industrial sectors are classified according to the Global Industry Classification Standard (GICS), see table 1.2. The inter-sector correlation is visible in the off-diagonal blocks, whereas the intra-sector correlation is visible in the blocks on the diagonal. For later discussion, we emphasize that the stripes in these correlation matrices indicate the structuring of the market in industrial sectors, see, e.g., [63].

We see that the correlation matrix changes over time. The reason, therefore, is that the business relations between companies change over time. The question arises why one does not reduce the length of the time series T to better capture the current state of the market. The answer lies in the fact that correlation matrices are noise dressed. By reducing T the measurement noise increases [64]. Different approaches have been developed to reduce the noise and improve the estimation of correlation matrices [65–68]. Nevertheless, when measuring correlations there is a trade-off between generating measurement noise and keeping the time window length T short enough to assure currentness.

We will also use the covariance matrix

$$\Sigma = \sigma C \sigma \tag{1.10}$$

where the diagonal matrix

$$\sigma = \mathrm{diag}\left(\sigma_1(t), \ldots, \sigma_K(t)\right) \tag{1.11}$$

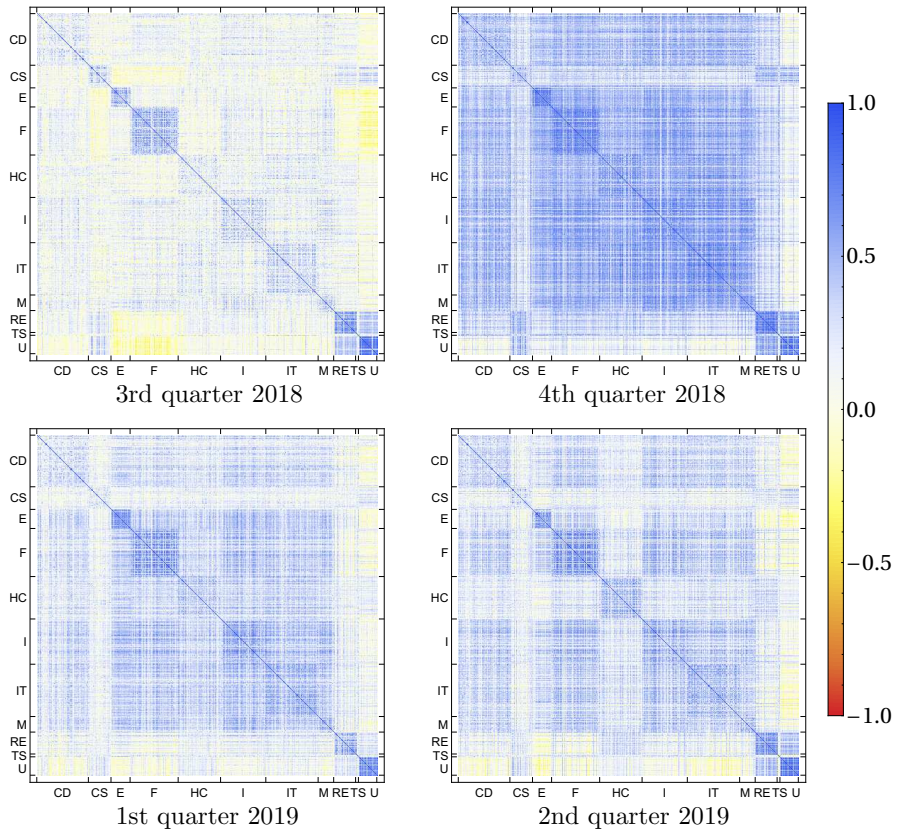

Figure 1.3.: Correlation matrices for 481 stocks from S&P500 index for four consecutive quarters beginning with the third quarter of 2018.

contains the standard deviations. The covariance matrix is not normalized and contains the variances and covariances. Setting $A = \sigma M$, we may write

$$\Sigma = \frac{1}{T} A A^{\dagger} \tag{1.12}$$

for the covariance matrix.

1.5. Copulae

The Pearson correlation coefficient only accounts for the linear dependence of observables. Nonlinear dependencies are not captured in an appropriate manner. The Pearson correlation is only a good measure if the marginal distributions have finite variance. Moreover, we have to keep in mind that correlations or covariances

only fully grasp the mutual dependencies if the multivariate distributions are Gaussian, which is not the case for returns if Δt is too small. Often the statistical dependence is more complex and cannot be represented by a single number. To resolve this problem we use the concept of copulae which were first introduced by Abe Sklar in 1959 [69, 70]. The joint probability distribution holds all the information of statistical dependency. Moreover, it includes the marginal distributions of each observable which can be calculated by integrating it over the full support of the residual observables. The marginal distributions have different shapes for observables underlying different processes. Hence it is not possible to directly compare the statistical dependence of different systems by means of the joint probability distribution.

The main idea of copulae is to separate the functional dependence of the observables from their marginal distributions. This allows comparison of the pure statistical dependence of different systems. In a copula, the marginal distributions are transformed to uniform distributions. The pure statistical dependence is measured independently of the marginal distribution functions. A copula is the joint distribution of a multivariate random variable expressed as a function of the quantiles for the marginal distributions. Copulae are of advantage in contrast to correlation coefficients because they are able to better capture nonlinear dependencies of observables. Due to this advantage, copulae have gained rising popularity and are well-established in statistics and finance. For various studies of copulae in finance, see, e.g., [71–84]. For a more detailed description of copulae, see, e.g., [85]. In the following, we give a brief mathematical introduction to copulae for the bivariate case.

Let X and Y be two random variables with the joint cumulative distribution function $F_{X,Y}(x,y)$. The marginal cumulative distribution functions are $F_X(x)$ and $F_Y(x)$. The inverse cumulative distribution functions F_X^{-1} and F_Y^{-1} are the quantile functions. The copula $\mathrm{Cop}_{X,Y}(u,v)$ is defined as the joint cumulative distribution function of the quantiles of the marginal distributions

$$\mathrm{Cop}_{X,Y}(u,v) = F_{X,Y}\left(F_X^{-1}(u),F_Y^{-1}(v)\right) \ . \tag{1.13}$$

The dependence structure is separated from the marginal distributions. Thus, the copula contains the pure statistical dependence of the random variables independently of the marginal distributions. We are able to reverse equation (1.13) in order to generate a joint cumulative distribution out of a copula and marginal distributions

$$F_{X,Y}(x,y) = \mathrm{Cop}_{X,Y}\left(F_X(x),F_Y(y)\right) \ . \tag{1.14}$$

Instead of the copula itself, we will use the copula density $\mathrm{cop}_{X,Y}(u,v)$ which is defined as

$$\mathrm{cop}_{X,Y}(u,v) = \frac{\partial^2}{\partial u \partial v} \mathrm{Cop}_{X,Y}(u,v) \; . \tag{1.15}$$

Furthermore, we are interested in empirical copula densities which are obtained from empirical or simulation data.

1.6. Random Nature of Prices

Despite the fact that the formation of a stock price is the result of the traders' actions and hence a deterministic process, the time evolution of stock prices looks erratic. This is due to the vast number of individual trades leading to price changes. According to this observation, the price evolution of stocks is usually modeled by stochastic processes. The first one to mathematically describe the stochasticity of price movements was Louis Bachelier in 1900 [12]. His work comprises a stochastic analysis of stock and option markets. Five years later, Albert Einstein published a paper [13] describing the movement of small particles in a fluid which is called Brownian motion. Einstein used the same stochastic process as Bachelier used in his description of stock prices. The fact that two completely different processes can be modeled by the same stochastic process is not very surprising. On the one hand, as written above, the price formation is a result of the interaction of numerous trades of individual traders. On the other hand, the movement of a particle in a suspension results from many collisions with moving molecules in the fluid. This fact reveals one of many parallels of economics and physics.

The Brownian motion can be described by a Wiener process with drift

$$dS(t) = \mu dt + \sigma dW(t) \; . \tag{1.16}$$

It consists of a deterministic part μdt, where μ is the drift constant, and a stochastic part $\sigma dW(t)$, where σ is the volatility, $dW(t) = \epsilon\sqrt{dt}$ is a standard Wiener process and ϵ is a random variable which is independent at each infinitesimal time step. Importantly, ϵ is normalized to zero mean and the second moment is unity. It can be drawn from any distribution satisfying these conditions. A common choice is the standard normal distribution. The replacement $dW(t) = \epsilon\sqrt{dt}$ may be doubtful from a mathematical perspective, because the square root of a differential is not well defined. However it is a practical and common notation used by many physicists. The Brownian motion is capable of describing a time series of stock returns, but a price time series has additional features. First and most important, the price of a stock cannot be negative. Second, on a long time scale we expect to see an exponential drift of the stock price. Third, the fluctuations of a stock price depend

on its current value. If the price of a stock is low, we expect the volatility to be low as well. If the price increases so do the fluctuations and hence the volatility increases too. These three properties are not included in the Brownian motion (1.16). A much more realistic description, proposed by Matthew C. M. Osborne [86], is the geometric Brownian motion

$$dS(t) = S(t)\mu dt + S(t)\sigma\epsilon\sqrt{dt}\ . \tag{1.17}$$

If we draw ϵ from a standard normal distribution, the prices $S(t)$ are log-normally distributed. Moreover, they are always positive and show an exponential trend. The latter can easily be seen by setting $\sigma = 0$ which results in an ordinary differential equation that is solved by an exponential function.

The geometric Brownian motion has numerous applications in financial modeling. One of the most famous is the Black and Scholes model developed by Fisher Black and Myron Scholes [87] and Robert C. Merton [88] in 1973.

1.7. Random Matrix Theory

Random matrix theory (RMT) had its major breakthrough in the 1950s, when Eugene Wigner used it to describe the spectra of complex nuclei [89]. The idea of RMT is to replace the Hamiltonian of a system with a random matrix that shares certain properties with the Hamiltonian, such as symmetry or invariance against transformations. The motivation behind this idea is that in many cases the Hamiltonian is not known exactly, except for specific properties. RMT allows us to calculate statistical features, describing the general state of a system instead of the microscopic processes. Its approach is similar to ergodicity in thermodynamics. In RMT we average over ensembles of random matrices sharing similar properties with the system. In quantum chaos, for example, the average over a long spectrum equals the average over an ensemble of random matrices, provided the number of levels is large.

In finance, RMT is often used to study the statistical properties of empirical correlation matrices, see, e.g., [90–94]. Due to the finite length T of the return time series the correlation matrix is noise dressed and therefore, to some extent, random. Laurent Laloux et al. [64] compared the eigenvalue spectrum of a sample correlation matrix from S&P 500 stocks and the eigenvalue spectrum of theoretical predictions from RMT, based on the assumption of a purely random correlation matrix. They found a remarkable agreement between the bulk of the two distributions. Merely a few large eigenvalues are not in accordance with the RMT predictions. These outliers are stable in time and the largest one represents the collective market movement, while the others represent the industrial branches. These findings

allow for the reduced noise of correlation matrices. Moreover, RMT noise filtering techniques are beneficial for portfolio optimization [95–98].

In the studies mentioned, the correlation matrices were evaluated over a long time period. Using ergodicity, the statistical properties of large correlation matrices are predicted by means of the average of a fictitious ensemble of random matrices. In chapter 2 we use a different approach, where ergodicity reasoning is not evoked. Instead, by means of random matrices we will model a truly existing ensemble of non-stationary covariance matrices that exist as a consequence of non-stationarity.

1.8. Risk

The Basel Committee on Banking Supervision distinguishes between three major components of risk that a bank can face: market risk, credit risk and operational risk. In economics literature these three components are often supplemented by a fourth type of risk, the liquidity risk [99, 100]. Besides these, there are many other types and subtypes of financial risk [101].

The best known is market risk. Most of the studies in econophysics are devoted to it. It is the risk of change in the value of a financial position due to unexpected changes of market variables like the price of an asset or its volatility. Credit risk will play a large role throughout this thesis. It is the risk of not receiving promised repayments on an outstanding debt due to the default of the borrower. Operational risks include losses from internal failure, like human errors or fraud, and losses from external events. Its management falls under the liability of internal auditors. Liquidity risk arises due to the lack of available trading volume. If we want to sell a large number of shares at once, it could happen that too few buyers are willing to take the current offer. In that case we might not be able to sell everything or, more likely, we would have to accept lower prices. Alexander J. McNeil et al. consider liquidity as “oxygen for a healthy market” [100]. It is important to survive but mostly we are not aware of its presence. However the consequences are drastic and become immediately clear in its absence.

For a company or bank to stay in long-term business it is important to control the risk it faces. Therefore risk needs to be quantified. This is the task of quantitative risk management. In 1952 Harry Markowitz [102] laid the foundation for modern portfolio theory. He developed an approach to optimize the return of a portfolio by mapping it onto its risk, measured in terms of standard deviation. Given a risk tolerance, a portfolio manager can optimize the portfolio return up to an efficient frontier emerging out of the correlations between the assets. Generally, chances for larger returns in the future come along with higher risk. In the decades following Markowitz there has been a drastic growth in risk-management methodology.

Concepts such as Sharp Ratio, the Capital Asset Pricing Model and Arbitrage Pricing Theory have been developed.

Another major breakthrough was the option pricing model of Black and Scholes. Under some specific assumptions, such as the price of the option's underlying stock follows a geometric Brownian motion, they provide a method to calculate the time evolution of option prices. Since then many advanced risk measures have been developed. One of the most established risk measures is the Value at Risk (VaR). In probabilistic terms, Value at Risk VaR_α is the quantile of a loss distribution at a freely choosable confidence level α and for a predefined time horizon. Typical values for the confidence level are 0.95 or 0.99. If, for example, the $\mathrm{VaR}_{0.95}$ is 1 million dollars for one day, we have a 5% chance of loosing at least 1 million dollars within that one day. The crucial point in estimating VaR is the quality of the underlying distribution. When its tail behaves Gaussian it is most likely that the VaR underestimates the risk because it does not account for extreme events that occur in times of crisis. Another deficiency of VaR is that it is not subadditive [103, 104]. The consequence therefrom is that in specific cases a portfolio manager cannot see the desired diversification effect. In other words, the VaR of a portfolio can be higher than the sum of the stand-alone VaRs of its components. However Value at Risk is a very important risk measure and commonly used. It is the preferential method in the Basel Accords to quantify risk [105, 106].

Another important risk measure is the Expected Tail Loss (ETL), also known as Expected Shortfall. It can be interpreted as expected loss in an event exceeding the Value at Risk for a given confidence level α

$$\mathrm{ETL}_\alpha = \frac{1}{1-\alpha} \int_\alpha^1 \mathrm{VaR}_u \, du \; . \tag{1.18}$$

The ETL strongly depends on the tail of the loss distribution and belongs to the class of coherent risk measures [107, 108]. One advantage of these risk measures is that they are subadditive. Figure 1.4 shows a typical loss distribution with VaR and ETL for a credit portfolio. The loss distribution of a credit portfolio significantly differs from that of a portfolio of stocks. We come back to this point.

Systemic risk is the risk of a breakdown of an entire (financial) system, as opposed to risk related to the failure of individual parts. It captures the risk of a cascading failure which is caused by interlinkages within a financial system. The stability of a financial system is associated with systemic risk factors such as the concurrent default of numerous small obligors.

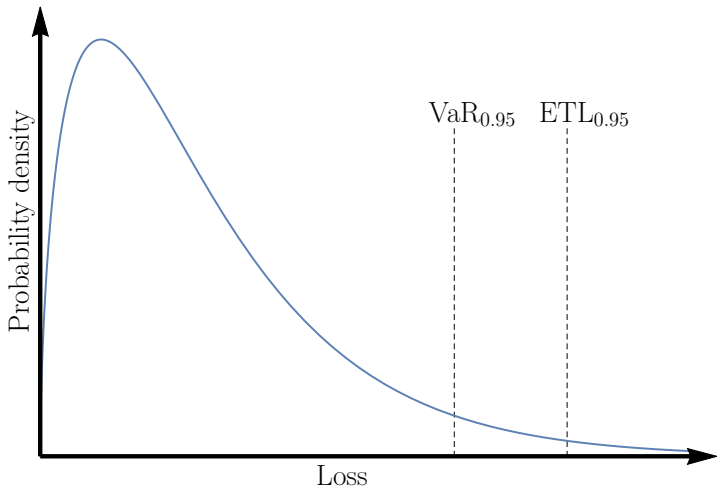

Figure 1.4.: Schematic loss distribution with $\mathrm{VaR}_{0.95}$ and $\mathrm{ETL}_{0.95}$ for a credit portfolio.

1.9. Credit Risk

To assess the impact of credit risk on the systemic stability of the financial markets and the economy as a whole is of considerable importance as the subprime crisis of 2007–2009 and the events following the collapse of Lehman Brothers drastically demonstrated [109–111]. The damage was not done by the default of one large debtor, but by the almost concurrent default of many small debtors. Most of the credit contracts were bundled into credit portfolios in the form of collateralized debt obligations (CDOs) [112–114]. Realistic estimates for credit risks and the possible losses, particularly of large portfolios, are important not only for the creditors, but also and maybe even more from a systemic viewpoint. A variety of different approaches exists, see [100, 115–122] for an overview. For a review on credit contagion, see [123–127], and for studies on practical investment and Value at Risk applications of copula theory in evaluating systemic risk, see [128, 129].

1.9.1. Phenomenology

A credit contract is a written agreement between two parties: the lending side, termed creditor, and the borrowing side, termed obligor or debtor. The obligor promises to repay an outstanding debt, termed face value, to the creditor. The face value is composed of the original amount of money lent by the creditor, termed principal, and a surplus defined by an interest rate and a risk compensation. The risk compensation usually depends on the creditworthiness of the obligor. A

common type of a credit is a bond. Many kinds of institutions, such as governments, states, cities, banks, companies, etc. sell bonds. The simplest form of a bond is a zero-coupon bond. The cash flow of a zero-coupon bond is limited to two dates, the date of issue and the maturity time, defined in the bond contract. At the date of issue the creditor lends the principal to the obligor. At maturity the obligor has to pay back the face value of the bond to the creditor. The debtor is not obliged to periodical payments of interest rates, the coupons, before maturity.

Risk arises due to the possibility that the obligor is not able to pay back his/her debt at maturity. For example such a default occurs if an obligor files for bankruptcy. Although a default is a rare event, it can cause huge losses for creditors. Especially in a credit portfolio, when correlations are present, defaults can occur simultaneously. For risk management purposes the probabilities of large losses are of central interest.

The problem to be addressed becomes ultimately a statistical one, as loss distributions for large portfolios of credit contracts have to be estimated. A schematic loss distribution for a credit portfolio is shown in figure 1.4. Typically, it has a very heavy right tail which is due to either unusually large single events, such as the Enron bankruptcy, or the simultaneous occurrence of many small events, as seen during the subprime crisis. Moreover, it is asymmetric because the maximum profit of the creditor is only the interest and risk compensation if no default occurs but the largest possible loss is the total loss of the money lent. It differs from the hypothetical loss distribution of market risk which is typically Gaussian. Generally a loss distribution of a credit portfolio is skewed and leptokurtic [116], and it has a δ peak at zero which corresponds to the case of non-default. Reducing the tail of the loss distribution would increase the stability of the financial system as a whole. Unfortunately the claim that diversification can lower the risk of a credit portfolio is questionable or even wrong, because often the correlations between the asset values are ignored. They are very important in a portfolio of credit contracts, e.g., in the form of collateralized debt obligations. In detailed studies, it was shown that the presence of even weak positive correlation diversification fails to reduce the portfolio risk [130, 131] for first passage models and for the Merton model [132–134]. Hence it is not possible to lower the tail risk significantly by enlarging the number of credit contracts in a credit portfolio. In general, diversification is not always fruitful [135–139].

1.9.2. Credit Ratings

A long-established way of quantifying credit risk is to determine the creditworthiness of an obligor by means of its credit rating. Credit ratings provide an ordinal ranking of default risks for obligors on a fixed time scale. The rankings are based on complex rating processes performed by credit rating agencies. Two of the largest and most

famous agencies are Standard & Poor's (S&P) and Moody's. The agencies use rating categories from best to lowest which is AAA for S&P and Aaa for Moody's, to CCC for S&P and C for Moody's, respectively. Moreover there is also the category of default. The possibility of moving from one credit rating to another is called migration risk. Transition probabilities for the migration from one rating to another in a fixed time period, usually one year, are typically given in rating transition matrices. The transition matrices are estimated by historical default data [140–142]. For studies on migration risk, see, e.g., [143–145].

1.9.3. Credit Risk Models

We distinguish two main categories of current credit risk models [146]: structural models and reduced-form models.

A model of default is called a structural model when it tries to explain the mechanism that leads to the default [100]. In these models, one makes assumptions about the time evolution of risk factors such as the price of an asset. A default occurs if the asset value falls below a certain threshold representing liabilities. The progenitor of all structural credit risk models is the Merton model [147]. It assumes a zero-coupon debt structure due at maturity time T_{M} and the equity of a company is modeled by a stochastic process such as the geometric Brownian motion. The equity of the company can be viewed as an European call option on its asset value with strike price equal to the face value F of the debt. Thus it is possible to apply the Black and Scholes framework to the problem of credit risk modeling. In contrast to the Merton model where the asset value at maturity decides about default, in first passage structural models default can happen at any time if the asset value falls below a certain threshold [148, 149]. Structural models provide a "microscopic" view as they trace defaults back to stochastic processes modeling the state of individual obligors. For a review on structural models, see, e.g., [150].

In reduced-form models the exact mechanism leading to a default of an obligor is left unspecified. The foundation of reduced-form models is the assumption of a functional dependency between macroscopic observables or risk factors and the default rate of an obligor. For example, the default time of an obligor can be modeled as a random variable whose distribution depends on economic observables that have to be calibrated with current market data. Reduced-form models are widely used in practice. They provide an abstract description of default events. For studies of reduced-form models, see, e.g., [118, 151–154].

There are many industry models for credit risk, such as CreditMetrics by JP Morgan [155], KMV by Moody's KMV [156], CreditRisk+ by Credit Suisse [157] and CreditPortfolioView by McKinsey & Company [158]. For a comparative analysis of these models, see [117].

1.10. Master Equations

Rare events sometimes tend to have extreme consequences [159]. Therefore, we are interested to know rather precisely how probable such events are. To obtain an appropriate description of (complex) systems which allows us to calculate rare events we use statistical methods. Especially, if the information about the system is incomplete, we use a probabilistic description to make statements about its evolution. In other words, if the information about the system is incomplete, it is not possible to give an exact prediction of its state at a future time. In general, an ensemble of identical systems which are all prepared in the same initial state, say $n_0 = n(t_0)$, will develop into different states $n(t)$ at the same time t for $t > t_0$. The information available, however, is the probability $p(n(t)|n_0)$ to reach a particular state $n(t)$, given that the system has been in the initial state n_0. The master equation is a central tool to determine the time evolution systems with restricted information [160, 161]. The general form of a master equation in discrete form reads

$$\frac{dP(n,t)}{dt} = \sum_m w(n,m)P(m,t) - \sum_m w(m,n)P(n,t) \ , \tag{1.19}$$

where $P(n,t)$ is the probability to find the system in state n at time t and $w(n,m)$ are the transition rates, i.e., the transition probabilities per unit of time to reach state n from state m. The master equation represents a set of homogeneous first order differential equations for the time evolution of the probability $P(n,t)$. The name "master equation" was originally coined in 1940 by Arnold T. Nordsieck, Willis E. Lamb and George E. Uhlenbeck [162].

Despite its simplicity it is not possible, apart from a few exceptions [163–167], to solve the master equation analytically [168–171]. Hence, other methods are called for. There are many kinds of numerical simulations [172–175] to model the stochastic kinetics. The stochastic simulation algorithm [176–178] simulates sample paths of the underlying stochastic process, especially for master equations describing chemical reactions. Due to limited computational resources, simulations are not appropriate for large systems and not for the determination of rare events either. An approximation of the master equation is obtained by a Fokker-Planck equation [179, 180]. To this end one has to apply a van Kampen system size expansion [181]. There are many other methods to find approximative solutions of master equations, such as the T-factor method [182].

An approach we are particularly interested in is based on the Wentzel-Kramers-Brillouin (WKB) approximation to master equations [183–185]. To this end, we transform the master equation by means of a generating function into a time-dependent "Schrödinger equation", which is solved by methods known from semi-classics.

1.11. Outline of the Thesis

In the previous sections we have established basic knowledge about financial markets, credit risk and master equations. Financial markets are complex systems that show a high degree of non-stationarity. This is a serious challenge which needs to be addressed by future risk managers for proper estimation of risk. The non-stationarity manifests itself in the mutual dependencies between stocks which are usually measured by correlation coefficients. Correlations have a significant impact on the distributions of credit risk. The financial crisis 2008–2009 showed in a drastic way that the misjudgment of credit risk, based on the correlated default of many small obligors, can lead to severe consequences. Fortunately, this was a rare event, and for this very reason, we are interested in the statistics of rare events which we consider for reacting systems.

The thesis is organized as follows: In chapter 2 we review recent progress of our group in modeling credit risk for correlated assets. In order to model non-stationarity for correlation matrices we employ a new interpretation of the Wishart model. We obtain an ensemble averaged asset return distribution which accounts for the non-stationarity. We use the Merton model to calculate the loss distribution for a portfolio of credit contracts. Moreover, we present results based on numerical simulations for the dependence of portfolio losses for two non-overlapping credit portfolios.

In chapter 3 we analytically calculate the multivariate joint loss distribution of several credit portfolios on a non-stationary market. We use this distribution to calculate the portfolio loss correlation of two non-overlapping creditors. We see that increasing the size of a portfolio on one market does not lead to a considerable decrease of its tail risk. To lower the risk of large losses, one is advised to split the investment onto different markets. We quantify this effect by calculating the loss distribution of a portfolio investing into two on average uncorrelated markets. We extend the Merton model by analyzing a subordinated debt structure of two creditors. Here, the senior creditor is protected by the junior subordinated creditor from losses.

Chapter 4 covers rare event statistics for reacting systems. In particular, we consider chemical reactions that can be described by master equations. In order to solve these master equations we transform them into a time-dependent "Schrödinger equation" and apply a WKB-type-of approximation. We extend a method put forward by Vlad Elgart and Alex Kamenev [186].

We summarize this thesis in chapter 5.

2. Credit Risk Meets Random Matrices

2.1. Introduction

The previous chapter underlines the importance of taking asset correlations into account when it comes to the estimation of risk, especially credit risk. The covariance and correlation matrix of asset values changes in time [63, 187–190], exhibiting an important example of the non-stationarity, which is always present in financial markets. This non-stationarity has significant influence on the loss distribution of credit risk. It has to be accounted for in order to give a realistic risk estimation.

Recently, progress has been made to analytically solve the Merton model [147] in a most general setting of a correlated market and even in the realistic case of fluctuating correlations between the assets.

Here, we review an approach [134, 191–193] which uses the fact that the set of different correlation matrices measured in a smaller time window that slides through a longer dataset can be modeled by an ensemble of random correlation matrices. The asset values are found to be distributed according to a correlation averaged multivariate distribution [134, 191, 192, 194]. This assumption is confirmed by detailed empirical studies. Applied to the Merton model, this ensemble approach drastically reduces, as a most welcome side effect, the number of relevant parameters. We are left with only two, an average correlation between asset values and a measure for the strength of the fluctuations. The special case of zero average correlation has been previously considered [195]. The limiting distribution for a portfolio containing an infinite number of assets is also given, providing a quantitative estimate for the limits of diversification benefits. We also report the results of Monte Carlo simulations for the general case of empirical correlation matrices that yield the Value at Risk and Expected Tail Loss.

Another important aspect is comprised of concurrent losses of different portfolios. Concurrent extreme losses might impact the solvencies of major market participants, considerably enlarging the systemic risks. From an investor's point of view, buying CDOs allows one to hold a "slice" of each contract within a given portfolio [112–114]. Such an investor might be severely affected by significant concurrent credit portfolio losses. It is thus crucial to assess in which way and how strongly the losses of different portfolios are coupled. In the framework of the Merton model and the

ensemble average, losses of two credit portfolios are studied, which are composed of statistically-dependent credit contracts. Since correlation coefficients only give full information in the case of Gaussian distributions, the statistical dependence of these portfolio losses is investigated by means of copulas. The approach discussed here differs from the one given in [196], as Monte Carlo simulations of credit portfolio losses with empirical input from S&P 500 data and Nikkei 225 data are run and the resulting empirical copulas are analyzed in detail. There are many other aspects causing systemic risk such as fire sales spillover [197].

We review recent work on how to take into account the non-stationarity of asset correlations into credit risk [134, 191–193]. To make the chapter self-contained, it is preceded by a brief sketch of the Wishart model and a discussion of its re-interpretation to model non-stationary correlations.

This chapter is organized as follows: We introduce the Merton model in section 2.2. In section 2.3, we introduce random matrix theory for non-stationary asset correlations, including a sketch of the Wishart model for readers not familiar with random matrices. This approach is used in section 2.4 to account for fluctuating asset correlations in credit risk. In section 2.5, concurrent credit portfolio losses are discussed. Conclusions are given in section 2.6. The contents of this chapter are published in references [1, 2].

2.2. Merton Model

Here, we briefly explain the basic idea of the Merton model [147] and extend it considering a portfolio of K credit contracts. Each obligor in the portfolio is assumed to be a publicly-traded company. The basic idea is that the asset value $V_k(t)$ of company k is the sum of time-independent liabilities F_k and equity $E_k(t)$, i.e., $V_k(t) = F_k + E_k(t)$. The stochastic process $V_k(t)$ represents the unobservable asset (firm) value. This is indeed a weakness of the Merton model, which has often been discussed [150, 198]. We proceed by assuming that $V_k(t)$ can be estimated by the observable equity values [199]. This was Merton's original idea. He claimed that the equity of a company can be estimated by its market capitalization, i.e., the stock price of the company $S_k(t)$ times the number of stocks traded. Thus, one can trace back the changes in asset values to stock price returns. The debt has a simple structure: it consists of a zero coupon bond with face value F_k and maturity time T_{M}. We assume a frictionless market, i.e., no transaction costs, and the equity of the company can be traded without restrictions. The liabilities mature after some time T_{M}, and the obligor has to fulfill his/her obligations and make a required payment. Thus, he/she has to pay back the face value F_k without any coupon payments in between.

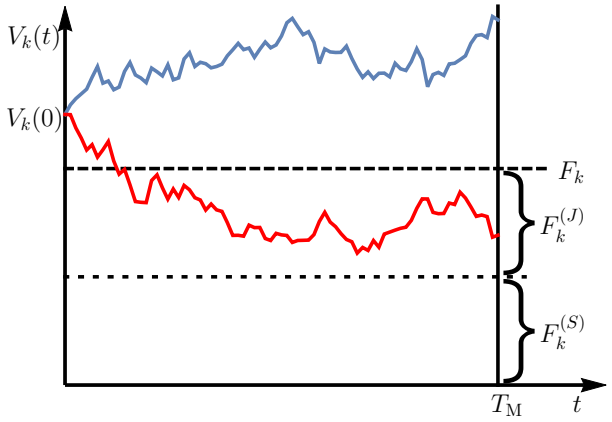

Figure 2.1.: Schematic visualization of the Merton model. A default occurs if the asset value at maturity $V_K(T_\mathrm{M})$ drops below the face value F_k. In the red sketched scenario, a default occurs only to the junior subordinated creditor while the senior creditor obtains no loss.

A default occurs only if at maturity, the asset value $V_k(T_\mathrm{M})$ is below the face value F_k. From a stockholders point of view, the value of his/her stock is reduced at maturity by the amount paid back. If the company defaults, i.e., when it is not able to pay back the debt, the stocks become worthless and the stockholders do not have to compensate the bondholders. Instead, the bondholders take over all assets of the company, liquidate them and distribute the revenue among themselves. In summary, the value of the stocks at maturity can be formulated as

$$S_k(T_\mathrm{M}) = \max(V_k(T_\mathrm{M}) - F_k, 0) \; . \tag{2.1}$$

Thus, according to the Black and Scholes model, the equity of the company can be viewed as an European call option on its asset value with strike price F_k. A visualization of the underlying process for a single asset is shown in figure 2.1. For the moment, we may ignore the fact that the face value F_k is composed as a sum of two face values $F_k = F_k^{(S)} + F_k^{(J)}$. This becomes important in chapter 3 when we take subordination of debt into account. The colored lines show two time-dependent asset values $V_k(t)$. In the blue case, the asset value of the company at maturity is above the face value and the promised payment can be made. In the red case, the asset value at maturity is below the face value F_k which results in a default.

In the spirit of the Merton model, $V_k(t)$ is modeled by a geometric Brownian motion

$$dV_k(t) = \mu_k V_k(t) dt + \sigma_k V_k(t) dW_k(t) \; , \tag{2.2}$$

where $dW_k(t)$ is a standard Wiener process and $V_k(0) > 0$ holds. The parameters of the stochastic process like drift μ_k and volatility σ_k can be estimated by empirical stock price data. Under the dynamics (2.2) the logarithm of the asset value at maturity is normally distributed [100]. In other words, the asset value at maturity is distributed according to a log-normal distribution and the default probability of the company is

$$P(V_k(T_\mathrm{M}) \leq F_k) = \Phi\left(\frac{\ln F_k/V_k(0) - (\mu_k - \sigma_k^2/2)\, T_\mathrm{M}}{\sigma_k\sqrt{T_\mathrm{M}}}\right) , \tag{2.3}$$

where $\Phi(x)$ is the cumulative function of the standard normal distribution

$$\Phi(x) = \frac{1}{\sqrt{2\pi}} \int_{-\infty}^{x} \exp\left(\frac{-z^2}{2}\right) dz \, . \tag{2.4}$$

The normalized loss for company k is

$$L_k = \frac{F_k - V_k(T_\mathrm{M})}{F_k}\, \Theta(F_k - V_k(T_\mathrm{M})) \, . \tag{2.5}$$

The Heaviside step function

$$\Theta(x) = \begin{cases} 0\,, & x < 0, \\ \frac{1}{2}\,, & x = 0, \\ 1\,, & x > 0, \end{cases} \tag{2.6}$$

guarantees that a loss is always larger than zero. This is necessary, because in the case $V_k(T_\mathrm{M}) > F_k$, the company is able to make the promised payment, and no loss occurs. In other words, the default criterion can be affiliated with the leverage at maturity $F_k/V_k(T_\mathrm{M})$. If the leverage is larger than one, a default occurs, and if the leverage is below one, no default occurs. The corresponding normalized loss given default (LGD) for $F_k > V_k(T_\mathrm{M})$ is

$$LGD_k = \frac{F_k - V_k(T_\mathrm{M})}{F_k} \, . \tag{2.7}$$

It differs from (2.5) by the Heaviside step function. The loss given default is the actual loss, if a company defaults.

In the following, we consider a portfolio of credit contracts for K companies. The total portfolio loss L is a sum over the individual losses weighted by their fractions

f_k in the portfolio

$$L = \sum_{k=1}^{K} f_k L_k \qquad , \qquad f_k = \frac{F_k}{\sum_{i=1}^{K} F_i} \ . \tag{2.8}$$

The aim is to describe the average portfolio loss distribution $p(L|\Sigma)$, which depends on the covariance matrix Σ. It can be expressed by means of a filter integral

$$p(L|\Sigma) = \int\limits_{[0,\infty)^K} d[V] g(V|\Sigma) \delta \left(L - \sum_{k=1}^{K} f_k L_k \right) \ , \tag{2.9}$$

where $g(V|\Sigma)$ is the multivariate distribution of all correlated asset values at maturity time T_{M}, Σ is the covariance matrix, $V = (V_1(T_{\mathrm{M}}), \ldots, V_K(T_{\mathrm{M}}))$ is the K component vector of the asset values and the measure $d[V]$ is the product of all differentials

$$d[V] = \prod_{k=1}^{K} dV_k \ . \tag{2.10}$$

This is equivalent to a $K-1$-fold convolution, which is expressed in terms of a filter integral by means of the Dirac delta function $\delta(x)$. We notice the complexity of the integral (2.9) as the losses (2.5) involve Heaviside functions. In order to calculate the portfolio loss distribution (2.9) we first need to specify the multivariate distribution of the correlated asset values $g(V|\Sigma)$. It is obtained by the more easily accessible distribution $g(r|\Sigma)$ where r is the return vector consisting of the returns

$$r_k(t) = \frac{V_k(t + \Delta t) - V_k(t)}{V_k(t)} \ , \tag{2.11}$$

defined analogously to (1.2). Here, Δt is the return horizon, which corresponds to the maturity time, i.e.,

$$\Delta t = T_{\mathrm{M}} \tag{2.12}$$

because we are interested in changes of the asset values over the time period T_{M} and we assume all credit contracts to have the form of zero coupon bonds.

The crucial problem is that the asset values show fluctuating correlations in the course of time. This non-stationarity has to be taken into account by the distribution $g(r|\Sigma)$ when larger time scales like one year or more are considered. Our goal is to calculate average loss distributions that take the non-stationarity of

the covariances into account

$$\langle p\rangle(L|\Sigma) = \int\limits_{[0,\infty)^K} d[V]\langle g\rangle(V|\Sigma)\delta\left(L - \sum_{k=1}^{K} f_k L_k\right) . \tag{2.13}$$

We will argue that this is achieved by properly averaging the multivariate distribution $g(V|\Sigma)$, resulting in $\langle g\rangle(V|\Sigma)$.

2.3. Random Matrix Theory for Non-Stationary Asset Correlations

In the following, we introduce a random matrix theory based on the Wishart model in order to take non-stationary asset correlations into account. First, we sketch the salient features of the Wishart model for correlation and covariance matrices.

2.3.1. Wishart Model for Correlation and Covariance Matrices

Financial markets are highly correlated systems, and risk assessment always requires knowledge of correlations or, more generally, mutual dependencies. Correlation or covariance matrices can be measured for arbitrary systems in which the observables are time series. About ninety years ago, Wishart [200, 201] put forward a random matrix model to assess the statistical features of the correlation or covariance matrices by comparing to a Gaussian null hypothesis. Consider the K values $A_k(t),\ k = 1,\ldots,K$ at a fixed time t, which form the K component data vector $A(t) = (A_1(t),\ldots,A_K(t))^\dagger$. Now, suppose that we draw the entries of this vector from a multivariate Gaussian distribution with some covariance matrix Σ_0, say, meaning that

$$\widetilde{w}(A(t)|\Sigma_0) = \frac{1}{\det^{1/2}(2\pi\Sigma_0)} \exp\left(-\frac{1}{2}A^\dagger(t)\Sigma_0^{-1}A(t)\right) \tag{2.14}$$

is the probability density function. We now make the important assumptions that, first, the data vectors are statistically independent for different times t and, second, the distribution (2.14) has exactly the same form for all times $t = 1,\ldots,T$ with the same covariance matrix Σ_0. Put differently, we assume that the data are from a statistical viewpoint, Markovian and stationary in time. The probability density

function for the entire model data matrix A is then simply the product

$$\begin{aligned} w(A|\Sigma_0) = & \prod_{t=1}^{T} \widetilde{w}(A(t)|\Sigma_0) \\ = & \frac{1}{\det^{T/2}(2\pi\Sigma_0)} \exp\left(-\frac{1}{2}\mathrm{tr}A^\dagger\Sigma_0^{-1}A\right) \ . \end{aligned} \tag{2.15}$$

This is the celebrated Wishart distribution for the data matrix A, which predicts the statistical features of random covariance matrices. By construction, we find for the average of the model covariance matrix $AA^\dagger/T$

$$\langle\frac{1}{T}AA^\dagger\rangle \ = \ \int d[A]w(A|\Sigma_0)\frac{1}{T}AA^\dagger \ = \ \Sigma_0 \ , \tag{2.16}$$

where the angular brackets indicate the average over the Wishart random matrix ensemble (2.15) and where $d[A]$ stands for the flat measure, i.e., for the product of the differentials of all independent variables

$$d[A] = \prod_{k,t} dA_k(t) \ . \tag{2.17}$$

We notice that in the random matrix model, each $A_k(t)$ is one single random variable; both the index k and the argument t are discrete. Hence, the $dA_k(t)$ is not the differential of a function, rather it is simply the differential of the random variable $A_k(t)$. The Wishart ensemble is based on the assumptions of statistical independence for different times, stationarity and a multivariate Gaussian functional form. The covariance matrix Σ_0 is the input for the mean value of the Wishart ensemble about which the individual random covariance matrices fluctuate in a Gaussian fashion. The strength of the fluctuations is intimately connected with the length T of the model time series. Taking the formal limit $T \to \infty$ reduces the fluctuations to zero, and all random covariance matrices are fixed to Σ_0. It is worth mentioning that the Wishart model for random correlation matrices has the same form. If we replace A with M and Σ_0 with C_0, we find the Wishart distribution that yields the statistical properties of random correlation matrices.

The Wishart model serves as a benchmark and a standard tool in statistical inference [201] by means of an ergodicity argument: the statistical properties of individual covariance or correlation matrices may be estimated by an ensemble of such matrices, provided their dimension K is large. Admittedly, this ergodicity argument does not necessarily imply that the probability density functions are multivariate Gaussians. Nevertheless, arguments similar to those that lead to the central limit theorem corroborate the Gaussian assumption, and empirically, it was

seen to be justified in a huge variety of applications. A particularly interesting application of the Wishart model for correlations in the simplified form with $C_0 = 1_K$ was put forward by the Paris and Boston econophysics groups [64, 90] who compared the eigenvalue distributions (marginal eigenvalue probability density functions) of empirical financial correlation matrices with the theoretical prediction. They found good agreement in the bulk of the distributions, which indicates a disturbing amount of noise-dressing in the data due to the relatively short lengths of the empirical time series with considerable consequences for portfolio optimization methods [67, 68, 91, 97, 202, 203].

2.3.2. New Interpretation and Application of the Wishart Model

Financial markets are well known to be non-stationary, i.e., the assumption of stationarity is only meaningful on short time scales and is bound to fail on longer ones. Non-stationary complex systems pose fundamental challenges [204–207] for empirical analysis and for mathematical modeling [208, 209]. An example from finance is comprised of the strong fluctuations of the sample standard deviations σ_k, measured in different time windows of the same length T [53, 54], as shown in figure 1.2 (c). Financial markets demonstrated their non-stationarity in a rather drastic way during the recent years of crisis. Here, we focus on the non-stationarity of the correlations. Their fluctuations in time occur, e.g., because the market expectations of the traders change, the business relations between the companies change, particularly in a state of crisis, and so on. To illustrate how strongly the $K \times K$ correlation matrix C as a whole changes in time, we show it for subsequent time windows in figure 1.3.

Clearly, the non-stationary fluctuations of the correlations influence all deduced economic observables, and it is quite plausible that this effect will be strong for the statistics of rare, correlated events. In the sequel, we will show that the tails of the loss distributions in credit risks will be particularly sensitive to the non-stationarity of the correlations. We will also extend the Merton model of credit risk to account for the non-stationarity. To this end, we will now put forward a re-interpretation of the Wishart random matrix model for correlation matrices [191]. As mentioned in section 2.3.1, the Wishart model in its original and widely-used form is based on the assumption of stationarity. Using ergodicity, it predicts statistical properties of large individual correlation and covariance matrices with the help of a fictitious ensemble of random matrices. Ergodicity means that averages of one single system over a very long time can be replaced by an average over an ensemble of matrices or other mathematical structures, which represent all possible systems of the same kind. We now argue that the Wishart model may be viewed as an ensemble of random matrices that models a truly existing ensemble of non-stationary covariance

matrices. The elements of this ensemble model are in a statistical sense a set of covariance matrices, which result from a measurement. In the re-interpretation of the Wishart model the issue of ergodicity does not arise. Four elements in this latter ensemble are shown in figure 1.3; the whole ensemble consists of all correlation matrices measured with a window of length T sliding through a set of much longer time series of length T_{tot}. The size of the truly existing ensemble is thus T_{tot}/T if the windows do not overlap. The average correlation or covariance matrices C_0 or Σ_0 are simply the sample averages over the whole time series of length T_{tot}. We have K time series divided into pieces of length T that yield the truly existing ensemble. To model it with an ensemble of random matrices, we have to employ data matrices A with K rows, representing the model time series, but we are free to choose their length N. As argued above, the length of the time series controls the strength of the fluctuations around the mean. Thus, we use $K \times N$ random data matrices A and write

$$w(A|\Sigma_0) \;=\; \frac{1}{\det^{N/2}(2\pi\Sigma_0)} \exp\left(-\frac{1}{2}\mathrm{tr}A^{\dagger}\Sigma_0^{-1}A\right) \tag{2.18}$$

for the probability density function. The $K \times K$ mean covariance matrix Σ_0 is the input and given by the sample mean using the whole time series of length T_{tot}. This is our re-interpreted Wishart model to describe fluctuating, non-stationary covariance or correlation matrices. Importantly, ergodicity reasoning is not evoked here, and it would actually be wrong. It is also worth mentioning that we are not restricted to large matrix dimensions.

Next, we reveal that the non-stationarity in the correlations induces generic, i.e., universal features in financial time series of correlated markets. We begin with showing that the returns are to a good approximation multivariate Gaussian distributed, if the covariance matrix Σ is fixed. We begin with assuming that the distribution of the K dimensional vectors $r(t) = (r_1(t), \ldots, r_K(t))$ for a fixed return interval Δt while t is running through the dataset is given by

$$g(r|\Sigma) \;=\; \frac{1}{\sqrt{\det(2\pi\Sigma)}} \exp\left(-\frac{1}{2}r^{\dagger}\Sigma^{-1}r\right) \;, \tag{2.19}$$

where we suppress the argument t of r in our notation. We test this assumption on a dataset consisting of daily data of $K = 306$ continuously-traded companies in the S&P 500 index between 1992 and 2012. We divide the time series in windows of length $T = 25$ trading days, which is short enough to ensure that the sampled covariances can be viewed as constant within these windows. We aggregate the data, i.e., we rotate the return vector into the eigenbasis of Σ and normalize with the corresponding eigenvalues. As seen in figure 2.2, there is good agreement with a Gaussian over at least four orders of magnitude; details of the analysis can be

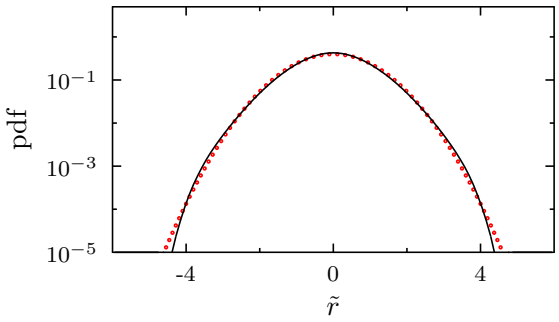

Figure 2.2.: Aggregated distribution of normalized returns $\tilde{r}$ for fixed covariances from the S&P 500 dataset, $\Delta t = 1$ trading day and window length $T = 25$ trading days. The circles show a normal distribution, the scale is logarithmic. Taken from [191].

found in [191]. To account for the non-stationarity of the covariance matrices, we replace them with random matrices

$$\Sigma \quad \longrightarrow \quad \frac{1}{N} A A^\dagger \ , \tag{2.20}$$

drawn form the distribution (2.18). We emphasize that the random matrices A have dimension $K \times N$. The larger the N, the more terms contribute to the individual matrix elements of $AA^\dagger/N$, eventually fixing them for $N \to \infty$ to the mean Σ_0. The fluctuating covariances alter the multivariate Gaussian (2.19). We model this by the ensemble averaged return distribution

$$\langle g \rangle (r|\Sigma_0,N) \ = \ \int d[A] g \left(r \middle| \frac{1}{N} A A^\dagger \right) w(A|\Sigma_0) \ , \tag{2.21}$$

which parametrically depends on the fixed empirical covariance matrix Σ_0, as well as on N. The ensemble average can be done analytically [191] and results in

$$\langle g \rangle (r|\Sigma_0,N) = \frac{\sqrt{N}^K}{\sqrt{2}^{N-2}\Gamma(N/2)\sqrt{\det(2\pi\Sigma_0)}} \frac{\mathcal{K}_{(K-N)/2}\left(\sqrt{N r^\dagger \Sigma_0^{-1} r}\right)}{\sqrt{N r^\dagger \Sigma_0^{-1} r}^{(K-N)/2}} \ , \tag{2.22}$$

where $\mathcal{K}_\nu$ is the modified Bessel function of the second kind of order ν. In the data analysis below, we will find $K > N$. Since the empirical covariance matrix Σ_0 is fixed, N is the only free parameter in the distribution (2.22). For large N, it approaches a Gaussian. The smaller N, the heavier the tails, for $N = 2$ the

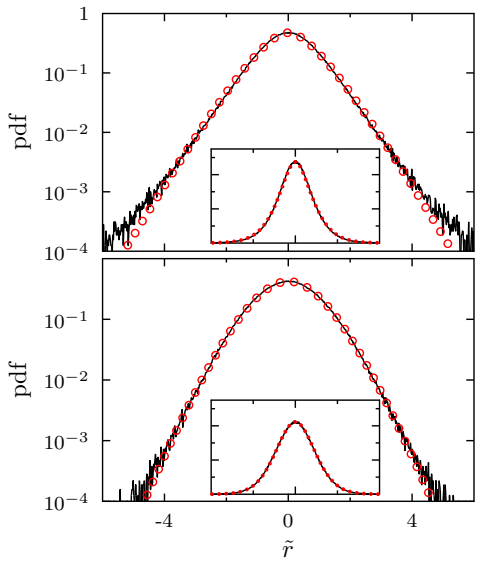

Figure 2.3.: Aggregated distribution of the rotated and scaled returns $\tilde{r}$ for $\Delta t = 1$ (**top**) and $\Delta t = 20$ (**bottom**) trading days on a logarithmic scale. The circles correspond to the aggregation of the distribution (2.22). Taken from [191].

distribution is exponential. Importantly, the returns enter $\langle g \rangle(r|\Sigma_0,N)$ only via the bilinear form $r^\dagger \Sigma^{-1} r$.

To test our model, we again have to aggregate the data, but now for the entire S&P 500 dataset from 1992–2012, i.e., $T_{\text{tot}} = 5275$ days, see figure 2.3. We find $N = 5$ for daily returns, i.e., $\Delta t = 1$ trading day and $N = 14$ for $\Delta t = 20$ trading days. Furthermore, a more detailed comparison with larger datasets for monthly returns is provided in figure 2.4. Here, stocks taken from the S&P 500 index and stocks taken from NASDAQ are used. In the top left corner, the dataset consists of 307 stocks taken from the S&P 500 index, which are continuously traded in the period 1992–2012. The other datasets following clockwise are: 439 stocks from S&P 500 index in the time period 2002–2012, 2667 stocks from NASDAQ in the time period 2002–2012 and 708 stocks from NASDAQ in the time period 1992–2012. We find values around $N = 20$ for monthly returns. Both datasets are taken from Yahoo Finance [210].

There is a good agreement between the model and data. Importantly, the distributions have heavy tails, which result from the fluctuations of the covariances; the smaller the N, the heavier. For small N, there are deviations between theory and data in the tails. Three remarks are in order. First, one should clearly distinguish this multivariate analysis from the stylized facts of individual stocks,

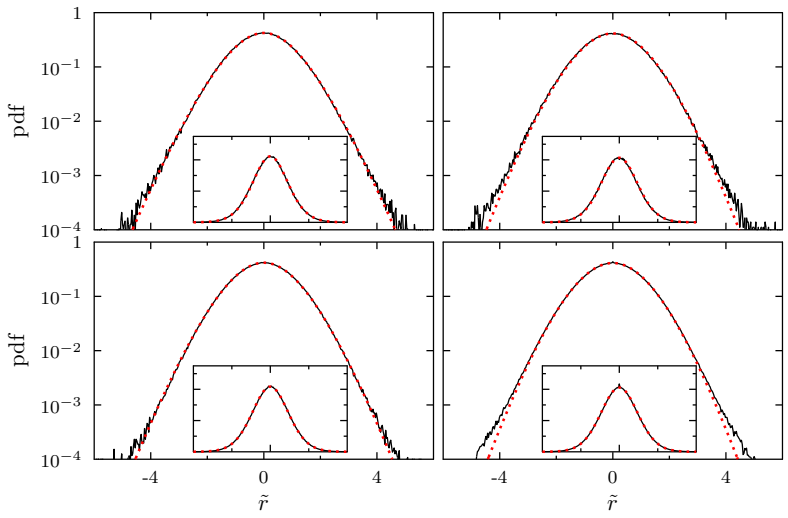

Figure 2.4.: Aggregated distribution for the normalized monthly returns with the empirical covariance matrix on a logarithmic scale. The black line shows the empirical distribution; the red dotted line shows the theoretical results. The insets show the corresponding linear plots. **Top** left/right: S&P 500 (1992–2012)/(2002–2012); **bottom** left/right: NASDAQ (1992–2012)/(2002–2012). Taken from [192].

which are well known to have heavy-tailed distributions. This is to some extent accounted for in our model, as seen in the bottom part of figure 2.3. In the top part, the tails are heavier because the time interval Δt is much shorter. To further account for this, we need to modify the Wishart model by using a distribution different from a Gaussian one [211]. Second, figure 1.3 clearly shows that the empirical ensemble of correlation matrices has inner structures, which are also contained in our model, because the mean Σ_0 enters. Third, an important issue for portfolio management is that the random matrix approach reduces the effect of fluctuating correlations to one single parameter characterizing its strength. Hence, the fluctuation strength of correlations in a given time interval can directly be estimated from the empirical return distribution without having to estimate the correlations on shorter time intervals [194].

In the mathematics and economics literature, dynamic models based on Wishart processes were introduced, involving multivariate stochastic volatilities [212, 213]. Various quantities such as leverage, risk premia, prices of options and Wishart autoregressive processes are calculated and discussed. These studies are related to ours, although our focus is not on the processes, rather on the resulting distributions,

because we wish to directly model multivariate return distributions in a non-stationary setting.

2.4. Modeling Fluctuating Asset Correlations in Credit Risk

Structural credit risk models employ the asset value at maturity to derive default events and their ensuing losses. Thus, the distribution that describes the asset values has to be chosen carefully. One major requirement is that the distribution is in good accordance with empirical data. This goal can be achieved by using the random matrix approach for the asset correlations, discussed in section 2.3. Based on [134, 192], we discuss the Merton model together with the random matrix approach and reveal various results for the average portfolio loss distribution, VaR and ETL.

2.4.1. Random Matrix Approach

As described in section 2.3, the random matrix approach can be used to cope with the non-stationary asset correlations. The average asset value distribution $\langle g \rangle (V|\Sigma_0,N)$ is obtained by averaging a multivariate normal distribution over an ensemble of Wishart distributed correlation matrices. Thus, we calculate the loss distribution as an ensemble average. From (2.9), we find

$$\langle p \rangle (L|\Sigma_0,N) = \int\limits_{[0,\infty)^K} d[V] \langle g \rangle (V|\Sigma_0,N) \delta \left(L - \sum_{k=1}^{K} f_k L_k \right) . \tag{2.23}$$

Again, we emphasize that the ensemble truly exists as a consequence of the non-stationarity. As a side effect of the random matrix approach, the resulting distribution depends only on two parameters: the $K \times K$ average covariance matrix Σ and the free parameter N, which controls the strength of the fluctuations around the average covariance matrix. N behaves like an inverse variance of the fluctuations; the smaller the N, the larger the fluctuations become. Both parameters have to be determined by historical stock price data.

The average asset value distribution depends on the $K \times K$ mean covariance matrix Σ_0. To circumvent the ensuing complexity and to make analytical progress,

we assume an effective average correlation matrix

$$C_0 = (1-c)\mathbb{1}_K + ce_K e_K^\dagger = \begin{bmatrix} 1 & c & c & \dots \\ c & 1 & c & \dots \\ c & c & 1 & \dots \\ \vdots & \vdots & \vdots & \ddots \end{bmatrix} \tag{2.24}$$

where all off-diagonal elements are equal to c. Here, $\mathbb{1}_K$ is the $K \times K$ unit matrix and e_K is a K component vector containing ones. The average correlation is calculated over all assets for the selected time horizon. We emphasize that only the effective average correlation matrix C_0 is fixed; the correlations in the random matrix approach fluctuate around this mean value. In the sequel, whenever we mention a covariance matrix with an effective correlation matrix, we denote it as an effective covariance matrix, and whenever we mention a fully-empirical covariance matrix where all off-diagonal elements differ from another, we denote it as an empirical covariance matrix or a covariance matrix with a heterogeneous correlation structure. Using the assumption (2.24), analytical tractability is achieved, but it also raises the question whether the data can still be described well. To compare the result with the data, one has to rotate and scale the returns again, but instead of using the empirical covariance matrix the covariance matrix with the effective average correlation structure has to be applied. The results for monthly returns, using the same dataset as in figure 2.4, are shown in figure 2.5. Still, there is a good agreement between the average asset value distribution with the assumption (2.24) and the data. This leads to the conclusion that the approximation is reasonable. Considering the parameter N_{eff}, which is needed to describe the fluctuations around the effective average correlation matrix, values around $N_{\text{eff}} = 4$ are found. In contrast to the larger values around $N = 20$, which describe the distributions best in the case of an empirical correlation matrix, the lower values in the case of an effective correlation matrix with average correlation c are needed to describe the larger fluctuations around this average. This result corroborates the interpretation of N as an inverse variance of the fluctuations. Now, the correlation structure of a financial market is captured solely by two parameters: the effective average correlation coefficient c and parameter N, which indicates the strength of the fluctuations around this average. Both parameters have to be estimated from empirical data.

If we studied non-averaged quantities depending on a specific correlation structure, approach (2.24) would be much less likely to give satisfactory results. The choice has two major advantages. First, we achieve analytical tractability, which can be seen later on in section 3.2.1; second, we can describe the complexity of a correlated market with only two parameters.

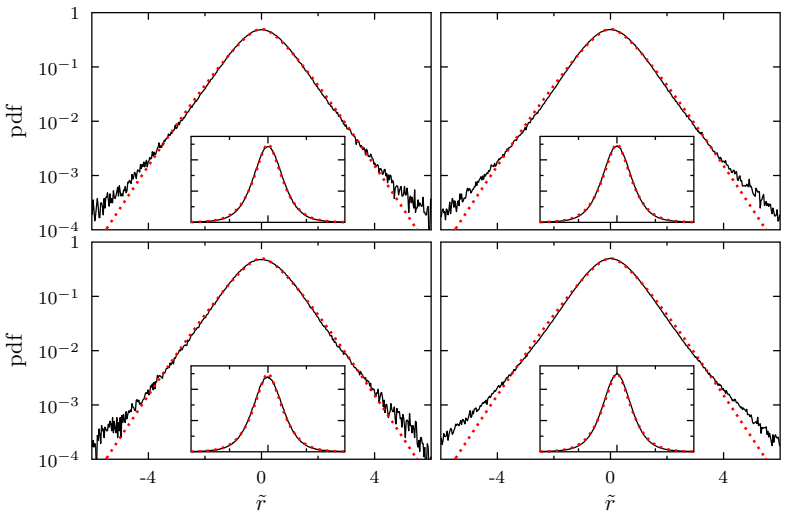

Figure 2.5.: Aggregated distribution for the normalized monthly returns with the effective correlation matrix on a logarithmic scale. The black line shows the empirical distribution; the red dotted line shows the theoretical results. The insets show the corresponding linear plots. **Top** left/right: S&P 500 (1992–2012)/(2002–2012); **bottom** left/right: NASDAQ (1992–2012)/(2002–2012). The average correlation coefficients are $c = 0.26$, 0.35, 0.21 and 0.25, respectively. Taken from [192].

2.4.2. Average Loss Distribution

Having shown the quality of the random matrix approach, we may now proceed in calculating the average portfolio loss distribution (2.23). We deduce the average distribution for the asset values $\langle g \rangle (V|\Sigma_0,N)$ from the result (2.22) for the returns. In the Merton model, it is assumed that the asset values $V_k(t)$ follow a geometric Brownian motion with drift and volatility constants μ_k and ρ_k, respectively. This leads to a multivariate Gaussian of the form (2.19) for the returns, which is consistent with the random matrix approach. Therefore, according to Itô's Lemma [214], we perform a change of variables

$$r_k \longrightarrow \ln \frac{V_k(T_\mathrm{M})}{V_{k0}} - \left(\mu_k - \frac{\rho_k^2}{2}\right) T_\mathrm{M} \,, \tag{2.25}$$

with $V_{k0} = V_k(0)$ and the volatilities

$$\rho_k = \frac{\sigma_k}{\sqrt{T_\mathrm{M}}} \,, \tag{2.26}$$

where σ_k is the sample standard deviation in connection with (1.7). Expression (2.22) can now be rewritten using Fourier integrals. After employing and adjusting the steps in [134], we arrive at the double integral

$$\begin{aligned}\langle g\rangle\,(V|c,N) = \frac{1}{2^{N/2}\Gamma(N/2)} \int_0^\infty dz z^{N/2-1} e^{-z/2} \sqrt{\frac{N}{2\pi z}} \sqrt{\frac{N}{2\pi z(1-c)T}}^K \\ \times \int_{-\infty}^{\infty} du \exp\left(-\frac{N}{2z}u^2\right) \\ \times \prod_{k=1}^K \frac{1}{V_k\rho_k} \exp\left[-\frac{N}{2z(1-c)T\rho_k^2}\left(\ln\frac{V_k}{V_{k0}} - \left(\mu_k - \frac{\rho_k^2}{2}\right)T + \sqrt{cT}u\rho_k\right)^2\right].\end{aligned} \tag{2.27}$$

The random matrix model of non-stationarity together with the effective average correlation matrix results in an expression for the joint multivariate distribution of the asset values in terms of a bivariate average of the product of geometric Brownian motions over a χ^2 distribution in z and a Gaussian in u. We do not perform the u integration yet because we will factorize the V_k integrals when computing the loss distribution (2.23) later on.

In order to calculate the average portfolio loss distribution, we assume a large portfolio in which all face values F_k are of the same order $1/K$ and carry out an expansion for large K. The analytical result is

$$\begin{aligned}\langle p\rangle(L|c,N) = \frac{1}{\sqrt{2\pi}2^{N/2}\Gamma(N/2)} \int_0^\infty dz\ z^{N/2-1} e^{-z/2} \sqrt{\frac{N}{2\pi}} \\ \times \int_{-\infty}^{+\infty} du \exp\left(-\frac{N}{2}u^2\right) \frac{1}{\sqrt{M_2(z,u)}} \exp\left(-\frac{(L-M_1(z,u))^2}{2M_2(z,u)}\right)\end{aligned} \tag{2.28}$$

for the average loss distribution with

$$M_1(z,u) = \sum_{k=1}^K f_k m_{1k}(z,u) \tag{2.29}$$

and

$$M_2(z,u) = \sum_{k=1}^K f_k^2 \left(m_{2k}(z,u) - m_{1k}^2(z,u)\right)\ . \tag{2.30}$$

The j-th moments $m_{jk}(z,u)$ are

$$m_{jk}(z,u) = \int_{-\infty}^{\hat{F}_k} d\hat{V}_k \left(1 - \frac{V_{k0}}{F_k} \exp\left(\sqrt{z}\hat{V}_k + \left(\mu_k - \frac{\rho_k^2}{2}\right) T_{\mathrm{M}}\right)\right)^j \times \sqrt{\frac{N}{2\pi(1-c)T_{\mathrm{M}}\rho_k^2}} \exp\left(-\frac{N}{2(1-c)T_{\mathrm{M}}\rho_k^2}\left(\hat{V}_k + \sqrt{cT_{\mathrm{M}}}u\rho_k\right)^2\right) , \tag{2.31}$$

see [134]. The changed variable is $\hat{V}_k = (\ln(V_k(T_{\mathrm{M}})/V_{k0}) - (\mu_k - \rho_k^2/2)T_{\mathrm{M}})/\sqrt{z}$ with the upper bound for the integral (2.31)

$$\hat{F}_k = \frac{1}{\sqrt{z}}\left(\ln\frac{F_k}{V_{k0}} - \left(\mu_k - \frac{\rho_k^2}{2}\right)T_{\mathrm{M}}\right) . \tag{2.32}$$

The integrals in (2.28) have to be evaluated numerically.

To further illustrate the results, we assume homogeneous credit portfolios. A portfolio is said to be homogeneous when all contracts have the same face value $F_k = F$ and start value $V_k(0) = V_0$ and the same parameters for the underlying stochastic processes like volatility $\rho_k = \rho$ and drift $\mu_k = \mu$. Of course, this does not mean that all asset values follow the same path from $t = 0$ to maturity T_{M} because underlying processes are stochastic.

It is often argued that diversification significantly reduces the risk in a credit portfolio. In the context mentioned here, diversification solely means the increase of the number K of credit contracts in the credit portfolio on the same market. The limit distribution for an infinitely large portfolio provides information about whether this argument is right or wrong. We thus consider a portfolio of size $K \to \infty$ and find the limiting distribution

$$\langle p\rangle(L|c,N)\Big|_{K\to\infty} = \frac{1}{2^{N/2}\Gamma(N/2)}\sqrt{\frac{N}{2\pi}} \times \int_0^\infty dz\, z^{N/2-1}e^{-z/2}\exp\left(-\frac{N}{2}u_0^2\right)\frac{1}{|\partial m_1(z,u)/\partial u|_{z,u_0}} , \tag{2.33}$$

where $u_0(L,z)$ is the implicit solution of the equation

$$L = m_1(z,u_0) . \tag{2.34}$$

We drop the second index k of the first moment $m_1(z,u_0)$ from (2.31), since we consider a homogeneous portfolio. To arrive at the result (2.33), we use standard methods of the theory of generalized functions and distributions [215]. We now

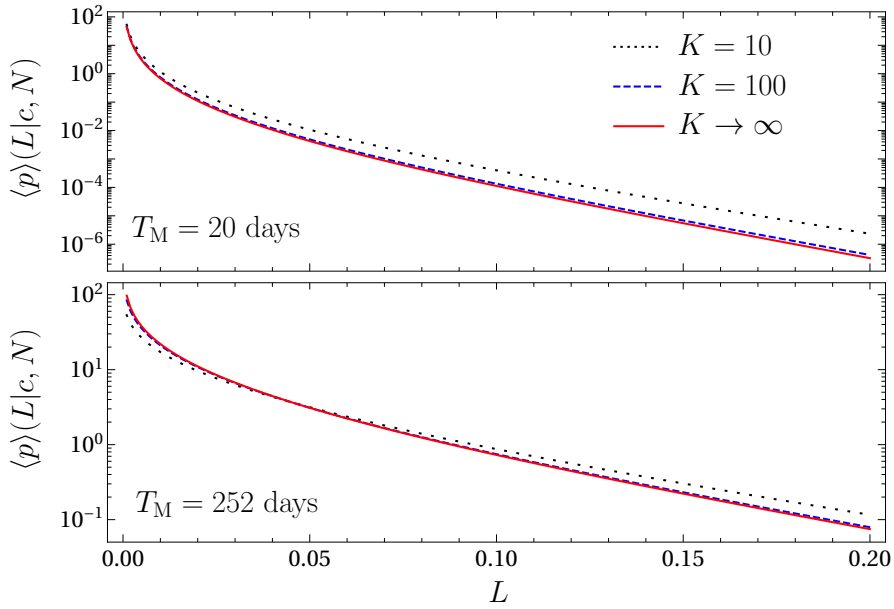

Figure 2.6.: Average portfolio loss distribution for different portfolio sizes of $K = 10$, $K = 100$ and the limiting case $K \to \infty$. At the **top**, the maturity time is one month; at the **bottom**, it is one year. The scale is logarithmic.

display the average loss distribution for different K. The model depends on four parameters, which can be calibrated by empirical data. Three of them, the average drift μ, the average volatility ρ and the average correlation coefficient c, can be directly calculated from the data. The fourth parameter N, controlling the strength of the fluctuations, has to be determined by fitting the average asset value distribution onto the data. The resulting average portfolio loss distribution $\langle p \rangle (L|c,N)$ for correlation averaged asset values is shown in figure 2.6. Different portfolio sizes $K = 10{,}100$ and $K \to \infty$ and two different maturity times $T_M = 20$ trading days and $T_M = 252$ trading days are shown. For the estimation of the empirical parameters, the S&P 500 dataset in the time period 1992–2012 is used. The parameters for $T_M = 20$ trading days are $N = 4.2$, $\mu = 0.013$ month^{-1}, $\rho = 0.1$ month$^{-1/2}$ and an average correlation coefficient of $c = 0.26$, shown on the top, and for a maturity time of $T_M = 1$ year $N = 6.0$, $\mu = 0.17$ year^{-1}, $\rho = 0.35$ year$^{-1/2}$ and an average correlation coefficient of $c = 0.28$, shown on the bottom. Moreover, a face value of $F = 75$ and an initial asset value of $V_0 = 100$ are used. There is always a slowly decreasing heavy-tail. A significant decrease of the risk of large losses cannot be achieved by increasing the size of the credit portfolio. Instead, the distribution quickly converges to the limiting distribution $K \to \infty$. This drastically reduces the effect of diversification. In a quantitative manner, it is thus shown

that diversification does not work for credit portfolios with correlated asset values. Speaking pictorially, the correlations glue the obligors together and let them act to some extent like just one obligor.

The values of the average correlation coefficient c and the parameter N also influence the average loss distribution. The larger the average correlation c and the smaller the parameter N, the heavier are the tails of the distribution and the more likely is the risk of large losses.

2.4.3. Adjustability to Different Market Situations

The non-stationarity of financial markets implies that there are calm periods where the markets are stable, as well as periods of crisis such as the period 2008–2010; see, e.g., for the volatility in figure 1.2 (c). Observables describing the market behavior in different periods vary significantly. Consequently, the loss distribution, particularly its tail, strongly changes in different market situations. Our model fully grasps this effect.

Importantly, we are able to adjust the four parameters drift, volatility, average correlation coefficient and parameter N, to different periods, i.e., different market situations. This is a significant feature of the model. To demonstrate the adjustability of our model based on the random matrix approach, we consider the two periods 2002–2004 and 2008–2010. The first period is rather calm, whereas the second includes the global financial crisis. We determine the average parameters for monthly returns of continuously-traded S&P 500 stocks, shown in Table 2.1. For each period, we take the corresponding parameters and calculate the average portfolio loss distribution; see figure 2.7. As anticipated, we find a much more pronounced tail risk in times of crisis. This is mainly due to the enlarged average correlation coefficient in times of crisis. Consequently, we are able to adjust the model to various periods. It even is possible to adjust the parameters and hence the tail behavior dynamically.

Time Horizon for Estimation	K	N_{eff}	ρ in month$^{-1/2}$	μ in month^{-1}	c
2002–2004	436	5	0.10	0.015	0.30
2008–2010	478	5	0.12	0.010	0.46

Table 2.1.: Average parameters used for two different time horizons. The values are taken from [192].

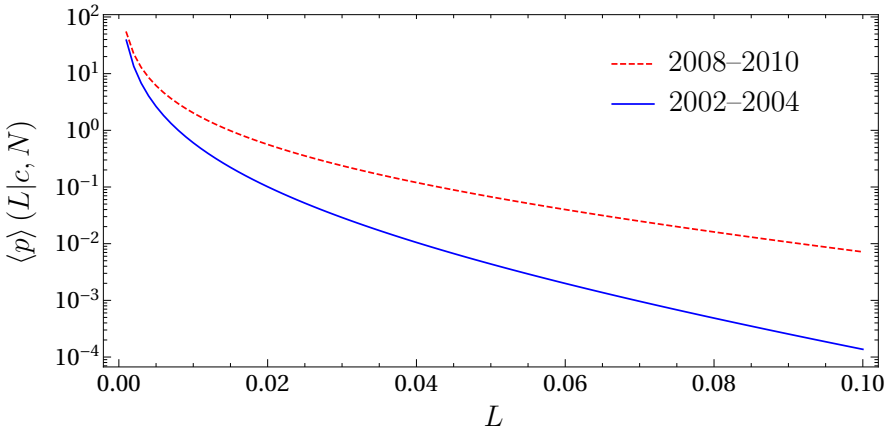

Figure 2.7.: Average loss distribution for different parameters taken from Table 2.1 on a logarithmic scale. The dashed line corresponds to the global financial crisis 2008–2010; the solid line corresponds to the calm period 2002–2004.

The setting discussed here includes avalanche or contagion effects only indirectly when calibrated to a market situation in the state of crisis. Direct modeling of contagion is provided in [127, 216].

We estimate the value of the correlations by empirical data. However, the multivariate return distribution (2.22) that we construct is strongly non-Gaussian and describes the empirical data well. Thus, in the present context copulas, which capture the lower tail dependence, are not needed. However, a comparison with copulas can be found in [83].

Moreover, by adjusting the parameter N, we are able to control the strength of the fluctuations around the mean correlation coefficient. The larger the N, the smaller the fluctuations are. In the case $N \to \infty$, the fluctuations are suppressed and the correlation matrix becomes stationary. Hence, the average return distribution (2.22) becomes a multivariate Gaussian and the benefits of the random matrix approach are not given anymore. The result for the average portfolio loss distribution is

$$\lim_{N\to\infty} \langle p \rangle (L|c,N) = \frac{1}{\sqrt{2\pi}} \int_{-\infty}^{\infty} du \exp\left(-\frac{u^2}{2}\right) \frac{1}{\sqrt{2\pi M_2(u)}} \exp\left(-\frac{(L-M_1(u))^2}{2M_2(u)}\right) \tag{2.35}$$

with

$$M_1(u) = \sum_{k=1}^{K} f_k m_{1k}(u) \tag{2.36}$$

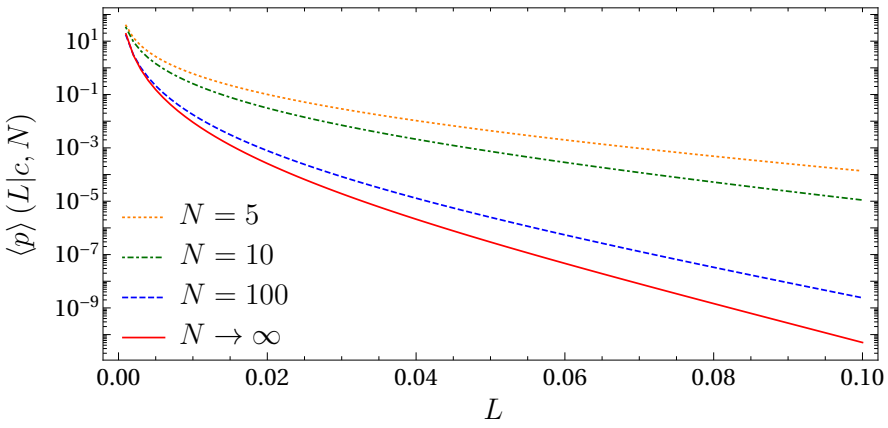

Figure 2.8.: Average portfolio loss distribution for a homogeneous market and different values of N on a logarithmic scale. The portfolio size is $K = 100$.

and

$$M_2(u) = \sum_{k=1}^{K} f_k^2 \left(m_{2k}(u) - m_{1k}^2(u) \right) \ . \tag{2.37}$$

The j-th moments

$$\begin{aligned} m_{jk}(u) = \int_{-\infty}^{\hat{F}_k} d\hat{V}_k \ & \left(1 - \frac{V_{k0}}{F_k} \exp\left[\hat{V}_k + \left(\mu_k - \frac{\rho_k^2}{2} \right) T_{\mathrm{M}} \right] \right)^j \\ & \times \frac{1}{\sqrt{2\pi(1-c) T_{\mathrm{M}} \rho_k^2}} \exp\left(\frac{1}{2(1-c) T_{\mathrm{M}} \rho_k^2} \left(\hat{V}_k + \sqrt{c T_{\mathrm{M}}} u \rho_k \right)^2 \right) \ , \end{aligned} \tag{2.38}$$

are very similar to the moments $m_{jk}(z,u)$ in (2.31).

In figure 2.8, we compare the portfolio loss distribution for a fixed correlation coefficient of $c = 0.3$ for different values of N. The tail of the loss distribution clearly decreases with increasing N. The larger N becomes, the smaller are the outliers of the random correlations around the mean correlation coefficient. This shows the benefit of our random matrix approach compared to standard methods using stationary asset correlations and a multivariate Gaussian for the asset return distribution. Due to the asymmetry of credit risk, outliers that exceed the average correlation coefficient by far have a much stronger impact on the loss distribution than outliers which remain below the average correlation coefficient. This effect is more pronounced for smaller N and leads to an increasing tail.

2.4.4. Value at Risk and Expected Tail Loss

The approximation of an effective correlation matrix facilitated analytical progress, but importantly, the average asset return distribution still fits empirical data well when using this approximation. We now show that this approximation is also capable of estimating the Value at Risk and the Expected Tail Loss. We compare the results obtained in this approximation with the results obtained for an empirical covariance matrix. This is also interesting from the risk management perspective because it is common to estimate the covariance matrix over a long period of time and use it as an input for various risk estimation methods. Put differently, we are interested in the quality of risk estimation using an effective correlation matrix and taking fluctuating correlations into account.

The comparison of the effective correlation matrix with the empirical correlation matrix cannot be done analytically. Hence, Monte Carlo simulations to calculate the VaR and ETL are carried out. For each asset, its value at maturity time T_{M} is simulated and the portfolio loss according to (2.8) is calculated. All assets have the same fraction in the portfolio. For different time horizons, the empirical covariance matrix, volatilities and drifts for monthly returns of the S&P 500 stocks are calculated. In addition, the parameter N is determined as described above. In the calm period 2002–2004, we find a rather large parameter value of $N = 14$ for the empirical covariance matrix, whereas during the financial crisis in 2008–2010, we find $N = 7$. This once more illustrates the meaning of N as an inverted variance of the fluctuations.

The relative deviations of the VaR and ETL for different quantiles of the effective covariance matrix from the empirical covariance matrix are calculated. This is done in two different ways. First, one may assume a fully-homogeneous portfolio where additional to the effective correlation matrix the average values for volatility and drift for each stock are used. Second, one may use the effective correlation matrix and the empirically-obtained values for volatility and drift for each stock. It turns out that in most cases, the effective correlation matrix together with homogeneous volatility and drift underestimates the risk. In contrast, if one uses heterogeneous volatilities and drifts and the effective correlation matrix, one finds a satisfactory agreement compared to the full empirical covariance matrix; for detailed analysis, see [192]. In the latter case, the effective covariance matrix slightly overestimates the VaR and ETL in most cases. Hence, the structure of the correlation matrix does not play a decisive role in the risk estimation. This is so because the loss distribution is always a multiply-averaged quantity. A good estimation of the volatilities, however, is crucial.

The benefit of the random matrix approach is shown by comparing the VaR calculated for $N \to \infty$ and for different values of N. The case $N \to \infty$ does not

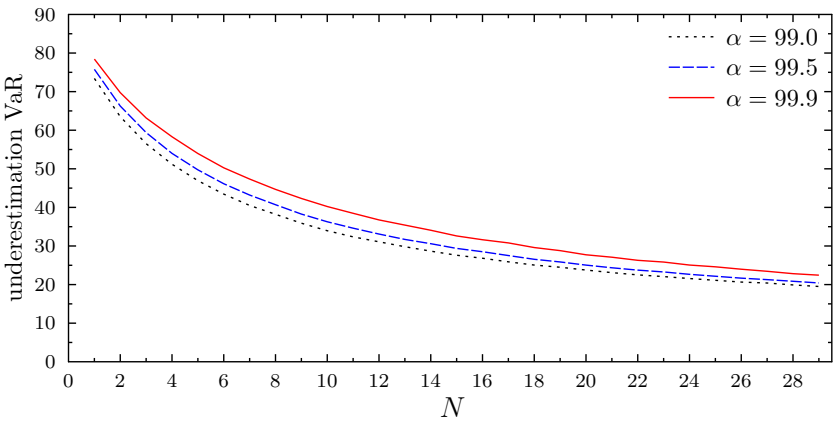

Figure 2.9.: Underestimation of the VaR if fluctuating asset correlations are not taken into account. The empirical covariance matrix is used and compared for different values of N. The scale is linear. Taken from [192].

allow fluctuations of the covariance matrix. This means that we use stationary correlations, which turn the distribution $\langle g \rangle(V|\Sigma_0,N)$ of the asset values at maturity into a multivariate log-normal distribution. Thus, for $N \to \infty$, the benefits of the random matrix approach are disabled. The underestimation of the VaR by using stationary correlations, i.e., $N \to \infty$, is measured in terms of the relative deviation from the VaR calculated for empirical values of N. The empirical covariance matrix and the empirical, i.e., heterogeneous, volatilities and drifts calculated in the period 2006–2010 are used. The results are shown in figure 2.9. Here, different quantiles $\alpha = 0.99, 0.995, 0.999$ are used. For the empirically-observed parameter $N = 12$, the VaR is underestimated between 30% and 40%. Hence, to avoid a massive underestimation of risk, the fluctuations of the asset correlations must be accounted for.

2.5. Concurrent Credit Portfolio Losses

In the previous section, solely one single portfolio on a financial market was considered. Here, based on [193], we consider the problem of concurrent portfolio losses where two non-overlapping credit portfolios are taken into account. We discuss the statistical dependencies for homogeneous and empirical S&P 500- and Nikkei-based credit portfolios by means of copulas.

2.5.1. Simulation Setup

We consider two non-overlapping credit portfolios, which are set up according to figure 2.10, in which the financial market is illustrated by means of its correlation matrix. The two portfolios are marked as black rimmed squares. Both portfolios include K contracts, which means they are of equal size and no credit contract is contained in either portfolio. Despite the fact that the portfolios are non-overlapping, they are correlated due to non-zero correlations in the off-diagonal squares.

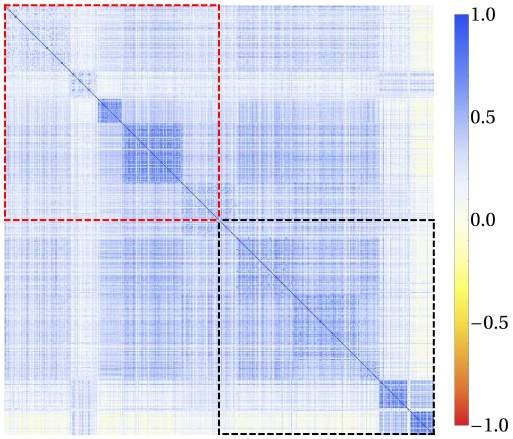

Figure 2.10.: Heterogeneous correlation matrix for 481 stocks from S&P 500 index in the period January 2018 to July 2019 illustrating a financial market. The two rimmed squares correspond to two non-overlapping credit portfolios.

The joint bivariate distribution of the losses $L^{(1)}$ and $L^{(2)}$ of two credit portfolios

$$p(L^{(1)},L^{(2)}|\Sigma) = \int\limits_{[0,\infty)^K} d[V]g(V|\Sigma)\delta\left(L^{(1)} - \sum_{k=1}^{K} f_k^{(1)}L_k^{(1)}\right)\delta\left(L^{(2)} - \sum_{k=1}^{K} f_k^{(2)}L_k^{(2)}\right) \tag{2.39}$$

is defined analogously to (2.9). Here, the upper index indicates the corresponding portfolio. The normalized losses $L_k^{(b)}$ and portfolio losses $L^{(b)}$, as well as the fractions $f_k^{(b)}$ for $b = 1,2$ are defined analogously to (2.5) and (2.8), respectively. The total face value $F_k = F_k^{(1)} + F_k^{(2)}$ is the sum over the face values for both portfolios. We remark that for two non-overlapping portfolios, one of the addends is always zero.

With this simulation setup, the correlated asset values $V_k(T_\mathrm{M})$ for each contract are simulated several thousand times to calculate the portfolio losses and herefrom

the empirical portfolio loss copula. In particular, we will analyze the copula density, which is illustrated by means of a normalized two-dimensional histogram. Hence, when speaking of a copula, we rather mean its density. To obtain a better understanding of the mutual dependencies, which are expressed by the empirical copula, it is compared to a Gaussian copula. This Gaussian copula is fully determined by the correlation coefficient of the portfolio losses.

To systematically study the influence of different parameters on the portfolio loss copula, it is helpful to analyze homogeneous portfolios first. The most generic features can be found by focusing on asset correlations and drifts. The simulation is run in two different ways. First, we consider Gaussian dynamics for the stock price returns. This means that the asset values at maturity time T_{M} are distributed according to a multivariate log-normal distribution. We notice that in the case of Gaussian dynamics, the fluctuations of the random correlations around the average correlation coefficient are zero. This corresponds to the case $N \to \infty$. Second, we use fluctuating asset correlations, employing a parameter value of $N_{\mathrm{eff}} = 5$ in accordance with the findings of [192] for an effective correlation matrix; see Table 2.1. For the simulation, the parameters $\mu = 10^{-3}\,\mathrm{day}^{-1}$, $\rho = 0.03\,\mathrm{day}^{-1/2}$ and leverages $F/V_0 = 0.75$ are chosen. The portfolios are of size $K = 50$, the maturity time is $T_{\mathrm{M}} = 1\,\mathrm{year}$ and a market with vanishing asset correlation, i.e., $c = 0$, is considered. The resulting copulas are shown in figure 2.11. For $N \to \infty$, the loss copula is constant. This result is quite obvious. Due to the Gaussian dynamics and $c = 0$, the asset values are uncorrelated and statistically independent. Therefore, the portfolio losses, which are derived from those independent quantities, do not show mutual dependencies either. The resulting copula is an independence copula, which agrees with a Gaussian loss copula for a portfolio loss correlation of $\mathrm{Corr}(L^{(1)},L^{(2)}) = 0$. In the color code, only white appears. The difference of the empirical copula and the Gaussian copula within each bin is illustrated by means of a color code. The color bar on the right-hand side indicates the difference between the two copulas. The colors yellow to red imply a stronger dependence by the empirical copula in the given (u,v)-interval than predicted by the Gaussian copula. The colors turquoise to blue imply a weaker dependence of the empirical copula than a Gaussian copula predicts. White implies that the local dependence is equal. The empirical average loss correlation calculated from the simulation outcomes is zero and corroborates this result.

In the bottom panel of figure 2.11, the combination of $c = 0$ and $N_{\mathrm{eff}} = 5$ is shown. The deviations from the independence copula are striking. They emerge because we included according to the random matrix approach fluctuating asset correlations around the average correlation $c = 0$. In that way, positive, as well as negative correlations are equally likely. Having a look at the copula histograms, we find a significant deviation from the Gaussian copula. A Gaussian copula is

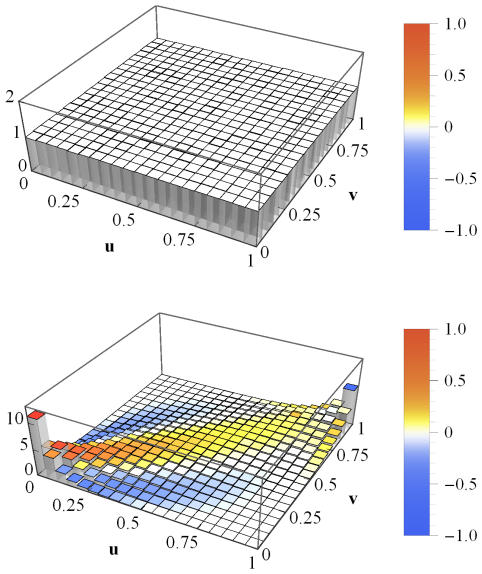

Figure 2.11.: Average loss copula histograms for homogeneous portfolios with vanishing average asset correlations $c = 0$. The asset values are multivariate log-normal ($N \to \infty$) in the top figure and multivariate heavy-tailed ($N_{\text{eff}} = 5$) in the bottom figure. The color bar indicates the local deviations from the corresponding Gaussian copula. Taken from [193].

always symmetric regarding the line spanning from (0,1) to (1,0). Nevertheless, the portfolio loss correlation is $\text{Corr}(L^{(1)},L^{(2)}) = 0.752$. The deviations from the Gaussian copula, which is determined by the calculated correlation coefficient, can be seen on the color code. Especially in the (1,1) corner, which is related to concurrent extreme losses, we see that the empirical copula shows a weaker dependence than the Gaussian copula. We still have to answer the question why the portfolio losses exhibit such a strong positive correlation, although the average asset correlation is set to zero in the simulation. First, as explained before, credit risk is highly asymmetric. For example, if in a credit portfolio, one single contract generates a loss, it is already sufficient enough that the whole portfolio generates a loss. The company defaulting may just cause a small portfolio loss, but still, it dominates all other non-defaulting and maybe prospering companies. In other words, there is no positive impact of non-defaulting companies on the portfolio losses. All those non-defaults are projected onto zero. Second, the fluctuating asset correlations imply a division of the companies into two blocks. The companies show positive correlations within the blocks and negative correlations across them. Due to the aforementioned fact that non-defaulting companies have no positive

impact on the loss distribution, the anti-correlations contribute to the portfolio loss correlation in a limited fashion. They would act as a risk reduction, which is limited according to the asymmetry of credit risk. On the other side, positive correlations within the blocks imply a high risk of concurrent defaults.

We now investigate the impact of the drift. All non-defaulting companies are projected onto a portfolio loss equal to zero. The influence of these projections onto zero and therefore the default-non-default ratio can be analyzed in greater detail by varying the drift of the asset values. For example, if a strong negative drift is chosen, it is highly likely that all companies will default at maturity.

We consider Gaussian dynamics with an average asset correlation of $c = 0.3$ and a volatility of $\rho = 0.02\,\mathrm{day}^{-1/2}$ and different values of μ. Figure 2.12 shows the resulting copulas for three different drift parameters. In the top panel, a drift of $\mu = 10^{-3}\,\mathrm{day}^{-1}$ is chosen, which leads to a non-default ratio of 39.1% and an estimated portfolio loss correlation of $\mathrm{Corr}(L^{(1)},L^{(2)}) = 0.851$. One finds a significant deviation from a symmetric Gaussian copula. In the middle and bottom panel, a drift of $\mu = 3\times10^{-4}\,\mathrm{day}^{-1}$ and $\mu = -3\times10^{-3}\,\mathrm{day}^{-1}$ is chosen, which leads to non-default ratios of 12.8% and zero, respectively. The estimated portfolio loss correlations increase as the non-default ratios decrease, and one finds a correlation of $\mathrm{Corr}(L^{(1)},L^{(2)}) = 0.904$ and $\mathrm{Corr}(L^{(1)},L^{(2)}) = 0.954$, respectively. Moreover, we see that the empirical copula turns ever more Gaussian if the percentage of non-defaults decreases. Finally, at a default probability of 100%, the empirical loss copula is a Gaussian copula. This is seen in the bottom panel where no color except for white appears. In the middle and top panel, we see deviations from the Gaussian copula. Especially in the (1,1) corner, we see that the empirical copula exhibits a stronger dependence than predicted by the corresponding Gaussian copula. In both cases, the statistical dependence of large concurrent portfolio losses is underestimated by the Gaussian copula.

We infer that an increase in default probability yields an increase in portfolio loss correlation. In addition, we conclude that the loss of information, which is caused by the projections onto zero, is responsible for the observed deviations of the statistical dependencies from Gaussian copulas.

2.5.2. Empirical Credit Portfolios

Now, more realistic portfolios with heterogeneous parameters are considered. To systematically study the influence of heterogeneity, only the volatility is initially chosen to be heterogeneous. Afterwards, we will proceed with the analysis of fully-heterogeneous portfolios. The empirical parameters like asset correlation, drift and volatility are determined by historical datasets from S&P 500 and Nikkei 225 stocks.

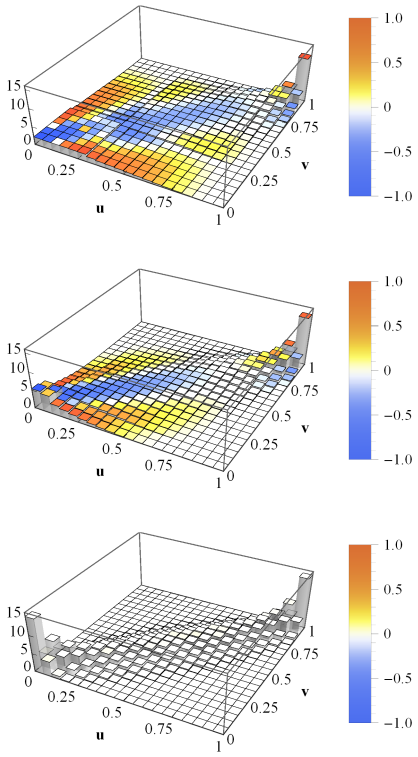

Figure 2.12.: Average loss copula histograms for homogeneous portfolios with asset correlations $c = 0.3$. The asset values are multivariate log-normal ($N \to \infty$). The drifts are $\mu = 10^{-3}\,\mathrm{day}^{-1}$ (**top**), $3 \times 10^{-4}\,\mathrm{day}^{-1}$ (**middle**) and $-3 \times 10^{-3}\,\mathrm{day}^{-1}$ (**bottom**). The color bar indicates the local deviations from the corresponding Gaussian copula. Taken from [193].

In order to avoid any effect due to a specific parameter choice, the average over thousands of simulations run with different parameter values is calculated.

We begin with investigating the heterogeneity of single parameters. Gaussian dynamics with an average asset correlation $c = 0.3$ and a homogeneous large negative drift of $\mu = -3 \times 10^{-3}\,\mathrm{day}^{-1}$ is considered. Due to the large negative drift, we have seen that in the case of an additional homogeneous volatility, the resulting dependence structure is a Gaussian copula. A rather simple heterogeneous portfolio is constructed when only the daily volatilities are considered random. For each contract, the volatility is drawn from a uniform distribution in the open interval (0,0.25). The resulting average portfolio loss copula is shown in figure 2.13. We again compare the average copula calculated by the simulation outcomes with

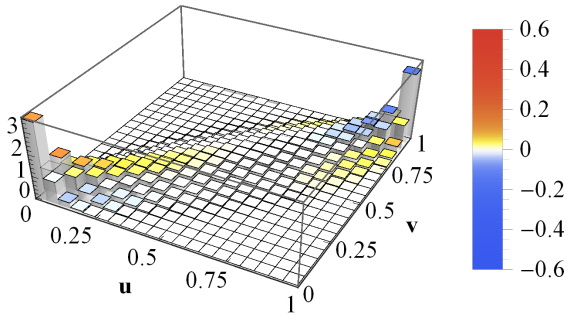

Figure 2.13.: Average loss copula histograms for two portfolios with heterogeneous volatilities drawn from a uniform distribution in the interval (0,0.25). The color bar indicates the local deviations from the corresponding Gaussian copula. Taken from [193].

the average over the corresponding Gaussian copulas determined by the portfolio loss correlation. Surprisingly, the single parameter heterogeneity is sufficient to cause deviations from the Gaussian copula. The coloring shows deviations of the empirical copula from the Gaussian copula especially in the vicinity of the (0,0) and (1,1) corners. We come to the conclusion that a choice of one or more heterogeneous parameters, i.e., a large variety in different parameters for each portfolio, alters the dependence structure from an ideal Gaussian copula. The more heterogeneous the portfolios become, the larger the deviations from the symmetric Gaussian copula.

So far, there are two causes for non-Gaussian empirical copulas: the loss of information, induced by the projections of non-defaults onto zero, as well as parameter heterogeneity.

We now turn to empirical portfolios. Before starting the simulation, the empirical parameters have to be defined. The dataset consists of stock return data from 272 companies listed on the S&P 500 index and from 179 companies listed on the Nikkei 225 index. It is sampled in a 21-year interval, which covers the period January 1993–April 2014. To set up a realistic, fully-homogeneous portfolio, drifts, volatilities and correlations are calculated from this empirical dataset. Moreover, in [191], it was shown that annual returns behave normally for empirical asset values. To match these findings, the Gaussian dynamics for the stock price returns is applied. To obtain an average empirical portfolio loss copula, one first averages over different pairs of portfolios and then averages over randomly chosen annual time intervals taken out of the 21-year period. By averaging over different pairs of portfolios, results that are due to specific features of two particular portfolios are avoided. We consider three different cases, which are shown in figure 2.14. In the first case, which is shown in the top panel, one portfolio is drawn from

S&P 500 stocks and the other is drawn from Nikkei 225 stocks. In the second case (middle panel), both portfolios are drawn from S&P 500 stocks, and in the third case (bottom panel) both are drawn from Nikkei 225 stocks.

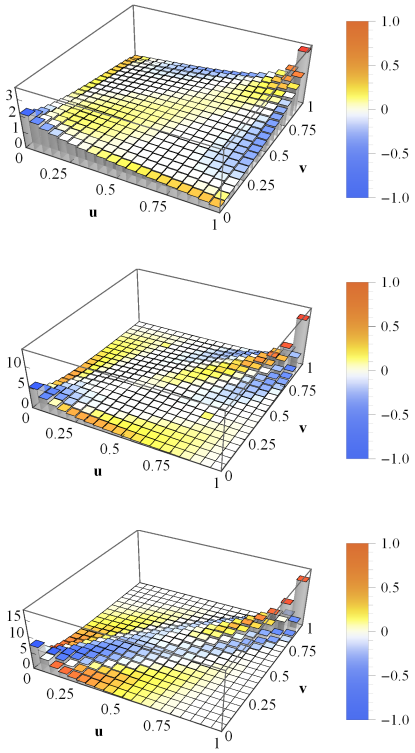

Figure 2.14.: Time averaged loss copula histograms for two empirical copulas of size $K = 50$. The asset values are multivariate log-normal ($N \to \infty$). **Top**: Portfolio 1 is always drawn from S&P 500 and Portfolio 2 from Nikkei 225; **middle**: both portfolios are drawn from S&P 500; **bottom**: both portfolios are drawn from Nikkei 225. The color bar indicates the local deviations from the corresponding Gaussian copula. Taken from [193].

In all three cases, we find deviations of the empirical copula from the Gaussian copula. Especially the dependence of the extreme events is much more pronounced than by the prediction of a Gaussian copula. This can be seen in the (1,1) corner, where the colors indicate that the tails are much more narrow and pointed compared to the Gaussian copula. On the other side, the tails in the (0,0) corner are flatter compared to a Gaussian copula. The asymmetry regarding the line spanned by (1,0) and (0,1) leads to the conclusion that extreme portfolio losses occur more

often simultaneously than in the case of small portfolio losses. Hence, an extreme loss of one portfolio is very likely to also yield an extreme loss of the other portfolio. This dependence is much stronger than predicted by a Gaussian copula. Thus, modeling portfolio loss dependencies by means of Gaussian copulas is deeply flawed and might cause severe underestimations of the actual credit risk.

Another important aspect of credit risk can be analyzed by considering different portfolio sizes. So far, only rather small portfolios of size $K = 50$ were chosen. Increasing the size of the portfolios leads to a rise in portfolio loss correlation. This behavior can be explained by the decrease of the idiosyncrasies of large portfolios. Moreover, it explains why the empirical loss copulas in figure 2.14 are almost perfectly symmetric regarding the line spanned by (0,0) and (1,1). Portfolios based on the S&P 500 dataset with a size of $K = 50$ and an average asset correlation of $c = 0.27$ each reveal an significant average loss correlation of $\mathrm{Corr}(L^{(1)},L^{(2)}) = 0.779$. Even if we decrease the size to $K = 14$ companies, an average portfolio loss correlation of $\mathrm{Corr}(L^{(1)},L^{(2)}) > 0.5$ is found. This reveals that high dependencies among banks are not only limited to "big players", which hold portfolios of several thousand contracts. Furthermore, small institutions show noticeable dependencies even though their portfolios are non-overlapping.

2.6. Conclusions

The motivation for the studies that we reviewed here was two-fold. First, the massive perturbations that shook the financial markets starting with the subprime crisis of 2007–2009 sharpened the understanding of how crucial the role of credits is for the stability of the economy as a whole in view of the strong interdependencies. Better credit risk estimation is urgently called for, particularly for rare, but drastic events, i.e., for the tails of the loss distributions. Particularly, the often claimed benefit of diversification has to be critically investigated. Second, the ubiquitous non-stationarity in financial markets has to be properly accounted for in the models. The financial crisis illustrates in a painful way that decisive economic quantities strongly fluctuate in time, ruling out elegant, but too simplistic equilibrium approaches, which fail to grasp the empirical situation.

This two-fold motivation prompted a random matrix approach to tackle and eventually solve the Merton model of credit risk for fully-correlated assets. A proper asset value distribution can be calculated by an ensemble average of random correlation matrices. The main ingredient is a new interpretation of the Wishart model for correlation or covariance matrices. While it was originally meant to describe generic statistical features resulting from stationary time series, i.e., eigenvalue densities and other quantities for large correlation matrices, the new interpretation grasps non-stationary correlation matrices by modeling a truly existing, measured

set of such correlation matrices with an ensemble of random correlation matrices. Contrary to the original interpretation of the Wishart model, ergodicity reasoning is not applied, and a restriction to large matrices is not needed, either.

According to the Merton model, stock price data instead of data on asset values can be used to calibrate the required parameters. This is quite valuable because empirical data on asset values are not easy to obtain, whereas stock price data are commonly available. Considering long time horizons, the sample statistics of returns can be described by a multivariate mixture of distributions. The resulting distribution is the average of multivariate normal distribution over an ensemble of Wishart-distributed covariance matrices. This random matrix approach takes the fluctuating asset correlations into account. As a very nice side effect, the random matrix approach reduces the number of parameters that describe the correlation structure of the financial market to two. Both of them can be considered as macroscopic. One parameter is a mean correlation coefficient of the asset values, and the other parameter describes the strength of the fluctuations around this average. Furthermore, the random matrix approach yields analytical tractability, which allows one to derive an analytical expression for the loss distribution of a portfolio of credit contracts, taking fluctuating asset correlations into account. In a quantitative manner, it is shown that in the presence of asset correlations, diversification fails to reduce the risk of large losses. This is substantial quantitative support and corroboration for qualitative reasoning in the economic literature. Furthermore, it is demonstrated that the random matrix approach can describe very different market situations. For example, in a crisis, the mean correlation coefficient is higher, and the parameter governing the strength of the fluctuations is smaller than in a quite period, with considerable impact on the loss distribution.

In addition, Monte Carlo simulations were run to calculate VaR and ETL. The results support the approximation of an effective average correlation matrix if heterogeneous average volatilities are taken into account. Moreover, the simulations show the benefit of the random matrix approach. If the fluctuations between the asset correlations are neglected, the VaR is underestimated by up to 40%. This underestimation could yield dramatic consequences. Therefore, the results strongly support a conservative approach to capital reserve requirements.

Light is shed on intrinsic instabilities of the financial sector. Sizable systemic risks are present in the financial system. These were revealed in the financial crisis of 2007–2009. Up to that point, tail-dependencies between credit contracts were underestimated, which emerged as a big problem in credit risk assessment. This is another motivation for models like ours that take asset fluctuations into account.

The dependence structure of credit portfolio losses was analyzed within the framework of the Merton model. Importantly, the two credit portfolios operate on the same correlated market, no matter if they belong to a single creditor

or bank or to different banks. The instruments to analyze the joint risk are correlations and copulas. Correlations break down the dependence structure into one parameter and represent only a rough approximation for the coupling of portfolio losses. In contrast, copulas reveal the full dependence structure. For two non-overlapping credit portfolios, we found concurrent large portfolio losses to be more likely than concurrent small ones. This observation is in contrast to a symmetric Gaussian behavior as described by correlation coefficients. Risk estimation by solely using standard correlation coefficients yields a clear underestimation of concurrent large portfolio losses. Hence, from a systemic viewpoint, it is really necessary to incorporate the full dependence structure of joint risks.

3. Extreme Portfolio Loss Correlations in Credit Risk

3.1. Introduction

We have seen the effects of non-stationary asset correlations on credit risk estimation in chapter 2. To describe the non-stationarity, we use a random matrix approach which results in a multivariate asset return distribution averaged over the fluctuating correlation matrices. This approach preserves, as a much appreciated side effect, analytical tractability and drastically reduces the number of parameters. In this chapter, we analytically study the mutual dependence of losses for different creditors in the case of overlapping credit portfolios. To obtain a comprehensive understanding of systemic credit risk, it is important to study and model the mutual dependence of losses of different portfolios. Here, we are interested in the multivariate joint probability loss distribution that contains all the information on the individual losses as well as their dependence structure.

We analytically calculate the multivariate joint loss distribution of several credit portfolios on a non-stationary market. To this end, we apply the Merton model to several credit portfolios simultaneously. Our study is a multivariate extension of the model presented in section 2.4. The fluctuating asset correlations are taken into account by means of the random matrix approach which is presented in section 2.3. We have seen that the effect of diversification is drastically limited for one portfolio. We now analyze the effect of diversification on two non-overlapping credit portfolios which operate on the same market. Particularly, we calculate the portfolio loss correlation depending on the size of the portfolios as well as on the average asset correlation in the market. In addition, we derive a limiting distribution for infinitely large credit portfolios. Our analytical results corroborate the results from section 2.5. We find that, for two disjoint credit portfolios, diversification does not work in a correlated market. We show that significant correlations of the losses emerge not only for large portfolios with thousands of credit contracts, but also for small portfolios only consisting of a few credit contracts. For an analytic study of large corporate bond and loan portfolios, see [217].

A general and simple method to reduce risk is provided by the proverb: “Don’t put all of your eggs in one basket”. Applied to finance, this means that risk can

be reduced by investing in different assets which exhibit small correlations or even anti-correlations instead of investing in high correlated assets [102, 218]. To quantify this effect, we consider a single credit portfolio that operates on several markets which are on average uncorrelated. We are able to derive a limiting distribution for an infinitely large credit portfolio. We compare its loss distribution with the loss distribution of a portfolio operating on a single market. The tail risk of a portfolio operating on two on average uncorrelated markets is lower than in the tail risk of a portfolio operating on just one market. Nevertheless, the effect of diversification by enlarging the size of the credit portfolio is limited.

Furthermore, we include subordination levels [148, 219, 220], which were established in CDOs to protect the more senior tranches from high losses. We analytically corroborate the observation that an extreme loss of the subordinated creditor is likely to also yield a large loss of the senior creditor.

This chapter is organized as follows: In section 3.2, we generalize the Merton model for a subordinated debt structure of two creditors and derive the corresponding multivariate portfolio loss distributions. Section 3.3 presents the generalized Merton model for a multivariate setting which lacks subordination. We calculate the joint portfolio loss distributions for several creditors. We extend the average asset return distribution for the case of several on average uncorrelated markets. In section 3.4, we present our results for empirical estimated parameters. We conclude our observations in section 3.5. The contents of this chapter are published in reference [2].

3.2. Merton Model Including Subordination

We extend the Merton model to a multivariate scenario with two creditors and K correlated obligors with asset values or economic states $V_k(t)$, $k = 1, \ldots, K$ at time t. Each obligor may hold a credit contract from each creditor. In the Merton model, the asset values $V_k(t)$ are estimated by the stock prices of the corresponding obligors. Thus, we assume that all K obligors are companies that can be traded on a stock market. Following the description in section 2.2, we claim that the asset values follow a geometric Brownian motion. Furthermore, we assume subordinated debt where at maturity time T_{M} the senior creditor is paid out first and the junior subordinated creditor is only paid out if the senior creditor regained the full promised payment. Hence, losses are first absorbed by the junior tranche and the subordinated debt structure protects the senior tranche.

Suppose each obligor has to pay back the face value F_k at maturity time T_{M}. We consider large time scales such as one year or one month. The face value of each obligor is composed of the face value of the senior creditor $F_k^{(S)}$ and the

face value of the junior subordinated creditor $F_k^{(J)}$, which is $F_k = F_k^{(S)} + F_k^{(J)}$. A default occurs if the asset value at maturity time T_M drops below the face value, i.e., $V_k(T_\mathrm{M}) < F_k$ for at least one obligor. The severity of the loss depends on the value of the obligors $V(T_\mathrm{M})$ at maturity. For $F_k > V_k(T_\mathrm{M}) > F_k^{(S)}$, the default is completely defrayed by the junior subordinated creditor meaning that the senior creditor does not incur any loss. The senior creditor will incur a loss only when the junior subordinated creditor will sustain a total loss, i.e., for $V_k(T_\mathrm{M}) < F_k^{(S)}$. A visualization of the underlying process for a single asset is shown in figure 2.1. The colored lines show two time-dependent asset values $V_k(t)$. In the blue case, the asset value of the company at maturity is above the face value and the promised payment can be made. In the red case, the asset value at maturity is below the total face value F_k but still above the face value of the senior creditor $F_k^{(S)}$, which results in a default of the junior creditor, while the senior creditor regains the full promised payment.

The normalized loss $L_k^{(S)}$ that a senior creditor and the normalized loss $L_k^{(J)}$ that a junior subordinated creditor is suffering can be expressed as

$$L_k^{(S)} = \left(1 - \frac{V_k(T_\mathrm{M})}{F_k^{(S)}}\right) \Theta\left(F_k^{(S)} - V_k(T_\mathrm{M})\right), \tag{3.1}$$

$$L_k^{(J)} = \left(1 - \frac{V_k(T_\mathrm{M}) - F_k^{(S)}}{F_k^{(J)}} \Theta\left(V_k(T_\mathrm{M}) - F_k^{(S)}\right)\right) \Theta\left(F_k - V_k(T_\mathrm{M})\right) . \tag{3.2}$$

The Heaviside step functions ensure that the losses are strictly positive. We introduce the fractional face values $f_k^{(S)}$ and $f_k^{(J)}$ for the senior and junior subordinated creditors

$$f_k^{(S)} = \frac{F_k^{(S)}}{\sum_{l=1}^K F_l^{(S)}} \qquad \text{and} \qquad f_k^{(J)} = \frac{F_k^{(J)}}{\sum_{l=1}^K F_l^{(J)}} , \tag{3.3}$$

respectively. This enables us to define the normalized portfolio losses $L^{(S)}$ and $L^{(J)}$ for the senior and junior subordinated creditors as weighted sums

$$L^{(S)} = \sum_{k=1}^K f_k^{(S)} L_k^{(S)} \qquad \text{and} \qquad L^{(J)} = \sum_{k=1}^K f_k^{(J)} L_k^{(J)} , \tag{3.4}$$

respectively. Our aim is to derive the bivariate distribution $p(L^{(S)},L^{(J)}|\Sigma)$ of the portfolio losses, which depends on the covariance matrix Σ. This can be done by integrating over all portfolio values and filtering those that lead to a given bivariate

total loss $(L^{(S)},L^{(J)})$

$$p(L^{(S)},L^{(J)}|\Sigma) = \int d[V]g(V|\Sigma)\,\delta\left(L^{(S)} - \sum_{k=1}^{K} f_k^{(S)} L_k^{(S)}\right)\delta\left(L^{(J)} - \sum_{k=1}^{K} f_k^{(J)} L_k^{(J)}\right), \tag{3.5}$$

where $g(V|\Sigma)$ is the multivariate distribution of the correlated asset values of the obligors at maturity and Σ is the covariance matrix of the asset values, which is in our model well estimated by that of the stock prices. Using the Fourier representation of the δ function [215] as well as equations (3.1) and (3.2), we find

$$\begin{aligned} p(L^{(S)},L^{(J)}|\Sigma) = \frac{1}{(2\pi)^2} \int_{-\infty}^{\infty} d\nu^{(S)} e^{-i\nu^{(S)}L^{(S)}} \int_{-\infty}^{\infty} d\nu^{(J)} e^{-i\nu^{(J)}L^{(J)}} \\ \times \prod_{k=1}^{K} \left[\int_{0}^{F_k^{(S)}} dV_k \exp\left(i\nu^{(S)} f_k^{(S)} \left(1 - \frac{V_k}{F_k^{(S)}}\right) + i\nu^{(J)} f_k^{(J)} \right) \right. \\ \left. + \int_{F_k^{(S)}}^{F_k} dV_k \exp\left(i\nu^{(J)} f_k^{(J)} \left(1 - \frac{V_k - F_k^{(S)}}{F_k^{(J)}}\right)\right) + \int_{F_k}^{\infty} dV_k \right] g(V|\Sigma)\,, \end{aligned} \tag{3.6}$$

where we split the V_k integrals in three parts. This representation will become handy later on, especially when determining the non-analytic parts of the loss distribution.

Our goal is to calculate average joint portfolio loss distributions. In order to make analytical progress and to take fluctuating asset correlations into account, we use the random matrix approach combined with the assumption of an effective average correlation matrix which is discussed in section 2.3. According to equation (3.6), the average joint portfolio loss distribution can be expressed as

$$\begin{aligned} \langle p\rangle(L^{(S)},L^{(J)}|c,N) = \int d[V]\langle g\rangle(V|c,N)\,\delta\left(L^{(S)} - \sum_{k=1}^{K} f_k^{(S)} L_k^{(S)}\right) \\ \times \delta\left(L^{(J)} - \sum_{k=1}^{K} f_k^{(J)} L_k^{(J)}\right)\,, \end{aligned} \tag{3.7}$$

where the average asset value distribution including an effective average correlation matrix is (2.27).

3.2.1. Average Loss Distribution

We work out the average loss distribution (3.7) using the results for the average distribution $\langle g \rangle (V|c,N)$ from section 2.4. After inserting equation (2.27) into equation (3.6), we obtain

$$\begin{aligned}\langle p \rangle \left(L^{(S)},L^{(J)}|c,N\right) = &\frac{1}{(2\pi)^2 2^{N/2}\Gamma(N/2)} \int_0^\infty dz z^{N/2-1} e^{-z/2} \sqrt{\frac{N}{2\pi z}} \int_{-\infty}^{\infty} du \exp\left(-\frac{N}{2z}u^2\right) \\ &\times \int_{-\infty}^{\infty} d\nu^{(S)} e^{-i\nu^{(S)}L^{(S)}} \int_{-\infty}^{\infty} d\nu^{(J)} e^{-i\nu^{(J)}L^{(J)}} \mathcal{I}\left(\nu^{(S)},\nu^{(J)},z,u\right),\end{aligned} \tag{3.8}$$

with the term

$$\mathcal{I}\left(\nu^{(S)},\nu^{(J)},z,u\right) = \prod_{k=1}^{K} \left\{1 + \sum_{j=1}^{\infty} \frac{i^j}{j!} m_{j,k}^{(SD)}\left(\nu^{(S)},\nu^{(J)},z,u\right) + \sum_{j=1}^{\infty} \frac{\left(i\nu^{(J)} f_k^{(J)}\right)^j}{j!} m_{j,k}^{(J)}(z,u)\right\} \tag{3.9}$$

and

$$m_{a,k}^{(SD)}\left(\nu^{(S)},\nu^{(J)},z,u\right) = \sum_{j=0}^{a} \binom{a}{j} \left(\nu^{(S)} f_k^{(S)}\right)^j \left(\nu^{(J)} f_k^{(J)}\right)^{a-j} m_{j,k}^{(S)}(z,u) \tag{3.10}$$

and the moments

$$\begin{aligned}m_{j,k}^{(S)}(z,u) = &\int_{-\infty}^{\hat{F}_k^{(S)}} d\hat{V}_k \left(1 - \frac{V_{k0}}{F_k^{(S)}} \exp\left(\sqrt{z}\hat{V}_k + \left(\mu_k - \frac{\rho_k^2}{2}\right)T_{\mathrm{M}}\right)\right)^j \\ &\times \sqrt{\frac{N}{2\pi(1-c)T_{\mathrm{M}}\rho_k^2}} \exp\left[\frac{N}{2(1-c)T_{\mathrm{M}}\rho_k^2}\left(\hat{V}_k + \sqrt{cT_{\mathrm{M}}}u\rho_k\right)^2\right]\end{aligned} \tag{3.11}$$

$$\begin{aligned}m_{j,k}^{(J)}(z,u) = &\int_{\hat{F}_k^{(S)}}^{\hat{F}_k} d\hat{V}_k \left(1 + \frac{F_k^{(S)}}{F_k^{(J)}} - \frac{V_{k0}}{F_k^{(J)}} \exp\left(\sqrt{z}\hat{V}_k + \left(\mu_k - \frac{\rho_k^2}{2}\right)T_{\mathrm{M}}\right)\right)^j \\ &\times \sqrt{\frac{N}{2\pi(1-c)T_{\mathrm{M}}\rho_k^2}} \exp\left[\frac{N}{2(1-c)T_{\mathrm{M}}\rho_k^2}\left(\hat{V}_k + \sqrt{cT_{\mathrm{M}}}u\rho_k\right)^2\right],\end{aligned} \tag{3.12}$$

where we use the change of variables $\hat{V}_k = (\ln V_k/V_{k0} - (\mu_k - \rho_k^2/2)T)/\sqrt{z}$ with proper adjustment of the integration bounds $\hat{F}_k$ and $\hat{F}_k^{(S)}$. The moments $m_{j,k}^{(S)}(z,u)$

and $m_{j,k}^{(J)}(z,u)$ are given in appendix A for $j = 0,1,2$. The term $m_{j,k}^{(SD)}\left(\nu^{(S)},\nu^{(J)},z,u\right)$ formally corresponds to those events that lead to a loss large enough that the senior creditor is affected. We use a binomial sum for the decoupling of the $\nu^{(S)}$ and $\nu^{(J)}$ integrals later on.

Now, we assume large portfolios where all face values are of the same order, to carry out an approximation to the second order in $f_k^{(S)}$ and $f_k^{(J)}$ by performing steps generalizing the one in [134]. This is justified when we consider all face values are of the same order, so all fractional face values are of order $1/K$. We finally arrive at

$$\begin{aligned}\langle p\rangle\left(L^{(S)},L^{(J)}|c,N\right) = \frac{1}{2^{N/2}\Gamma(N/2)}\int_0^\infty dz z^{N/2-1}e^{-z/2}\sqrt{\frac{N}{2\pi}}\int_{-\infty}^{\infty} du\exp\left(-\frac{N}{2}u^2\right)\\ \times\frac{1}{\sqrt{2\pi M_2^{(S)}(z,u)}}\exp\left(-\frac{\left(L^{(S)}-M_1^{(S)}(z,u)\right)^2}{2M_2^{(S)}(z,u)}\right)\\ \times\frac{1}{\sqrt{2\pi M_2(z,u)}}\exp\left(-\frac{\left(L^{(J)}-M_1(L^{(S)},z,u)\right)^2}{2M_2(z,u)}\right)\end{aligned} \tag{3.13}$$

for the average distribution with

$$M_1(L^{(S)},z,u) = M_1^{(J)}(z,u) + \sum_{k=1}^K f_k^{(J)}f_k^{(S)}N_k^{(S)}(z,u)\frac{L^{(S)}-M_1^{(S)}(z,u)}{M_2^{(S)}(z,u)}, \tag{3.14}$$

$$M_2(z,u) = M_2^{(J)}(z,u) - \frac{1}{M_2^{(S)}(z,u)}\left(\sum_{k=1}^K f_k^{(J)}f_k^{(S)}N_k^{(S)}(z,u)\right)^2, \tag{3.15}$$

$$M_1^{(S)}(z,u) = \sum_{k=1}^K f_k^{(S)}m_{1,k}^{(S)}, \tag{3.16}$$

$$M_2^{(S)}(z,u) = \sum_{k=1}^K {f_k^{(S)}}^2\left(m_{2,k}^{(S)} - {m_{1,k}^{(S)}}^2\right), \tag{3.17}$$

$$M_1^{(J)}(z,u) = \sum_{k=1}^K f_k^{(J)}\left(m_{0,k}^{(S)} + m_{1,k}^{(J)}\right), \tag{3.18}$$

$$M_2^{(J)}(z,u) = \sum_{k=1}^K {f_k^{(J)}}^2\left(m_{0,k}^{(S)} + m_{2,k}^{(J)} - {m_{0,k}^{(S)}}^2 - {m_{1,k}^{(J)}}^2 - 2m_{0,k}^{(S)}m_{1,k}^{(J)}\right), \tag{3.19}$$

$$N_k^{(S)}(z,u) = m_{1,k}^{(S)}\left(1 - m_{0,k}^{(S)} - m_{1,k}^{(J)}\right)\ . \tag{3.20}$$

Thus, we expressed the average loss distribution as double average of Gaussians with mean values $M_1(L^{(S)},z,u)$ and $M_1^{(S)}(z,u)$ and variances $M_2(z,u)$ and $M_2^{(S)}(z,u)$ that non-trivially depend on the integration variables. To keep the notation transparent, we dropped the arguments of the functions $m_{j,k}^{(S)}(z,u)$ and $m_{j,k}^{(J)}(z,u)$. Due to the complexity of the last two expressions in equation (3.13), the z and u integrals have to be evaluated numerically. We notice that the normalization of the average distribution is, for $L_k^{(S)},L_k^{(J)} \in [0,1]$, only valid up to the order of our approximation. Later on, we will concentrate on the contributions of no default.

3.2.2. Homogeneous Portfolio

Apart from the large K approximation, all results above are valid in general and apply to all portfolios for which the individual fractional face values are of order $1/K$. To further evaluate our results and to obtain a visualization, it is instructive to consider homogeneous portfolios, in which the senior and junior face values are equal

$$F_k^{(S)} = F_0^{(S)} \qquad \text{and} \qquad F_k^{(J)} = F_0^{(J)}, \tag{3.21}$$

such that

$$f_k^{(S)} = f_k^{(J)} = \frac{1}{K} \, . \tag{3.22}$$

Furthermore, we assume that the stochastic processes have the same initial values, drifts and volatilities,

$$V_{k0} = V_0 \, , \qquad \mu_k = \mu_0 \, , \qquad \rho_k = \rho_0 \, . \tag{3.23}$$

Of course, this does not mean that the realized stochastic processes are the same. By dropping the dependence of k, the moments $m_{a,k}^{(S)}(z,u) = m_{a,0}^{(S)}(z,u)$ and $m_{j,k}^{(J)}(z,u) = m_{j,0}^{(J)}(z,u)$ and thus the average distribution $\langle p \rangle \, (L^{(S)},L^{(J)}|c,N)$ can be computed much faster.

3.2.3. Non-Analytic Parts of the Loss Distribution

Only the full dynamics of our model without any approximations gives us information on the contribution of the non-analytic part of the average loss distribution. In particular, absence of losses is reflected in non-analytic δ functions at zero. To examine this, we start from the averaged version of equation (3.6) by inserting the distribution of asset values for a homogeneous portfolio with an effective average

correlation matrix

$$\begin{aligned}\langle g\rangle_{\mathrm{h}}(V|c,N) &= \frac{1}{2^{N/2}\Gamma(N/2)}\int_0^\infty dz z^{N/2-1}e^{-z/2}\sqrt{\frac{N}{2\pi z}}\int_{-\infty}^{\infty}du\exp\left(-\frac{N}{2z}u^2\right)\\ &\quad\times\left(\sqrt{\frac{N}{2\pi z(1-c)T_{\mathrm{M}}}}\frac{1}{V\rho_0}\right)^K\\ &\quad\times\exp\left[-\frac{KN}{2z(1-c)T_{\mathrm{M}}\rho_0^2}\left(\ln\frac{V}{V_0}-\left(\mu_0-\frac{\rho_0^2}{2}\right)T_{\mathrm{M}}+\sqrt{cT_{\mathrm{M}}}u\rho_0\right)^2\right]\\ &= \int_0^\infty dz\int_{-\infty}^{\infty}du f(z,u)\tilde{\omega}^K(V,z,u),\end{aligned} \tag{3.24}$$

with

$$f(z,u) = \frac{1}{2^{N/2}\Gamma(N/2)}z^{N/2-1}e^{-z/2}\sqrt{\frac{N}{2\pi z}}\exp\left(-\frac{N}{2z}u^2\right) \tag{3.25}$$

and

$$\begin{aligned}\tilde{\omega}(V,z,u) &= \sqrt{\frac{N}{2\pi z(1-c)T_{\mathrm{M}}}}\frac{1}{V\rho_0}\\ &\quad\times\exp\left[-\frac{N}{2z(1-c)T_{\mathrm{M}}\rho_0^2}\left(\ln\frac{V}{V_0}-\left(\mu_0-\frac{\rho_0^2}{2}\right)T_{\mathrm{M}}+\sqrt{cT_{\mathrm{M}}}u\rho_0\right)^2\right].\end{aligned} \tag{3.26}$$

Due to the homogeneity, the product in equation (3.6) also becomes a K-th power, to which we apply the multinomial theorem. We thus arrive at

$$\begin{aligned}\langle p\rangle\,(L^{(S)},L^{(J)}|c,N) = &\int_0^\infty dz \int_{-\infty}^{\infty} du f(z,u) \frac{1}{(2\pi)^2} \int_{-\infty}^{\infty} d\nu^{(S)} e^{-i\nu^{(S)}L^{(S)}} \int_{-\infty}^{\infty} d\nu^{(J)} e^{-i\nu^{(J)}L^{(J)}} \\ &\times \sum_{k_1+k_2+k_3=K} \binom{K}{k_1,k_2,k_3} \\ &\times \left(e^{i\nu^{(J)}/K} \int_0^{F_0^{(S)}} dV \exp\left(\frac{i\nu^{(S)}}{K}\left(1-\frac{V}{F_0^{(S)}}\right)\right)\tilde{\omega}(V,z,u)\right)^{k_1} \\ &\times \left(\int_{F_0^{(S)}}^{F_0} dV \exp\left(\frac{i\nu^{(J)}}{K}\left(1-\frac{V-F_0^{(S)}}{F_0^{(J)}}\right)\right)\tilde{\omega}(V,z,u)\right)^{k_2} \\ &\times \left(\int_{F_0}^{\infty} dV \tilde{\omega}(V,z,u)\right)^{k_3}\end{aligned} \tag{3.27}$$

with the multinomial coefficient

$$\binom{K}{k_1,k_2,k_3} = \frac{K!}{k_1!k_2!k_3!}\,. \tag{3.28}$$

From equation (3.27), we see that δ functions only appear under the condition $k_1 \cdot k_2 = 0$. For $k_1 = k_2 = 0$, we have no default at all. The only contribution to the distribution stems from the last integral in equation (3.27), leading to a δ peak $\delta(L_k^{(S)})\delta(L_k^{(J)})$ at the origin. This δ peak is associated with the absence of default neither on the junior nor on the senior level. The probability therefore is

$$\begin{aligned}P^{(\mathrm{ND})} = &\frac{1}{2^{N/2}\Gamma(N/2)} \int_0^\infty dz z^{N/2-1} e^{-z/2} \sqrt{\frac{N}{2\pi z}} \int_{-\infty}^{\infty} du \exp\left(-\frac{N}{2z}u^2\right) \\ &\times \left(\frac{1}{2} - \frac{1}{2}\,\mathrm{erf}\left[\sqrt{\frac{N}{2z(1-c)T_\mathrm{M}\rho_0^2}}\left(\ln\frac{F_0}{V_0} - \left(\mu_0 - \frac{\rho_0^2}{2}\right)T_\mathrm{M} + \sqrt{cT_\mathrm{M}}u\rho_0\right)\right]\right)^K,\end{aligned} \tag{3.29}$$

which obviously decreases with increasing K.

For $k_1 = 0, k_2 \neq 0$, we find the contribution of the events that lead to a total default of the junior subordinated creditor but not to a default of the senior creditor.

In this case, we have a single δ function $\delta(L_k^{(S)})$ that represents a moderate loss such that the senior subordinated creditor will not sustain a loss. The special case $k_1 \neq 0, k_2 = 0$ leads to a sum of δ functions $\delta(L_k^{(J)} - k_1/K)$ where k_1 runs from 1 to K. This is due to the sum in equation (3.27). These δ functions belong to the events where there is either no default at all or k_1 severe defaults such that, for $k_1 = 1,\ldots,K$ obligors, the junior subordinated creditor has a complete failure, i.e., $L_k^{(J)} = 1$ and the senior subordinated creditor may sustain a loss i.e., $L_k^{(S)} \geq 0$. All of these δ functions are not unmated. They are weighted with some integral prefactors to preserve the normalization of the distribution $\langle p \rangle (L^{(S)},L^{(J)}|c,N)$. Furthermore, the δ functions disappear when we only consider the loss given default, which in our model means $L^{(J)} > 0$ and also $L^{(S)} > 0$. The non-analytic parts cannot be obtained in the second order approximation we used to derive the average loss distribution (3.13).

3.2.4. Infinitely Large Portfolios

We now consider the case $K \to \infty$ for the homogeneous portfolio to analyze whether diversification works or not in the discussed multivariate scenarios. It has been shown that diversification does not work in a correlated univariate model with only one creditor, see [134].

The homogeneous versions of equations (3.15) and (3.17)

$$M_2(z,u) = \frac{1}{K}\left(m_{0,0}^{(S)} + m_{2,0}^{(J)} - {m_{0,0}^{(S)}}^2 - {m_{1,0}^{(J)}}^2 - 2m_{0,0}^{(S)} m_{1,0}^{(J)} - \frac{{m_{1,0}^{(S)}}^2 \left(1 - m_{0,0}^{(S)} - m_{1,0}^{(J)}\right)^2}{m_{2,0}^{(S)} - {m_{1,0}^{(S)}}^2} \right), \tag{3.30}$$

$$M_2^{(S)}(z,u) = \frac{1}{K}\left(m_{2,0}^{(S)} - {m_{1,0}^{(S)}}^2 \right), \tag{3.31}$$

imply that $M_2(z,u) \to 0$ as well as $M_2^{(S)}(z,u) \to 0$ for $K \to \infty$. This means that both Gaussians

$$\frac{1}{\sqrt{2\pi M_2^{(S)}(z,u)}} \exp\left(-\frac{\left(L^{(S)} - M_1^{(S)}(z,u)\right)^2}{M_2^{(S)}(z,u)} \right) \qquad \text{and}$$

$$\frac{1}{\sqrt{2\pi M_2(z,u)}} \exp\left(-\frac{\left(L^{(J)} - M_1(L^{(S)},z,u)\right)^2}{M_2(z,u)} \right)$$

in equation (3.13) become δ functions for $K \to \infty$. Thus, we arrive at

$$\begin{aligned}\langle p \rangle \left(L^{(S)},L^{(J)}|c,N\right)\Big|_{K\to\infty} &= \frac{1}{2^{N/2}\Gamma(N/2)} \int_0^\infty dz z^{N/2-1} e^{-z/2} \sqrt{\frac{N}{2\pi}} \int_{-\infty}^\infty du \exp\left(-\frac{N}{2}u^2\right) \\ &\quad \times \delta\left(L^{(S)} - M_1^{(S)}(z,u)\right) \delta\left(L^{(J)} - M_1(L^{(S)},z,u)\right) \\ &= \frac{1}{2^{N/2}\Gamma(N/2)} \int_0^\infty dz z^{N/2-1} e^{-z/2} \sqrt{\frac{N}{2\pi}} \int_{-\infty}^\infty du \exp\left(-\frac{N}{2}u^2\right) \\ &\quad \times \delta\left(L^{(S)} - m_{1,0}^{(S)}\right) \delta\left(L^{(J)} - m_{0,0}^{(S)} - m_{1,0}^{(J)}\right) \ .\end{aligned} \tag{3.32}$$

To make this equation numerically manageable, we use the identity

$$\delta\left(f(u)\right) = \sum_i \frac{\delta(u-u_i)}{|f'(u_i)|} \ , \tag{3.33}$$

where u_i are the roots of the function $f(u)$, with $f'(u_i) \neq 0$. This result is a direct consequence of the elementary theory of distributions [215]. Using this identity three times allows us to solve the remaining two integrals and we finally obtain the limiting loss distribution

$$\begin{aligned}\langle p \rangle \left(L^{(S)},L^{(J)}|c,N\right)\Big|_{K\to\infty} &= \frac{1}{2^{N/2}\Gamma(N/2)} \sqrt{\frac{N}{2\pi}} z_0^{N/2-1} \exp\left(-\frac{z_0}{2}\right) \\ &\quad \times \exp\left(-\frac{N}{2}{u^{(S)}}^2(L^{(S)},z_0)\right) \left|\frac{\partial}{\partial u}\, m_{1,0}^{(S)}(z_0,u)\Big|_{u=u^{(S)}(L^{(S)},z_0)}\right|^{-1} \\ &\quad \times \left|\frac{\partial}{\partial u}\left[m_{0,0}^{(S)}(z_0,u) + m_{1,0}^{(J)}(z_0,u)\right]_{u=u^{(S)}(L^{(S)},z_0)}\right|^{-1} \\ &\quad \times \left|\frac{\partial}{\partial z}\left[u^{(S)}(L^{(S)},z) - u^{(J)}(L^{(J)},z)\right]_{z=z_0}\right|^{-1} \ .\end{aligned} \tag{3.34}$$

Here, the implicit functions

$$u^{(S)} = u^{(S)}(L^{(S)},z) \quad \text{with} \quad 0 = L^{(S)} - m_{1,0}^{(S)}(z,u^{(S)}), \tag{3.35}$$

$$u^{(J)} = u^{(J)}(L^{(J)},z) \quad \text{with} \quad 0 = L^{(J)} - m_{0,0}^{(S)}(z,u^{(J)}) - m_{1,0}^{(J)}(z,u^{(J)}), \tag{3.36}$$

$$z_0 = z_0(L^{(S)},L^{(J)}) \quad \text{with} \quad u^{(S)}(L^{(S)},z_0) = u^{(J)}(L^{(J)},z_0) \ , \tag{3.37}$$

are unique and have to be calculated numerically. The dependence on $L^{(S)}$ and $L^{(J)}$ is now implicit in the functions $u^{(S)}$,$u^{(J)}$ and z_0. The very last derivatives in equation (3.34) can be done by using the implicit function theorem. They can

be traced back to derivatives of $m_{0,0}^{(S)}, m_{1,0}^{(S)}$ and $m_{1,0}^{(J)}$. The functions $m_{1,0}^{(S)}$ and $m_{0,0}^{(S)} + m_{1,0}^{(J)}$ are strictly monotonically increasing in u and z for fixed z and u, respectively. Thus, we can solve equations (3.35) and (3.36) locally to u, where we obtain $u^{(S)}$ and $u^{(J)}$. These equations can be derived by z using

$$\frac{\partial u^{(S)}}{\partial z}(L^{(S)},z_0) = - \left. \frac{\frac{\partial}{\partial z} m_{1,0}^{(S)}(z,u)}{\frac{\partial}{\partial u} m_{1,0}^{(S)}(z,u)} \right|_{u=u^{(S)}(L^{(S)},z_0)} \tag{3.38}$$

and

$$\frac{\partial u^{(J)}}{\partial z}(L^{(J)},z_0) = - \left. \frac{\frac{\partial}{\partial z} \left(m_{0,0}^{(S)}(z,u) + m_{1,0}^{(J)}(z,u) \right)}{\frac{\partial}{\partial u} \left(m_{0,0}^{(S)}(z,u) + m_{1,0}^{(J)}(z,u) \right)} \right|_{u=u^{(J)}(L^{(J)},z_0)} . \tag{3.39}$$

3.3. Absence of Subordination

Now, we consider the same model as discussed before, but without taking subordination into account. This means that a loss is evenly distributed among the creditors. This model is closely related to the simulation study [193] which we reviewed in section 2.5. We have $B \geq 2$ creditors with the face value $F_k^{(b)}$ of obligor k within creditor b, ($b = 1, \ldots, B$; $k = 1, \ldots, K$). The normalized loss of obligor k is

$$L_k^{(b)} = \begin{cases} \left(1 - \dfrac{V_k(T_{\mathrm{M}})}{F_k}\right) \Theta\left(F_k - V_k(T_{\mathrm{M}})\right) & \text{if } F_k^{(b)} > 0, \\ 0 & \text{else .} \end{cases} \tag{3.40}$$

The total face value of obligor k is the sum

$$F_k = \sum_{b=1}^{B} F_k^{(b)} . \tag{3.41}$$

In equation (3.40) for $F_k^{(b)} > 0$, the losses do not have any dependence on the obligors. In case of default, the creditors are not distinguished and suffer the same normalized loss. Hence, we set $L_k = L_k^{(b)}$. Again, we define the normalized portfolio

losses $L^{(b)}$ and the fractional face values $f_k^{(b)}$,

$$L^{(b)} = \sum_{k=1}^{K} f_k^{(b)} L_k \qquad \text{and} \qquad f_k^{(b)} = \frac{F_k^{(b)}}{\sum\limits_{k=1}^{K} F_k^{(b)}}\,, \tag{3.42}$$

corresponding to creditor b. The multivariate distribution of the total average loss is

$$\langle p \rangle \left(L|\Sigma_0,N\right) = \int d[V] \, \langle g \rangle \left(V|\Sigma_0,N\right) \delta\!\left(L - \sum_{k=1}^{K} f_k L_k\right), \tag{3.43}$$

with $L = (L^{(1)},\ldots,L^{(B)})^\dagger$ and $f_k = (f_k^{(1)},\ldots,f_k^{(B)})^\dagger$. We have already seen the bivariate case of this multivariate distribution in equation (2.39). We emphasize that, although written in the same form as the univariate distribution (2.23), the distribution (3.43) is multivariate. Adjusting our calculations from the subordinated case above and also applying a second order approximation for $f_k^{(b)}$, we arrive at the final result

$$\begin{aligned}\langle p \rangle \left(L|c,N\right) = {} & \frac{1}{2^{N/2}\Gamma(N/2)} \int_0^\infty dz z^{N/2-1} e^{-z/2} \sqrt{\frac{N}{2\pi}} \int_{-\infty}^{\infty} du \exp\left(-\frac{N}{2}u^2\right) \\ & \times \frac{1}{\sqrt{\det\left(2\pi M_2(z,u)\right)}} \exp\!\left(-\frac{1}{2}\left(L - M_1(z,u)\right)^\dagger M_2^{-1}(z,u)\left(L - M_1(z,u)\right)\right),\end{aligned} \tag{3.44}$$

where

$$M_1(z,u) = \sum_{k=1}^{K} f_k m_{1,k}(z,u), \tag{3.45}$$

and

$$M_2(z,u) = \sum_{k=1}^{K} D_k \left(m_{2,k}(z,u) - m_{1,k}^2(z,u)\right), \tag{3.46}$$

with the dyadic matrices

$$D_k = f_k f_k^\dagger \tag{3.47}$$

and with the moments $m_{j,k}(z,u)$ from (2.31). These have the same form as the moments in equation (3.11). This is not surprising because the scenario here refers to a subordinated debt structure with no junior subordinated creditor, i.e., where the face value of the junior subordinated creditor is zero. For the evaluation of the model in absence of subordination, we only consider heterogeneous portfolios

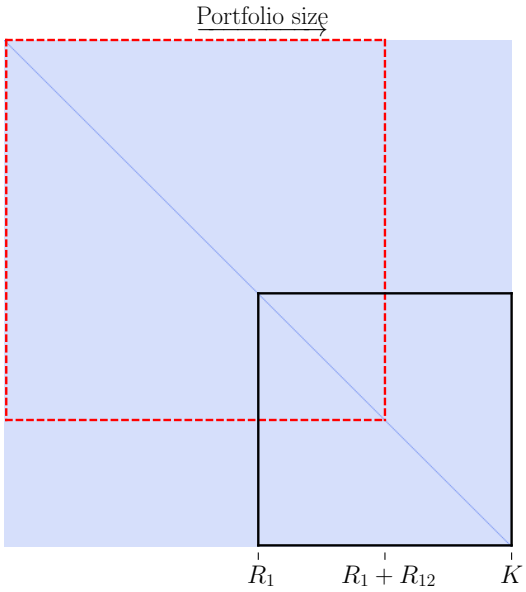

Figure 3.1.: Setup of the generalized model illustrating a financial market by means of its average effective correlation matrix. The two rimmed squares correspond to two partially overlapping portfolios.

for the whole market as homogeneous portfolios would lead to singular matrices D_k. Therefore, the losses would be exactly the same for all creditors and we could stick with the univariate case. It is suggestive to consider cases where the volume of credit differs among the creditors or to consider cases where the portfolios are non-overlapping or may only partially overlap.

Although our results are general, we now only consider $B = 2$ creditors to feasibly render a visualization. We denote them as creditor one and creditor two. Moreover, we address the most general set-up where two credit portfolios may partially overlap, see figure 3.1. Again, we consider K obligors in total. Let R_1 be the number of obligors with only one credit contract, say from creditor one. Let R_{12} be the number of creditors that raise credits from both creditors. These creditors correspond to the overlapping area in figure 3.1. The proportions correspond to the fractions $r_1 = R_1/K$ and $r_{12} = R_{12}/K$. Creditor one deals with $R_1 + R_{12}$ credits and creditor two deals with $K - R_1$ credits. This model, for example, also includes two disjoint portfolios, we just have to set $r_{12} = 0$. The face value of the R_{12} obligors consist of the sum of two face values $F_k = F_k^{(1)} + F_k^{(2)}$ that do not necessarily have the same size. For convenience, we consider homogeneous portfolios $F_k = F_0$ and we assume that the face values in the overlapping part of

the portfolios are equal within a portfolio but can differ across the portfolios. That means we introduce a parameter $\gamma \in [0,1]$ with $F_k^{(1)} = \gamma F_0$ and $F_k^{(2)} = (1-\gamma)F_0$.

For a market with homogeneous parameters, we find the result (3.44) with

$$M_1(z,u) = m_{1,0}(z,u) \begin{bmatrix} 1 \\ 1 \end{bmatrix}, \tag{3.48}$$

$$M_2(z,u) = \left(m_{2,0}(z,u) - m_{1,0}^2(z,u)\right) \frac{1}{K} \begin{bmatrix} \alpha_1 & \alpha_{12} \\ \alpha_{12} & \alpha_2 \end{bmatrix}, \tag{3.49}$$

where

$$\alpha_1 = \frac{r_1 + \gamma^2 r_{12}}{(r_1 + \gamma r_{12})^2}, \tag{3.50}$$

$$\alpha_{12} = \frac{\gamma(1-\gamma) r_{12}}{(r_1 + \gamma r_{12})(1 - r_1 - \gamma r_{12})}, \tag{3.51}$$

$$\alpha_2 = \frac{1 - r_1 - \gamma(2-\gamma) r_{12}}{(1 - r_1 - \gamma r_{12})^2} \ . \tag{3.52}$$

We notice $\alpha_{12} = 0$ for $\gamma = 0$ or $\gamma = 1$, i.e., for two disjoint portfolios.

3.3.1. Absence of Subordination and Infinitely Large Portfolios

In order to study the effect of diversification in the multivariate scenario, we now consider two infinitely large portfolios by taking the limit $K \to \infty$. We point out that r_1 and r_{12} do not scale with K in the case of two infinitely large portfolios. We will consider the case of one infinitely large portfolio and one portfolio of finite size later on. Now, the matrix $M_2(z,u)$ converges to a zero matrix. This implies that the exponential term and its prefactor converge to δ functions and we find the final result

$$\begin{aligned} \langle p \rangle \left(L^{(1)}, L^{(2)} | c, N\right)\Big|_{K\to\infty} = \frac{1}{2^{N/2}\Gamma(N/2)} \int_0^\infty dz z^{N/2-1} e^{-z/2} \sqrt{\frac{N}{2\pi}} \int_{-\infty}^\infty du \exp\left(-\frac{N}{2}u^2\right) \\ \times \delta\left(L^{(1)} - m_{1,0}(z,u)\right) \delta\left(L^{(2)} - L^{(1)}\right) \ . \end{aligned} \tag{3.53}$$

This result is quite remarkable. We point out first that there is no dependence on the structure of the portfolios anymore as the distribution (3.53) is independent of the parameters α_1,α_{12} and α_2. Second, the distribution (3.53) is practically identical to the univariate loss distribution of one creditor (2.33). Third, in the limiting case, the losses of both portfolios will always be equal to each other so

that they are perfectly correlated. In other words, the loss of one large creditor can be used as a forecast for the loss of another large creditor on the same market. This holds even if the creditors have disjoint portfolios and it also does not depend on the strength of the correlations across the asset values.

A different situation appears when we consider a portfolio of finite size and another infinitely large one. Due to the high asymmetry of the market shares of the portfolios, we solely examine two disjoint portfolios. Say, portfolio one is the finite one with R_1 companies. Then, the matrix element α_1 in equation (3.49) scales with K and α_2 converges to one. By calculating the limit $K \to \infty$, only one δ function emerges, and, by using property (3.33) of the δ function, we find

$$\begin{aligned}\langle p \rangle \left(L^{(1)},L^{(2)}|c,N\right)\Big|_{K\to\infty} &= \frac{1}{2^{N/2}\Gamma(N/2)} \int_0^\infty dz z^{N/2-1} e^{-z/2} \sqrt{\frac{N}{2\pi}} \exp\left(-\frac{N}{2}u_0^2\right) \\ &\times \sqrt{\frac{R_1}{2\pi(m_{2,0}(z,u_0) - m_{1,0}^2(z,u_0))}} \\ &\times \exp\left(-\frac{R_1(L^{(1)} - m_{1,0}(z,u_0))^2}{2(m_{2,0}(z,u_0) - m_{1,0}^2(z,u_0))}\right) \\ &\times \frac{1}{|\partial m_{1,0}(z,u)/\partial u|_{z,u_0}} ,\end{aligned} \tag{3.54}$$

where $u_0(L^{(2)},z)$ is an implicit function defined by

$$0 = L^{(2)} - m_{1,0}(z,u_0) . \tag{3.55}$$

We note that the dependence on $L^{(2)}$ in the limit distribution is encoded in $u_0(L^{(2)},z)$. Moreover, the above result is in line with the second order approximation even though one of the matrix elements does not scale with K.

3.3.2. Several on Average Uncorrelated Markets

So far, we have considered several credit portfolios which may or may not underlie subordination on just one market. We have seen that the effect of diversification is limited for one credit portfolio on one market. Now, we analyze one or several credit portfolios which operate on two or more markets which are, on average, uncorrelated. First, we have to derive the average asset value distribution.

This is an extension of unpublished work [221]. We define the number of uncorrelated markets to be β. In this case, the correlation matrix $C = \mathrm{diag}(C_1,\ldots,C_\beta)$ is block diagonal where $C_l = (1-c_l)\mathbb{1}_{K_l} + c_l e_{K_l} e_{K_l}^\dagger$ are matrices themselves with dimensions $K_l \times K_l$ for $l \in \{1,\ldots,\beta\}$. The correlation matrix C has dimension

$K \times K$ and therefore $\sum_{l=1}^{\beta} K_l = K$ holds. This block structure is not reflected in the random correlation matrices fluctuating about C, see equation (2.22). Hence, there are correlations between the blocks, only their average is zero. The correlation structure allows us to study the impact when going from one market to several markets. Within one market, we assume an effective correlation structure and, across the markets, we have an average correlation of zero. Importantly, this only means the absence of correlations on average. The correlations in our model and in reality fluctuate, implying that in any short instant of time, correlations can be present whose strength is governed by the parameter N. Furthermore, each market has its own standard deviation matrix $\sigma_l = \mathrm{diag}(\sigma_{l1},\ldots,\sigma_{lK_l})$ and drift vector $\mu_l = (\mu_{l1},\ldots,\mu_{lK_l})^\dagger$ for $l \in \{1,\ldots,\beta\}$. We properly extend the calculations in [134] with the difference that we have to apply l Fourier integrals, yielding

$$\begin{aligned}\langle g\rangle(V|c,N) = \frac{1}{2^{N/2}\Gamma(N/2)} \int_0^\infty dz z^{N/2-1} e^{-z/2} \sqrt{\frac{N}{2\pi z}}^{\beta} \sqrt{\frac{N}{2\pi z T}}^{K} \left(\prod_{l=1}^{\beta}\prod_{k=1}^{K_l} \frac{1}{V_{lk}\rho_{lk}}\right) \\ \times \prod_{l=1}^{\beta} \frac{1}{\sqrt{1-c_l}^{K_l}} \int_{-\infty}^{\infty} du_l \exp\left(-\frac{N}{2z}u_l^2\right) \\ \times \exp\left[-\frac{N}{2zT_{\mathrm{M}}} \sum_{k=1}^{K} \frac{\left(\ln\frac{V_{lk}}{V_{lk0}} - \left(\mu_{lk} - \frac{\rho_{lk}^2}{2}\right)T_{\mathrm{M}} + \sqrt{c_l T_{\mathrm{M}}} u_l \rho_{lk}\right)^2}{(1-c_l)\rho_{lk}^2}\right],\end{aligned} \tag{3.56}$$

with $c = \mathrm{diag}(c_1,\ldots,c_\beta)$.

This multiple integral depends on the number of markets β. The index l indicates each market, the index k indicates the asset in a specified market l. In general, the index pair (l,k) denotes the k-th asset on the l-th market.

3.3.3. Absence of Subordination on Several Markets

To calculate the multivariate portfolio loss distribution for several portfolios on several uncorrelated markets, we perform the same calculations as in section 3.3. We insert the average asset value distribution (3.56) into equation (3.43) with the slight difference that we have to replace the sum over k by two sums over l and k. We arrive at the final result, which is up to a prefactor formally identical to

equation (3.44)

$$\langle p\rangle\,(L|c,N) = \frac{1}{2^{N/2}\Gamma(N/2)}\int_0^\infty dz z^{N/2-1}e^{-z/2}\sqrt{\frac{N}{2\pi}}^{\beta}\int d[u]\exp\left(-\frac{N}{2}u^2\right) \times \frac{1}{\sqrt{\det\left(2\pi M_2(z,u)\right)}}\exp\Big(-\frac{1}{2}\left(L-M_1(z,u)\right)^\dagger M_2^{-1}(z,u)\left(L-M_1(z,u)\right)\Big), \tag{3.57}$$

with

$$M_1(z,u) = \sum_{l=1}^{\beta}\sum_{k=1}^{K_l} f_{lk}m_{1,l,k}(z,u_l), \tag{3.58}$$

$$M_2(z,u) = \sum_{l=1}^{\beta}\sum_{k=1}^{K_l} D_{lk}\left(m_{2,l,k}(z,u_l) - m_{1,l,k}^2(z,u_l)\right), \tag{3.59}$$

and

$$D_{lk} = f_{lk}f_{lk}^\dagger \tag{3.60}$$

and $u = (u_1,\ldots,u_\beta)$. Here, $d[u]$ denotes the product of all differentials du_l. The moments $m_{1,l,k}(z,u_l)$ and $m_{2,l,k}(z,u_l)$ are the same as in equation (2.31) including an additional index for each market $l \in \{1,\ldots\beta\}$. Analogously, f_{lk} is the extension of f_k for several markets. In this way, we are able to vary the parameters like drift and volatility across the markets. We found it useful depending on the size of β, to use polar or spherical coordinates for the evaluation of the multivariate u integral.

Finally, we analyze two disjoint infinitely large portfolios of same size, where each portfolio invests in a separate market. We start from distribution (3.57) and perform the limit $K \to \infty$. Again, we find two δ functions and, by applying equation (3.33) twice, we obtain

$$\langle p\rangle\,(L^{(1)},L^{(2)}|c,N)\Big|_{K\to\infty} = \frac{1}{2^{N/2}\Gamma(N/2)}\int_0^\infty dz z^{N/2-1}e^{-z/2}\frac{N}{2\pi}\exp\left(-\frac{N}{2}(u_{10}^2+u_{20}^2)\right) \times \left|\frac{\partial}{\partial u}m_{1,1,0}(z,u)\Big|_{z,u_{10}}\right|^{-1}\left|\frac{\partial}{\partial u}m_{1,2,0}(z,u)\Big|_{z,u_{20}}\right|^{-1}, \tag{3.61}$$

where

$$0 = L^{(1)} - m_{1,1,0}(z,u_{10}) \tag{3.62}$$

and

$$0 = L^{(2)} - m_{1,2,0}(z,u_{20}) \tag{3.63}$$

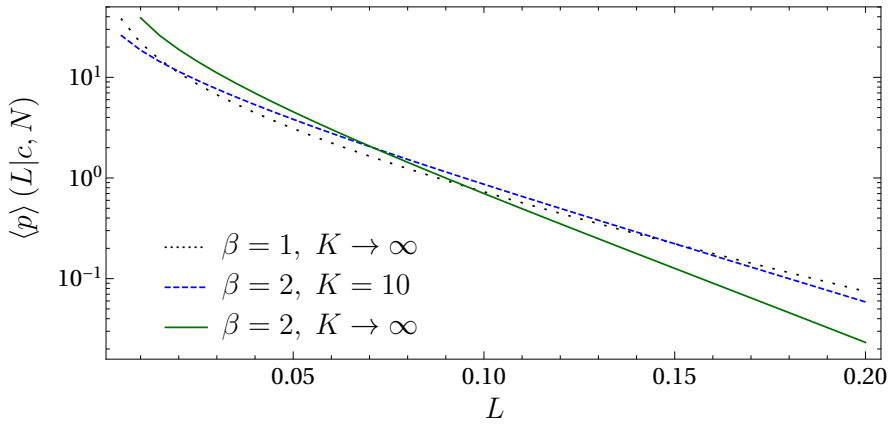

Figure 3.2.: Average loss distribution on a logarithmic scale for a different number of markets and market size. The markets are homogeneous and we choose a face value of $F_0 = 75$ and the initial asset value $V_0 = 100$.

define the implicit functions $u_{10}(L^{(1)},z)$ and $u_{20}(L^{(2)},z)$.

3.4. Visualization of the Results

We always employ the approximation (2.24) to the mean correlation matrix, which yields, as already emphasized, very good fits to empirical data due to the very nature of the ensemble average. Furthermore, we restrict our analysis to homogeneous portfolios.

3.4.1. One Portfolio, Two Markets

In the following, we use the same parameters as in section 2.4. These are determined by data consisting of 307 stocks from the S&P500 index traded in the period from 1992 to 2012. We find the following empirical results for $T_{\mathrm{M}} = 1$ year: $\mu = 0.17$ year^{-1}, $\rho = 0.35$ year$^{-1/2}$, $N = 6$ and $c = 0.28$.

We study the impact of investing into two uncorrelated markets. We thus assume two identical uncorrelated markets with the same average correlation coefficient. Furthermore, we assume the empirical parameters to be the same for both markets. The results are shown in figure 3.2. For a comparison, we also show the limiting distribution (2.33) for only one market $\beta = 1$ with the same parameters as in the case of two markets. As expected, we see that the diversification, i.e., the separation of the correlation matrix into two blocks leads to a reduction of large portfolio losses. Hence, reducing the risk of large losses can be achieved more effectively by

splitting the portfolio onto different uncorrelated markets than by solely increasing the number of credit contracts on one single market. Obviously, this is due to the on-average zero correlations in the off-diagonal blocks. A further reduction of the risk can only be achieved by either splitting the portfolio in more than two markets or investing into markets where the average correlation coefficient is low with little fluctuations. Nevertheless, by increasing the number of uncorrelated markets β, we obtain for $\beta \to \infty$ the same scenario as in the case of one market with average correlation zero. Here, the diversification effect is limited to the strength of the fluctuations N, where the pronounced tail of the loss distribution would only decrease for large N.

This effect has been discussed before, for example, in [222], in an empirical setting. We emphasize that our results make it possible to quantitatively model the effect of diversification. According to the adjustability of our model, the benefits of diversification can be modeled for different markets and different market situations.

3.4.2. Absence of Subordination and Disjoint Portfolios of Equal Size

Previously, we analyzed one portfolio on two markets. Here, we are interested in the case of two portfolios on one market. We begin with varying the number of companies K and study the corresponding impact on the multivariate loss distribution as well as on the default correlation and the default probabilities. Figure 3.3 shows the average loss distribution (3.44) with effective average correlation matrix and homogeneous parameters for two disjoint portfolios of equal size, for different market sizes $K = 10, 20, 100$ and empirical values for the parameters.

We choose the face value $F_0 = 75$ and the initial asset value $V_0 = 100$. The market parameters are the same as we used in the previous section. The distribution is symmetric. It converges to the limiting distribution (3.53) as K increases. We thus infer a high correlation of the portfolio losses even for a small number of obligors. The striking peak around the origin $L^{(1)} = L^{(2)} = 0$ corresponds to those events that lead to little portfolio losses. This peak arises because of the large drift we use for evaluation. Due to the positive drift, the overall number of companies that do not default is larger than the number of companies that default at maturity. Still, this peak does not represent the δ peak at the origin, which stands for the probability of total survival of all companies. It becomes clear when we calculate the survival probability for all companies. This probability does not depend on whether we have subordinated debt or not and it also does not depend on the composition of our portfolios, see equation (3.29). The effect of different drift parameters μ on the probability of zero portfolio loss is shown in figure 3.4.

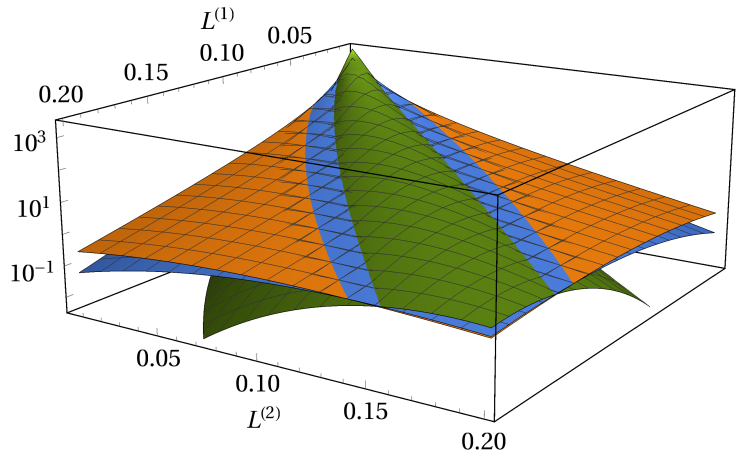

Figure 3.3.: Average loss distribution for two disjoint portfolios of same sizes on a logarithmic scale. We show different market sizes, $K = 10$ orange, $K = 20$ blue and $K = 100$ green. The parameters are $\mu = 0.17\,\text{year}^{-1}$, $\rho = 0.35\,\text{year}^{-1/2}$, $N = 6$, $c = 0.28$ and a maturity time of $T_\text{M} = 1\,\text{year}$.

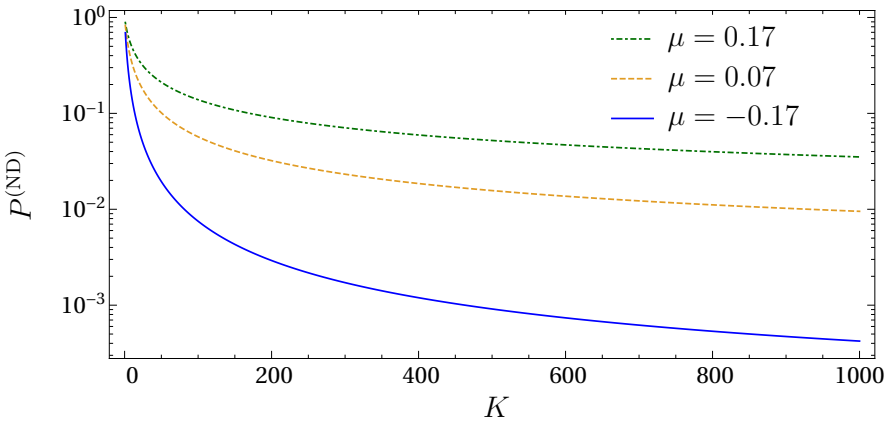

Figure 3.4.: Probability of zero portfolio loss depending on the portfolio size K for different drift parameters μ on a logarithmic scale.

For every value of μ, the probability of having zero total portfolio loss decreases with an increasing number of companies K. Hence, the weight of the δ peak on the portfolio loss distribution at $L^{(1)} = L^{(2)} = 0$ becomes smaller. This is quite intuitive; the larger the K, the more likely is the default of at least one company.

When looking at the portfolio loss correlations, we find large values for little or even zero asset correlation. For a market size of $K = 100$, i.e., each portfolio is

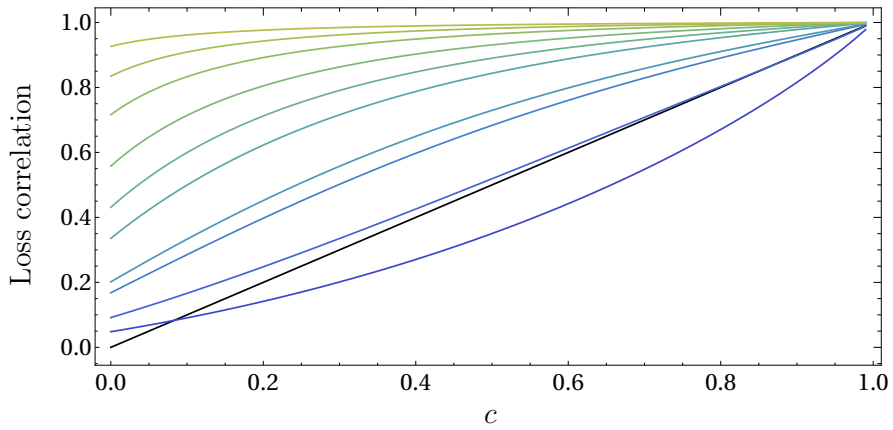

Figure 3.5.: Portfolio loss correlation on a linear scale depending on the asset correlation c. Both portfolios are homogeneous and have the same size. The market size K ranges from 2 (blue) over 4, 8, 10, 20, 30, 50, 100, 200 to 500 (green). The bisecting line is shown in black.

of size 50, we obtain for an average asset correlation of $c = 0$ a correlation of the portfolio losses of $\mathrm{Corr}(L^{(1)},L^{(2)}) = 0.71$. This high loss correlation is based on the fact that the asset correlations fluctuate around the mean asset correlation of zero. Due to this fluctuation, we have individual positive and negative correlations. The negative correlations only have a limited effect because the asymmetry of credit risk projects all non defaulting events onto zero while only defaulting events contribute to the loss distribution. Hence, the positive asset correlations dominate the negative ones causing a high portfolio loss correlation. The results are shown in figure 3.5.

They are in accordance with the simulation results in [193]. The portfolio loss correlation is a monotonic function of the asset correlation c. Depending on the number of companies, the portfolio loss correlation is a convex function (namely, $K = 2,4$) or a concave function ($K \geq 8$). However, we emphasize that these results are subject to the second order approximation, which yields better results the larger the K. Large numbers of K lead to very high loss correlations. This confirms that, even without average asset correlation, i.e., $c = 0$, the loss of one large portfolio serves as a forecast for another large portfolio. We substantiate this statement with figure 3.6. There, we show the loss correlation of two disjoint credit portfolios in dependence of the market size K for different values of the average effective market correlation. We find that the portfolio loss correlation rapidly increases with increasing market size.

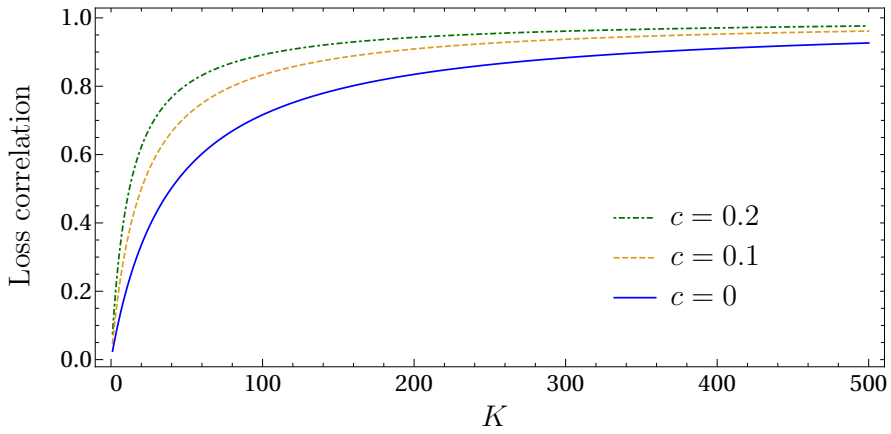

Figure 3.6.: Portfolio loss correlation on a linear scale depending on the market size K for different average asset correlations c. The credit portfolios are disjoint, homogeneous and have the same size.

3.4.3. Absence of Subordination and Disjoint Portfolios of Various Sizes

Looking at portfolios of various sizes yields much improved understanding of whether diversification works or not. To analyze this, we consider portfolio one with fixed size $R_1 = 10$ and we consider the overall size of the market $K = 30$, 110 and the limit $K \to \infty$. In this scenario, the market share of portfolio one will steadily decrease and converge to zero in the limiting case. Hereby, we are able to compare somewhat smaller portfolios with very large ones.

For our calculations, we use the same empirical parameters as before. The effect of different market sizes K on the loss distribution $\langle p \rangle \, (L^{(1)},L^{(2)}|c,N)$ is shown in figure 3.7. There are regions where we have heavy-tailed behavior of the distributions but also others where the distributions decay very fast. In this latter regions that always fulfill the condition $L^{(1)} > L^{(2)}$, the loss distribution decays considerably faster with increasing market size K. Hence, we find large deviations between the distributions of different market sizes. These deviations only play a minor role because they emerge at a significant low order of the loss distribution. In general, for increasing market size K, the second (larger) portfolio describes the market in a better manner. Hence, it is very unlikely for the first portfolio to suffer a big loss in times when the second portfolio of large size exhibits little loss. This explains the fast decay of the loss distribution in the $L^{(1)} > L^{(2)}$ corner. However, the most important fact is that, along the diagonal $L^{(1)} = L^{(2)}$ and in the upper corner $L^{(1)} < L^{(2)}$, significant deviations between the loss distributions for different market sizes do not occur. Here, we also observe heavy-tails of the loss

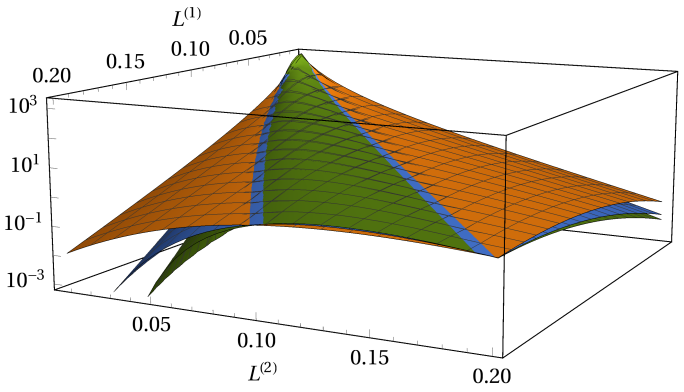

Figure 3.7.: Average loss distribution for portfolios of different sizes on a logarithmic scale. Portfolio one is of fixed size $R_1 = 10$ and the market size is $K = 30$ (orange), $K = 110$ (blue) and $K \to \infty$ (green). The parameters are $\mu = 0.17\,\text{year}^{-1}$, $\rho = 0.35\,\text{year}^{-1/2}$, $N = 6$, $c = 0.28$ and a maturity time of $T_\text{M} = 1\,\text{year}$.

distribution. Especially when we consider the diagonal, where the losses are equal, we find no deviations and, thus, no diversification at all. This means that increasing the size of portfolio two while keeping the size of portfolio one constant does not yield a decrease of concurrent large portfolio losses of equal size. Interestingly, it is more likely to find an event in the upper off-diagonal corner with $L^{(1)} < L^{(2)}$ than in the lower corner. This can be explained by the fluctuations around the mean correlation coefficient of $c = 0.28$ and the positive drift $\mu = 0.17\ \text{year}^{-1}$. The fluctuations ensure that there is a probability for the assets of portfolio one to be adversely correlated to the assets of portfolio two. Accordingly, there is a significant probability that the small portfolio one suffers no or little default while the second portfolio suffers a major one. This probability decreases when we enlarge the size of portfolio one while keeping the size of portfolio two fixed and still larger than the size of portfolio one. Due to the asymmetry of the portfolio loss distributions regarding the diagonal, we find lower portfolio loss correlations for the same market size than in the case of two equal sized portfolios, see figure 3.8. In contrast to two portfolios of equal size, there is a limit correlation of the portfolio losses depending on c in the limit $K \to \infty$. One clearly sees that the limiting curve is reached very quickly for increasing market size. This is due to the fixed size of portfolio one. Increasing its size and the market size would raise the portfolio loss correlation.

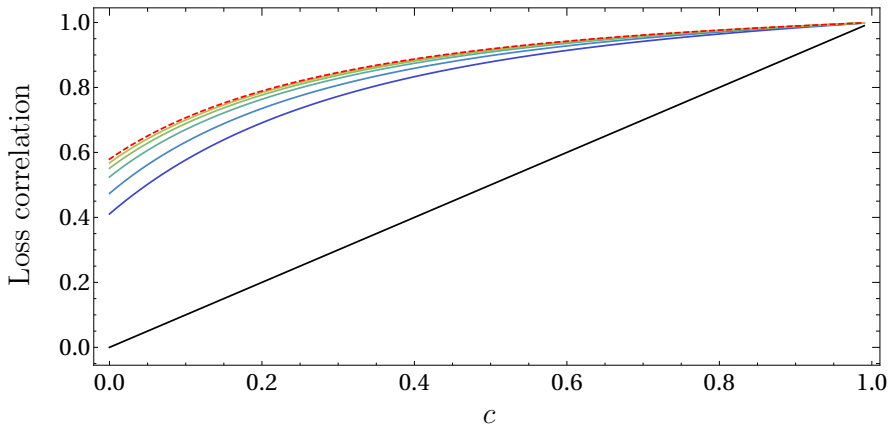

Figure 3.8.: Portfolio loss correlation as a function of asset correlation c on a linear scale. Portfolio one is of fixed size $R_1 = 10$ and the market size K ranges from 30 (blue) over 50, 100, 200 to 500 (green). The limiting curve $K \to \infty$ is shown as dashed red line and the bisecting line is shown in black.

3.4.4. Subordinated Debt

The subordinated debt structure brings a high degree of asymmetry into effect, see figure 3.9. We show the joint probability density of two equal-sized portfolios with face values $F_k^{(S)} = 37$ and $F_k^{(J)} = 38$. Both, senior and junior subordinated creditors operate on the entire market. By definition, the loss of the junior subordinated creditor is always larger or equal than the loss of the senior creditor. We thus have a cutoff along the diagonal line $L^{(S)} = L^{(J)}$. Besides the near region of a curved line, which we define as the back of the distribution, the number of obligors K influences the joint probabilities drastically. Along the back of the distribution, there is almost no deviation between the surfaces of the joint probability densities. Independent of K, the back of the distribution shows a heavy tail. Importantly, the curvature reaches for high losses of the junior subordinated creditor evermore to higher losses of the senior creditor. This is an important consequence in times of crisis. When the loss of the junior subordinated creditor becomes extremely large, it is most likely that also the senior creditor suffers a significant loss. Furthermore, we find that, in times of crisis, the majority of an additional loss will be distributed to the senior creditor when there is already a large loss of the junior subordinated creditor.

When we consider the marginal distributions of each creditor individually, we see that strong diversification effects do not exist, see figure 3.10. The upper three curves are the marginal distributions of the junior subordinated creditor and the

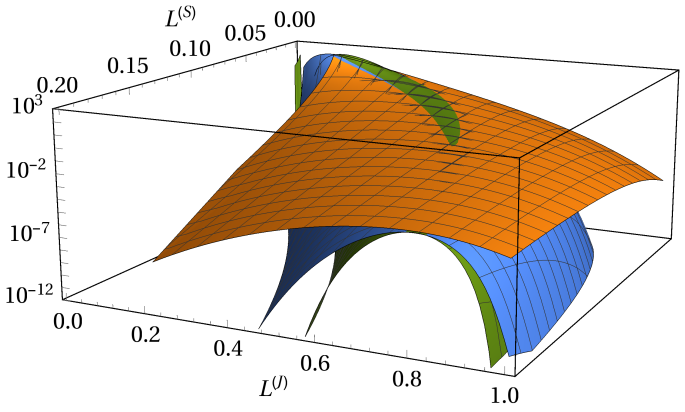

Figure 3.9.: Average portfolio loss distribution of a subordinated debt structure on a logarithmic scale. Both portfolios operate on the entire market. We show different market sizes $K = 10$ orange, $K = 200$ blue and $K \to \infty$ green.

lower three curves belong to the senior creditor. All distributions show heavy tails and the gap between the senior and junior subordinated creditor enlarges with increasing loss L. The size of this gap becomes smaller when the ratio $F_k^{(S)}/F_k^{(J)}$ becomes larger.

3.5. Conclusions

Within the Merton model, we calculated a multivariate joint average portfolio loss distribution, taking fluctuating asset correlations into account. We used a random matrix model, which is, most advantageously, analytically tractable and also empirically yields a good match of stock market data. The multivariate average asset value distribution depends on two parameters only, the effective average asset value correlation and the strength of the fluctuations around this average.

We showed that diversification is achieved much more efficiently by splitting a credit portfolio onto different markets that are, on average, uncorrelated than by solely increasing the number of credit contracts on one single market.

For two non-overlapping portfolios of equal size, we found a symmetric portfolio loss distribution. Studying the portfolio loss correlations, we showed that significant correlations emerge not only for large portfolios containing thousands of credit contracts, but also, in accordance with a second order approximation, for small portfolios containing only a few credit contracts. Two non-overlapping portfolios of

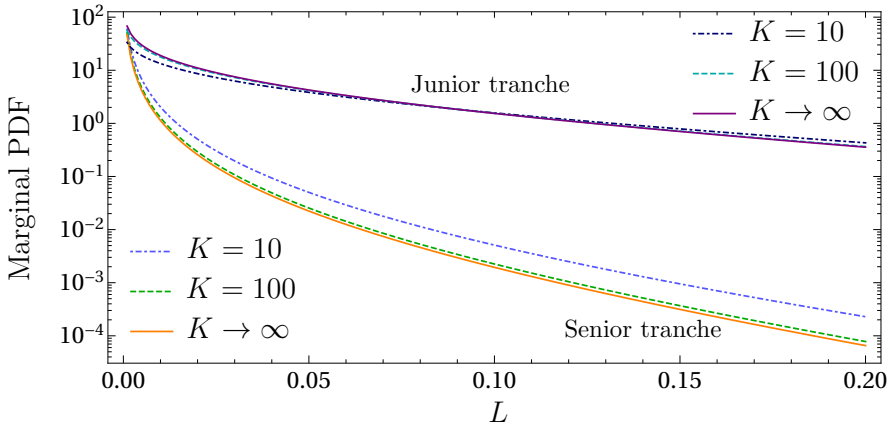

Figure 3.10.: Marginal distributions of senior and junior subordinated creditor on a logarithmic scale. The upper three lines belong to the junior subordinated creditor and the lower three lines to the senior creditor.

infinite size have a loss correlation of one and will always suffer the same relative loss.

When we analyzed two non-overlapping portfolios of different size, we found the loss correlations to be limited. Nevertheless, the distributions show heavy tails that make large concurrent portfolio losses likely.

Furthermore, we included subordinated debt, related to CDO tranches. At maturity time, the senior creditor is paid out first and the junior subordinated creditor only if the senior creditor regained the full promised payment. Here, we analytically substantiate that, in case of crisis, i.e., when a large loss of the junior subordinated creditor is highly likely, a large loss of the senior creditor is also very likely. Thus, the concept of subordination does not work as intended in times of crisis. In addition, the marginal distributions show that increasing the size of both portfolios fails to reduce the tail risk significantly.

There are some limitations of our model. Our approach is based on the Merton model, which as discussed in the literature, has some weaknesses, see, e.g., [150, 198]. Furthermore, due to the second order approximation in $f_k^{(S)}$ and $f_k^{(J)}$, necessary for analytical tractability, we assume that the face values of all companies are of the same order. Hence, in this approximation, we are not able to analyze the influence of one large company in the loss distribution. Credit default data is very hard to get, implying that we are unfortunately not able to compare the results of our model with empirical data. Nevertheless, our results, when compared to credit risk data in the future, provide an excellent test of the Merton model because we use stock market data for calibration.

The novelty of our approach is the ability to quantitatively model diversification effects that have been mainly qualitatively discussed in the economic literature. Hence, we corroborate qualitative reasoning in the economic literature. Additionally, by obtaining the joint portfolio loss distribution, further quantities such as any kind of risk measures can be calculated.

4. WKB-Type-of Approximation for Rare Event Statistics in Reacting Systems

4.1. Introduction

In the previous chapters we have seen that rare events are important in many situations, especially when their consequences are extreme. Often, demographic noise or intrinsic fluctuations which are based on stochasticity cause such events. There is a wide variety of applications where stochasticity plays a key role, such as chemical reactions [181, 223], population dynamics [224–228], epidemiology [229–233] and financial markets [234] to name a few examples. Another example for stochasticity is non-demographic, i.e. extrinsic, noise which arises due to interactions between the considered system and a noisy environment [235–238]. If one ignores the noise, many of such systems can be described by rate equations to obtain a macroscopic, deterministic description of average quantities of the system, particularly mean concentrations. This is referred to as the mean field approximation. However, we are interested in large deviations from a typical system behavior. For example, in population dynamics, this is the case when the average size of the population is large and we are interested in low population numbers. The state of this system is given by the population number at a distinct time. The probabilistic description of a stochastic system in such a state is given by the master equation [239, 240]. Since it is often not possible to solve the master equation analytically, one has to find an approximation, such as the Fokker-Planck equation. The Fokker-Planck equation, however, is reliable only for small deviations from the mean field approximation. It fails to give an accurate description of large deviations from the typical evolution of a system [241, 242]. Hence, other methods to calculate the rare event statistics are called for. In 2004 Vlad Elgart and Alex Kamenev [186] put forward an asymptotic method to calculate the rare event statistics in reaction-diffusion systems by formally relating it to semiclassics. A quantum problem can sometimes be solved by expanding to lowest order in $\hbar$ around the corresponding classical equations of motion. A "Hamiltonian" formulation of reaction-diffusion systems is developed which reformulates the master equation by means of a generating function as a "Schrödinger equation". The "semiclassical" dynamics of the corresponding Hamiltonian provides all the information necessary

for the analysis of rare event statistics. The existence of a small parameter allows the treatment analogous to a Wenzel-Kramers-Brillouin (WKB) approximation [243–247]. The WKB approximation is applied to the evolution equation of the generating function. For related studies on the WKB approximation see [183–185, 248–252] and for reviews see [253–255]. For stochastic population models the WKB approximation allows one also to calculate the mean extinction times and probabilities [256–259] and for switching rates in multistep reactions see [260].

Here, we consider single-species chemical reactions which can be described by master equations that give the time evolution of the probability $P_n(t)$ to find a distinct number of particles n at a given time t. One way of dealing with such systems is a spectral formulation and a stationary WKB approximation, see [248]. A different method is the time-dependent semiclassical approximation [186]. Both methods have different regimes of validity and accuracy. The time-dependent semiclassical approximation is accurate for $1 \ll n \leq \langle n \rangle$, where $\langle n \rangle$ denotes the average particle number which depends on time. In the region $n > \langle n \rangle$ the accuracy of this method breaks down and the spectral formulation and stationary WKB approximation is better suited. We generalize the time-dependent model [186] in such a way that reactions with more than two particles of one species can be analyzed. This is not possible in the original method since the corresponding equations cannot be solved analytically. Moreover, we include the calculation of the pre-exponential factor of the distribution. This was disregarded in the original method. Our main focus lies on the probability of rare events, i.e., to find our system in a state far away from the typical behavior. By means of the probabilities we are able to estimate many quantities such as the average extinction time and the lifetime distribution. Even though large deviations from a typical system behavior may be hardly observable, their probabilities are interesting for anyone who has to compensate probable risks which come along with these rare events. In more detail we consider systems which can have, depending on the initial condition, an absorbing state with zero particles left. In general, results for such systems are unavailable in analytical form. However, with our approach, we are able to compute the solution partially in analytical and partially in numerical form. Depending on the reaction scheme, we have to scale the corresponding parameters of the master equation in order to perform the WKB approximation in a proper way. We consider different types of reactions where we combine death or single annihilation, binary annihilation and triple annihilation. As a result we find a very good accordance between the WKB approximation and the exact solution of the master equation especially in the left tail of the distribution.

This chapter is organized as follows. In section 4.2 we go into the details of the approach and generalize it in such a way that more complex reactions like higher order annihilations can be analyzed. In section 4.3 we apply the method

on a set of examples which can either be solved exactly or by means of the WKB approximation and numerical calculus. We conclude in section 4.4. The contents of this chapter are published in reference [3].

4.2. Deeper Look at the Method

Consider a system consisting of identical particles which can react with each other according to different reaction schemes $i = 1, \ldots, m$. The chemical reactions can be described by master equations which give the time evolution of the probability to find a given number of particles in the system at a given time. A particular reaction occurs with probability $\lambda_i \Delta t$ with $\lambda_i \ll 1$ in the time interval $[t,t + \Delta t]$, where λ_i is the specific probability rate constant. Importantly, all λ_i are independent of Δt or the considered time interval. Since each particle may react with each other the system is fully described by the following master equation

$$\frac{d}{dt}P_n(t) = \sum_{i=1}^{m} \left(\lambda_i h_i(n - \nu_i)P_{n-\nu_i}(t) - \lambda_i h_i(n)P_n(t)\right) \tag{4.1}$$

where $P_n(t)$ denotes the probability to find n particles at time t, $h_i(n)$ is the number of combinations of reacting particles in the system under reaction scheme i when n particles are in the system, and ν_i is the change of particle number when the reaction i occurs, see [239]. In order to obtain a unique solution of the master equation we have to specify an initial condition. This can be any kind of normalized distribution like the Poisson distribution or for our sake we use a fixed particle number n_0 and hence the initial condition is

$$P_n(0) = \delta_{n,n_0} \ , \tag{4.2}$$

with the Kronecker delta

$$\delta_{n,n_0} = \begin{cases} 1 \, , & n = n_0, \\ 0 \, , & n \neq n_0 \end{cases} \ . \tag{4.3}$$

We introduce the auxiliary variable ξ which formally plays the role as a "position" and we also introduce the generating function

$$G(\xi,t) = \sum_{n=0}^{\infty} \xi^n P_n(t) \ . \tag{4.4}$$

The generating function has to fulfill the initial condition $P_n(0)$ which gives

$$G(\xi,0) = \xi^n \ . \tag{4.5}$$

Furthermore, from the conservation of probability, we find

$$G(1,t) = 1 \ . \tag{4.6}$$

By means of the generating function we are able to calculate the average particle number

$$\langle n \rangle = \sum_{n=0}^{\infty} n P_n(t) = \frac{\partial}{\partial \xi} G(\xi,t)\Big|_{\xi=1} \tag{4.7}$$

and the probability

$$P_n(t) = \frac{1}{n!} \frac{\partial^n}{\partial \xi^n} G(\xi,t)\Big|_{\xi=0} \ . \tag{4.8}$$

If the particle number n is large it is convenient to use Cauchy's integral formula

$$P_n(t) = \frac{1}{2\pi i} \oint d\xi \, G(\xi,t) \xi^{-n-1} \tag{4.9}$$

where the integration is performed over a closed contour encircling $\xi = 0$. Multiplying both sides of (4.1) with ξ^n and summing over all n yields the partial differential equation

$$\frac{\partial}{\partial t} G(\xi,t) = \hat{\mathcal{L}} G(\xi,t) \ , \tag{4.10}$$

where $\hat{\mathcal{L}}$ is a linear differential operator that includes powers of the expression $\partial/\partial\xi$. The requirement of analyticity of $G(\xi,t)$ yields "self-generated" boundary conditions. Besides the universal boundary condition $G(1,t) = 1$ the others are specific to the problem at hand. However, there is always the physical initial condition which is determined by the value of $P_n(0)$ and hence it is $G(\xi,0)$ that needs to be considered. The partial differential equation (4.10) can formally be written as a time-dependent "Schrödinger equation" with imaginary time

$$i\lambda \frac{\partial}{\partial i t} G(\xi,t) = \hat{H} G(\xi,t) \ , \tag{4.11}$$

where the right hand side contains the "Hamilton operator" $\hat{H}$ and we define $\lambda = \lambda_k$ for a fixed k. Now, we employ the formal analogy of the probability λ with Planck's constant $\hbar$. Moreover, in analogy to quantum mechanics we define the momentum operator

$$\hat{\pi} = -i\lambda \frac{\partial}{\partial \xi} \ , \tag{4.12}$$

which will acquire the meaning of a counting operator. By inserting the ansatz

$$G(\xi,t) = \varphi(\xi)\psi(it) \tag{4.13}$$

into (4.11) we can separate the variables ξ and t and find the two equations

$$i\lambda\frac{\partial}{\partial it}\psi(it) = E\psi(it) \tag{4.14}$$

$$\hat{H}\varphi(\xi) = E\varphi(\xi)\ . \tag{4.15}$$

We will interpret the constant E as energy or Hamilton function of our system. Up to this point we consider a probabilistic description of our problem, i.e., both variables ξ and t can be chosen independently from each other. However, the separation ansatz leads to the formal problem $G(1,t) = \varphi(1)\psi(it) = 1$ where t cannot be chosen arbitrarily. We will solve this problem by a semiclassical approximation in which we use the classical equations of motion that give an explicit dependence of both variables ξ and t.

The solution of equation (4.14) is

$$\psi(it) = \psi(0)e^{Et/\lambda}\ . \tag{4.16}$$

We solve the stationary "Schrödinger equation" (4.15) with a WKB approximation. We insert the ansatz

$$\varphi(\xi) = A(\xi)\exp(iS(\xi)/\lambda) \tag{4.17}$$

and separate the resulting equation into its real and imaginary parts. To solve the pair of differential equations we use the standard WKB assumption that all terms of second order or higher in the small parameter, here λ, can be neglected. The WKB approximation requires that the "quantum" fluctuations are weak, which is true as long as $\langle n(t)\rangle \gg 1$, i.e., for times not too long. In this regime we can apply the condition $\lambda \ll 1$. By putting all solutions of the differential equations together we find the solution for the generating function $G(\xi,t)$. This solution depends on a constant which has to be determined by the initial condition $G(\xi,0)$. Moreover, the generating function also depends on the energy E of our system. To make progress we have to determine the value of E.

Up to this point we used a probabilistic interpretation of the system where the variables ξ and t can be chosen independently from each other. To approximate the function $G(\xi,t)$ and determine the value of E we now go into semiclassics. The energy is given by the Hamilton function H which can be inferred from the "Hamilton operator" $\hat{H}$ and reads

$$H = H(\xi,\pi) = E \tag{4.18}$$

where π is the classical "momentum". The energy is an integral of motion with $dE/dt = 0$. The classical equations of motion in imaginary time are the "Hamilton equations"

$$\frac{d\xi}{dit} = \frac{\partial H}{\partial \pi} \tag{4.19}$$

$$\frac{d\pi}{dit} = -\frac{\partial H}{\partial \xi} \ . \tag{4.20}$$

Due to the classical equations of motion (4.19) and (4.20), the variables ξ and t are no longer independent of each other. From this point on, ξ and π are viewed as functions of t. We solve the energy E for π and insert the result into (4.19). Now, the first equation of motion contains only ξ and the constant energy E and we find

$$\frac{d\xi}{dit} = \tau(\xi,E) \ , \tag{4.21}$$

which gives the explicit classical dependence $\xi = \xi(t)$. Importantly, for the determination of the initial condition of the generating function we find

$$\xi(0) = \xi_0 \ . \tag{4.22}$$

In the original method [186] the assumption $\xi_0 = 1$ was made. In section 4.3.1 we show in a direct comparison between our and the original method the benefit of taking the variable ξ_0 into account, rather than making the approximation $\xi_0 = 1$. We do not solve the second equation of motion (4.20), instead we consider the mean field dynamics. If we are interested in the average particle number $\langle n \rangle$, we have to know the generating function in the vicinity of $\xi = 1$, see equation (4.7). This is the constant mean field solution $\bar{\xi} = 1$ which solves equation (4.19) because every permissible Hamilton function must satisfy the condition

$$H(1,\pi) = 0 \tag{4.23}$$

due to the normalization of probability. By application of the mean field solution the second equation of motion (4.20) has the solution $\bar{\pi}(t)$ where we specify the initial condition

$$\bar{\pi}(0) = \pi_0 \ . \tag{4.24}$$

Acting with the previously defined momentum operator $\hat{\pi}$ on the generating function at the mean field solution gives

$$\hat{\pi} G(\xi,t)\Big|_{\xi=1} = \frac{\lambda}{i} \frac{\partial G(\xi,t)}{\partial \xi}\Big|_{\xi=1} = \frac{\lambda}{i} \langle n \rangle = \bar{\pi}(t) \ . \tag{4.25}$$

The last equality holds because in the mean field approximation quantum mechanics has to coincide with classical mechanics. Thus, we call the operator $\hat{\pi}$ counting operator which gives the average particle number for a given time. As π_0 has to be constant for all times we can specify its value at time $t = 0$ where, due to the initial condition, we find $\langle n \rangle_{t=0} = n_0$ and therefore

$$\pi_0 = \frac{\lambda}{i} n_0 \ . \tag{4.26}$$

We note that E is constant and can also be expressed in terms of $\xi(0) = \xi_0$ and $\pi(0) = \pi_0$, i.e., $E = E(\xi_0) = E_0$. Equation (4.21) can be solved by integration. The formal solution is

$$\int_{\xi_0}^{\xi} \frac{d\xi'}{\tau(\xi',E)} = it \ . \tag{4.27}$$

If we allow for complex reactions the function $\tau(\xi,E)$ will become also complex. In many cases it might not be possible to solve the integral (4.27) analytically. Instead a numerical solution has to be taken into account. Examples therefore are the reaction which combines binary and single annihilation and the combined reaction up to third order annihilation which are discussed in section 4.3.3 and 4.3.4, respectively. This issue is the starting point of our more general approach to calculate the rare event statistics.

The initial condition $G(\xi,0) = \xi_0^{n_0}$ enables us to determine the constant in the generating function $G(\xi,t)$. But before we determine the value ξ_0 we first calculate the probability $P_n(t)$ by means of a saddle point approximation. At this point we have to make an important remark. As already discussed, the starting point of our analysis is a probabilistic description of the process. We proceed by using semiclassical methods in order to find an approximation for the generating function. Therefore we derive equations of motion that describe the classical trajectories for a constant energy E. The classical trajectories give an explicit dependence of the underlying variables which in our case are ξ, π and t. They cannot be chosen independently from each other. The value of the energy determines which trajectory in the phase space describes the relationship between ξ and t, i.e., $\xi = \xi(t)$. Eventually, we are interested in probabilities $P_n(t)$ again. Therefore, we have to leave the semiclassical description behind and turn back to a probabilistic description. In a probabilistic description the variables ξ and t are independent of each other and can also be chosen independently. Classically this means that we do not move along the trajectories anymore. This only applies if the energy depends on both variables, i.e., $E = E(\xi,t)$. In other words, when we go back from the semiclassical into the probabilistic description the energy does not remain constant. In that sense it is more intuitive to name the quantity E Hamilton function instead of energy. This non-constant Hamilton function can be explained

by a short example: In a conservative system the energy is fully determined by the initial conditions. It however differs for different initial conditions. In that sense, the Hamilton function describes, at the same time, a constant of motion and the same system at different energies. Hence, derivatives

$$E' = \frac{\partial E}{\partial \xi} \tag{4.28}$$

have to be taken into account when the saddle point approximation is performed.

The contour integral can be written as

$$P_n(t) = \frac{1}{2\pi i} \oint d\xi \, g(\xi) \exp(f(\xi,E)) \tag{4.29}$$

with the function $g(\xi)$ and the "free energy" $f(\xi,E)$ that are determined by the generating function $G(\xi,t)$ and the factor ξ^{-n-1} in Cauchy's integral formula (4.9). We add the term ξ^{-n} into the exponential because of its factor n which is supposed to be large. We calculate the integral by means of a saddle point approximation. This approximation is justified because we have a small λ and assume large n. Furthermore, we are interested in times t where $\langle n(t) \rangle$ is sufficiently smaller than n_0 but $\langle n(t) \rangle \gg 1$ still holds.

The saddle point approximation requires

$$\frac{\partial}{\partial \xi} f(\xi_s,E) = f'(\xi_s,E) = 0 \tag{4.30}$$

and we find with a non-constant energy $E(\xi,t)$ the derivative

$$f'(\xi,E) = \omega(\xi,E,E') \; . \tag{4.31}$$

For convenience we drop the arguments of $E(\xi,t)$. Pretending that the analytical solution of (4.21) is not known, i.e., when we have to evaluate the integral in (4.27) numerically, we have to determine E' in order to solve the saddle point equation $f'(\xi_s,E) = 0$. We obtain the derivative of E by deriving the solution of the classical equation of motion (4.27) with respect to ξ under the condition that the energy depends on ξ and the time t does not

$$0 = \frac{\partial}{\partial \xi} \int_{\xi_0}^{\xi} \frac{d\xi'}{\tau(\xi',E(\xi,t))} \; . \tag{4.32}$$

We remark that the integration is performed over the variable ξ' which is due to semiclassics not included in $E(\xi,t)$. By using the Leibniz rule we find

$$\begin{aligned} E' &= \frac{\partial E(\xi,t)}{\partial \xi} \\ &= \left(\tau(\xi,E(\xi,t)) \int_{\xi_0}^{\xi} \frac{d\xi'}{\tau^2(\xi',E(\xi,t))} \frac{\partial}{\partial E} \tau(\xi',E(\xi,t)) \right)^{-1} \\ &= \kappa(\xi,E) \, , \end{aligned} \tag{4.33}$$

which again is a function of ξ and E. The energy E can be expressed in dependence of ξ_0, i.e., $E = E(\xi_0)$. Due to this relation E' can also be expressed in terms of ξ and ξ_0, i.e., $E' = \kappa(\xi,\xi_0)$. Now, we can reduce the derivative

$$f'(\xi,E) = \omega(\xi,\xi_0) \tag{4.34}$$

on the two variables ξ and ξ_0 and the saddle point condition becomes

$$\omega(\xi_s,\xi_0) = 0 \, . \tag{4.35}$$

From its solution we obtain the relationship between ξ_s and ξ_0, i.e., $\xi_0 = \xi_0(\xi_s)$. Together with equation (4.27) this allows us to calculate a numeric value for ξ_s, by solving the integral equation

$$\int_{\xi_0(\xi_s)}^{\xi_s} \frac{d\xi'}{\tau(\xi',E_0(\xi_0(\xi_s)))} = it \, . \tag{4.36}$$

We note that the integral stems from the semiclassical part of our analysis, hence the energy E has to remain constant during integration. Furthermore we changed the upper limit in (4.27) to ξ_s which is valid, as the constant value of the energy depending on ξ_s has to be chosen accordingly. Finding a solution for ξ_s can be demanding, depending on the function $\tau(\xi,E)$ and the solution $\xi_0(\xi_s)$. Once, a solution for ξ_s is found the value of ξ_0 can be calculated. The last piece missing for the saddle point approximation is the second derivative of the free energy

$$f''(\xi,E) = \frac{\partial \omega(\xi,E,E')}{\partial \xi} + \frac{\partial \omega(\xi,E,E')}{\partial E} E' + \frac{\partial \omega(\xi,E,E')}{\partial E'} E'' \, , \tag{4.37}$$

with the second derivative of the energy

$$\begin{aligned} E'' &= \frac{\partial^2 E(\xi)}{\partial \xi^2} \\ &= -(E')^2 \Bigg\{ \frac{1}{E'\tau(\xi,E(\xi))} \frac{\partial}{\partial \xi}\tau(\xi,E(\xi)) + \frac{1}{\tau(\xi,E(\xi))} \frac{\partial}{\partial E}\tau(\xi,E(\xi)) \\ &+ E'\tau(\xi,E(\xi)) \int_{\xi_0}^{\xi} \frac{d\xi'}{\tau^2(\xi',E(\xi))} \left[\frac{\partial^2}{\partial E^2}\tau(\xi',E(\xi)) - \frac{2}{\tau(\xi',E(\xi))} \left(\frac{\partial}{\partial E}\tau(\xi',E(\xi)) \right)^2 \right] \Bigg\} . \end{aligned} \tag{4.38}$$

The value of E is determined by $E(\xi_0) = E_0$. Combining all pieces yields the final result for the probability

$$P_n(t) = \frac{1}{\sqrt{2\pi}} \frac{g(\xi_s)}{\sqrt{|f''(\xi_s,E)|}} \exp\left(f(\xi_s,E_0)\right) , \tag{4.39}$$

if $f''(\xi,E)$ is always real. This formalism works for every kind of reaction scheme. However, if the reactions become too complex, e.g. by involving higher order annihilations, it might become impossible to solve the required equations due to technical complications.

4.3. Some Examples

In the following we give some examples on how to apply the formalism which was described in the previous section.

4.3.1. Binary Annihilation Revisited

For the convenience of the reader we show how the known results of binary annihilation, studied in [186], fit into our generalized approach. This model can be solved analytically and exactly [165].

We consider a system where only the binary annihilation can possibly occur with probability rate λ. Once, this reaction takes place two particles form an inert aggregate. Since each particle may react with each other the system is fully described by the following master equation

$$\frac{d}{dt}P_n(t) = \frac{\lambda}{2}\left((n+2)(n+1)P_{n+2}(t) - n(n-1)P_n(t)\right) , \tag{4.40}$$

where $P_n(t)$ denotes the probability to find n particles at time t. According to equation (4.11) the corresponding time-dependent "Schrödinger equation" with imaginary time is

$$i\lambda\frac{\partial}{\partial it}G(\xi,t) = \frac{\lambda^2}{2}(1-\xi^2)\frac{\partial^2}{\partial\xi^2}G(\xi,t)\ , \tag{4.41}$$

where the right hand side can also be written in terms of the "Hamilton operator"

$$\hat{H} = \frac{\lambda^2}{2}(1-\xi^2)\frac{\partial^2}{\partial\xi^2} = -\frac{1}{2}(1-\xi^2)\hat{\pi}^2\ . \tag{4.42}$$

The separation ansatz $G(\xi,t) = \varphi(\xi)\psi(it)$ yields equation (4.16) for the time-dependent part and

$$E\varphi(\xi) = \frac{\lambda^2}{2}(1-\xi^2)\frac{\partial^2}{\partial\xi^2}\varphi(\xi) \tag{4.43}$$

for the stationary part. We solve the stationary "Schrödinger equation" with a WKB approximation. We insert the ansatz (4.17) and separate the resulting equation into its real and imaginary parts which yields

$$EA(\xi) = -\frac{\lambda^2}{2}(\xi^2-1)\left(A''(\xi) - \frac{1}{\lambda^2}A(\xi)\left(S'(\xi)\right)^2\right) \tag{4.44}$$

$$0 = 2A'(\xi)S'(\xi) + A(\xi)S''(\xi)\ . \tag{4.45}$$

Equation (4.45) can be simplified

$$\frac{d}{d\xi}A^2(\xi)S'(\xi) = 0 \tag{4.46}$$

which yields

$$A(\xi) = \frac{\tilde{c}}{\sqrt{S'(\xi)}} \tag{4.47}$$

with a constant $\tilde{c}$. In equation (4.44) we use the standard WKB assumption that all terms of second order in the small parameter, here λ, can be neglected. This gives the simplified differential equation

$$\frac{1}{2}(\xi^2-1)\left(S'(\xi)\right)^2 = E\ . \tag{4.48}$$

Its solution is

$$S(\xi) - S(\xi_0) = i\sqrt{2E}(\arccos\xi - \arccos\xi_0)\ , \tag{4.49}$$

with some initial value ξ_0. Now, we can put all terms together and obtain the generating function

$$G(\xi,t) = c\left(\frac{1-\xi^2}{2E}\right)^{1/4} \exp\left(-\frac{\sqrt{2E}}{\lambda}(\arccos\xi - \arccos\xi_0) + \frac{Et}{\lambda}\right), \tag{4.50}$$

where all constants have been put into c. Before determining this constant by the initial condition of the generating function, we first go into semiclassics. The Hamilton function is given by

$$H = E = \frac{1}{2}(\xi^2 - 1)\pi^2 \,. \tag{4.51}$$

The classical equations of motion in imaginary time are

$$\frac{d\xi}{dit} = \frac{\partial H}{\partial \pi} = (\xi^2 - 1)\pi \tag{4.52}$$

$$\frac{d\pi}{dit} = -\frac{\partial H}{\partial \xi} = -\xi\pi^2 \,. \tag{4.53}$$

We solve equation (4.51) for π and insert the solution into equation (4.52). The ensuing differential equation

$$\frac{d\xi}{dit} = \sqrt{2E(\xi^2 - 1)} \tag{4.54}$$

has the solution

$$\arccos\xi - \arccos\xi_0 = \sqrt{2E}t \,, \tag{4.55}$$

which is analogous to equation (4.27). The mean field dynamics gives us the average particle number. By application of the mean field solution $\bar{\xi} = 1$ the second equation of motion (4.53) has the solution

$$\bar{\pi}(t) = \frac{\lambda}{i}\langle n\rangle = \frac{\pi_0}{it\pi_0 + 1} \,. \tag{4.56}$$

The average particle number is

$$\langle n(t)\rangle = \frac{n_0}{n_0\lambda t + 1} \approx \frac{1}{\lambda t} \tag{4.57}$$

for $n_0 \gg 1$. The energy can be written as

$$E = E_0 = \frac{1}{2}(\xi_0^2 - 1)\pi_0^2 = \frac{\lambda^2}{2}n_0^2(1 - \xi_0^2) \,. \tag{4.58}$$

Now, we are able to determine the constant c in equation (4.50) with the initial condition $G(\xi,0) = \xi_0^n$

$$c = \xi_0^{n_0} \left(\frac{2E}{1-\xi_0^2} \right)^{1/4} . \tag{4.59}$$

Obviously, the normalization $G(1,t) = 1$ remains preserved. We calculate the probability $P_n(t)$ by means of the contour integral (4.9) and a saddle point approximation. The contour integral now reads

$$P_n(t) = \frac{1}{2\pi i} \frac{\xi_0^{n_0}}{(1-\xi_0^2)^{1/4}} \oint d\xi \, g(\xi) \exp(f(\xi,E)) \tag{4.60}$$

with

$$g(\xi) = \frac{1}{\xi}(1-\xi^2)^{1/4} \tag{4.61}$$

$$f(\xi,E) = -\frac{\sqrt{2E}}{\lambda}(\arccos\xi - \arccos\xi_0) + \frac{Et}{\lambda} - n\ln\xi. \tag{4.62}$$

The saddle point approximation requires $f'(\xi_s,E) = 0$ and we find with a non-constant Hamilton function $E(\xi,t)$

$$f'(\xi,E) = -\frac{E'}{\lambda}\left(\frac{\arccos\xi - \arccos\xi_0}{\sqrt{2E}} - t \right) + \frac{\sqrt{2E}}{\lambda} \frac{1}{\sqrt{1-\xi^2}} - \frac{n}{\xi} . \tag{4.63}$$

For convenience we drop the arguments of $E(\xi,t)$. We see that inserting the solution (4.55) of the classical equation of motion deletes the first bracket and yields

$$\frac{1}{\lambda t}(\arccos\xi_s - \arccos\xi_0) \frac{1}{\sqrt{1-\xi_s^2}} = \frac{n}{\xi_s} . \tag{4.64}$$

Interestingly, the E' term has been removed and with equation (4.58) we immediately obtain the relation $\xi_0 = \xi_0(\xi_s)$ according to equation (4.35)

$$\xi_0 = \sqrt{1 - \frac{n^2}{n_0^2} \frac{1-\xi_s^2}{\xi_s^2}} . \tag{4.65}$$

Combining equations (4.65), (4.58) and (4.55) yields an implicit equation for ξ_s which has to be solved by numerical methods. Having found the solution for ξ_s, a value for ξ_0 can be obtained by equation (4.65). In order to obtain the second derivative of the free energy we need E' which is according to equation (4.33)

$$E' = -\frac{\sqrt{2E}}{t\sqrt{1-\xi^2}} . \tag{4.66}$$

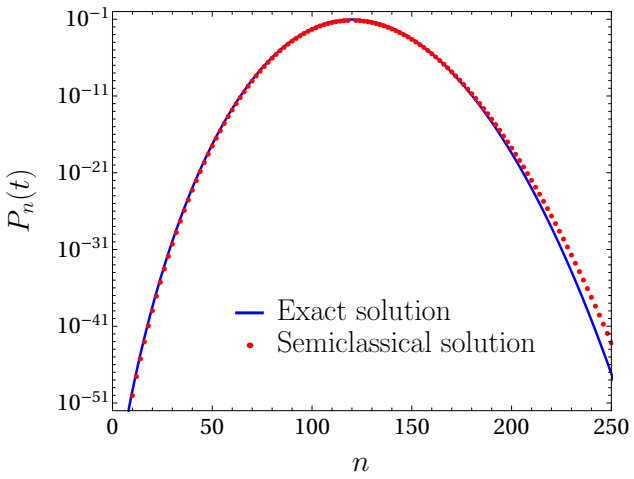

Figure 4.1.: Probability density distribution for the binary annihilation, see equation (4.40), at $t = 0.5$ on a logarithmic scale. Parameters are chosen as $n_0 = 300$ and $\lambda = 0.01$.

This result can directly be obtained by deriving equation (4.55). The second derivative of $f(\xi)$ at ξ_s can be simplified to

$$f''(\xi_s) = \frac{n\lambda t - \xi_s^2}{\lambda t(1-\xi_s^2)\xi_s^2} \approx \frac{n - \langle n\rangle \xi_s^2}{(1-\xi_s^2)\xi_s^2} \,, \tag{4.67}$$

which is always real for real ξ_s. Combining all pieces yields the final result for the probability

$$P_n(t) = \xi_0^{n_0} \sqrt{\frac{n_0 \xi_s}{2\pi n}} \left| \frac{1-\xi_s^2}{n - \langle n\rangle \xi_s^2} \right|^{1/2} \exp\left(-\frac{n^2}{2} \lambda t \frac{1-\xi_s^2}{\xi_s^2} - n \ln \xi_s \right) \,. \tag{4.68}$$

In figure 4.1 we compare the approximation (4.68) with the exact solution. We set $n_0 = 300$, $\lambda = 0.01$ and $t = 0.5$. The exact solution is calculated by numerical integration of the master equation. The maximum probability is around the average particle number which according to equation (4.57) is $\langle n(0.5)\rangle = 120$. Overall the approximation coincides over many orders of magnitude very well with the exact solution. We compare the new result (4.68) with the original one. In fact, we do not use the original result of [186], where the prefactor was included manually, we use the time-dependent solution of [248] that includes the prefactor by calculation. Figure 4.2 shows on a log-scale the ratios of the exact result and the semiclassical approximation for both, the new result (4.68) and the original result. Clearly, in the region $n \leq \langle n\rangle$ we see the high accuracy of the new result which outperforms

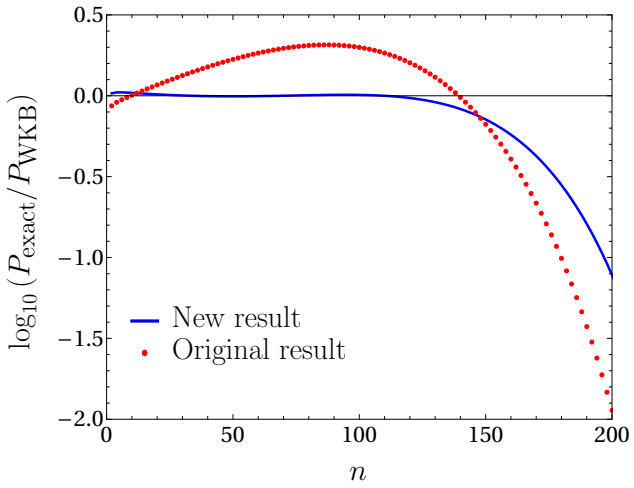

Figure 4.2.: Decadic logarithm of the ratio of the exact solution and the time-dependent WKB approximations. The solid line shows the new approximation (4.68), the circles show the original result. Parameters are chosen as $n_0 = 300$, $t = 1$ and $\lambda = 0.01$.

the original result. For large n the accuracy of the time-dependent semiclassical approximation deteriorates.

4.3.2. Single Annihilation

The simplest reaction is the single annihilation, where one particle forms an inert aggregate with probability rate λ. In terms of population dynamics this reaction is called death process. This process can be solved analytically and it is well known in literature, see, e.g. [163, 261]. Nevertheless, we apply the method to give a different representation how the model can be solved. Its master equation reads

$$\frac{d}{dt}P_n(t) = \lambda(n+1)P_{n+1}(t) - \lambda n P_n(t) \; . \tag{4.69}$$

This master equation can be solved exactly by different methods, see [163]. By means of the generating function (4.4) equation (4.69) can be written as "Schrödinger equation"

$$i\lambda\frac{\partial}{\partial it}G(\xi,t) = \lambda^2(1-\xi)\frac{\partial}{\partial\xi}G(\xi,t) = i\lambda(1-\xi)\hat{\pi}G(\xi,t) \; , \tag{4.70}$$

with the momentum operator $\hat{\pi}$. By applying the separation ansatz, we find the same formal solution for the time-dependent part as for the binary annihilation, see

equation (4.16). The ξ-dependent part of the separation ansatz is more interesting

$$E\varphi(\xi) = \lambda^2(1-\xi)\frac{\partial}{\partial\xi}\varphi(\xi) \ , \tag{4.71}$$

it has the exact solution

$$\varphi(\xi) = \varphi(\xi_0)\left(\frac{\xi_0 - 1}{\xi - 1}\right)^{E/\lambda^2} \ . \tag{4.72}$$

The classical energy is $E = i\lambda(1-\xi)\pi$ and the classical equations of motion are

$$\frac{d\xi}{dit} = i\lambda(1-\xi) \tag{4.73}$$

$$\frac{d\pi}{dit} = i\lambda\pi \ . \tag{4.74}$$

Both equations are easily solvable. The second equation gives the mean field dynamics resulting in the average particle number which is

$$\langle n\rangle = n_0 e^{-\lambda t} \ . \tag{4.75}$$

The solution for equation (4.73)

$$\xi = 1 + (\xi_0 - 1)e^{\lambda t} \tag{4.76}$$

can be inserted into equation (4.72) which yields

$$\varphi(\xi) = \varphi(\xi_0)e^{-Et/\lambda} \ . \tag{4.77}$$

Hence, we find the generating function

$$G(\xi,t) = \psi(t)\varphi(\xi) = \psi(0)\varphi(\xi_0) = G(\xi_0,0) = \xi_0^{n_0} \ . \tag{4.78}$$

In the last step we used the initial condition that at time $t = 0$ there are n_0 particles in the system. Solving equation (4.76) for ξ_0 and inserting into the generating function yields

$$G(\xi,t) = \left(1 + (\xi - 1)e^{-\lambda t}\right)^{n_0} \ . \tag{4.79}$$

The probability to find n particles at time t can be calculated by means of equation (4.8). We find

$$P_n(t) = \binom{n_0}{n}\left(1 - e^{-\lambda t}\right)^{n_0 - n} e^{-n\lambda t} \ . \tag{4.80}$$

4.3.3. Binary and Single Annihilation

We now consider a system where two reactions can occur. The binary annihilation occurs with probability rate λ and the single annihilation occurs with probability rate σ. Both probabilities are of the same order of magnitude. The master equation reads

$$\begin{aligned}\frac{d}{dt}P_n(t) = \frac{\lambda}{2}\left((n+2)(n+1)P_{n+2}(t) - n(n-1)P_n(t)\right) \\ + \sigma\left((n+1)P_{n+1}(t) - nP_n(t)\right) \ .\end{aligned} \tag{4.81}$$

Its corresponding "Schrödinger equation" for the generating function is

$$\begin{aligned}i\lambda\frac{\partial}{\partial it}G(\xi,t) &= \frac{\lambda^2}{2}(1-\xi^2)\frac{\partial^2}{\partial\xi^2}G(\xi,t) + \lambda\sigma(1-\xi)\frac{\partial}{\partial\xi}G(\xi,t) \\ &= -\frac{1}{2}(1-\xi^2)\hat{\pi}^2G(\xi,t) + i\sigma(1-\xi)\hat{\pi}G(\xi,t) \ ,\end{aligned} \tag{4.82}$$

where we use the momentum operator $\hat{\pi} = -i\lambda\partial/\partial\xi$ in the second line. The separation ansatz yields to the known result (4.16) for the time-dependent part and for the stationary part we find

$$E\varphi(\xi) = \frac{\lambda^2}{2}(1-\xi^2)\frac{\partial^2}{\partial\xi^2}\varphi(\xi) + \lambda\sigma(1-\xi)\frac{\partial}{\partial\xi}\varphi(\xi) \ . \tag{4.83}$$

In the manner of section 4.3.1 we use the ansatz $\varphi(\xi) = A(\xi)\exp(iS(\xi)/\lambda)$, sort the resulting equation for its real and imaginary part. Neglecting all terms scaling with λ^2 or $\lambda\sigma$ we find

$$E = \frac{1}{2}(\xi^2-1)\left(S'(\xi)\right)^2 \tag{4.84}$$

$$0 = \frac{\lambda}{2}(\xi+1)\left(2A'(\xi)S'(\xi) + A(\xi)S''(\xi)\right) + \sigma A(\xi)S'(\xi) \ . \tag{4.85}$$

The solution of equation (4.84) is the already discussed result (4.49). We can insert the derivatives of $S(\xi)$ and insert them into equation (4.85) to obtain a differential equation for $A(\xi)$ with the solution

$$A(\xi) = \tilde{c}(\xi^2-1)^{1/4}\left(\xi+1\right)^{-\sigma/\lambda} \ , \tag{4.86}$$

with a constant $\tilde{c}$. Hence, the generating function, fulfilling the initial condition $G(\xi_0,0) = \xi_0^{n_0}$, is

$$G(\xi,t) = \xi_0^{n_0} \left(\frac{\xi^2-1}{\xi_0^2-1}\right)^{1/4} \left(\frac{\xi_0+1}{\xi+1}\right)^{\sigma/\lambda} \times \exp\left(-\frac{\sqrt{2E}}{\lambda}(\arccos\xi - \arccos\xi_0) + \frac{1}{\lambda}Et\right) . \tag{4.87}$$

The classical energy is $E = \frac{1}{2}(\xi^2-1)\pi^2 - i\sigma(\xi-1)\pi$ and the classical equations of motion are

$$\frac{d\xi}{dit} = (\xi^2-1)\pi - i\sigma(\xi-1) = \sqrt{2E(\xi^2-1) - \sigma^2(\xi-1)^2} \tag{4.88}$$

$$\frac{d\pi}{dit} = -\xi\pi^2 + i\sigma\pi = -\pi\sqrt{2E + (\pi - i\sigma)^2} . \tag{4.89}$$

First, we evaluate the average particle number by means of the mean field dynamics

$$\frac{d\bar{\pi}}{dit} = -\bar{\pi}^2 + i\sigma\bar{\pi} . \tag{4.90}$$

The solution gives the average particle number

$$\langle n(t)\rangle = \frac{\sigma}{\lambda}\left(\frac{1}{1 - \frac{\lambda n_0}{\lambda n_0+\sigma}e^{-\sigma t}} - 1\right) . \tag{4.91}$$

In order to make analytical progress we simplify equation (4.88) furthermore by dropping the σ^2 term. This is fully consistent with the WKB method since by Taylor approximation the leading order of equation (4.88) is σ^2. Due to this approximation we find the same classical dynamics as in the case of binary annihilation, see equations (4.52) and (4.53). The solution for the corresponding classical equation of motion, determining ξ, is given in (4.55). Hence, the generating function has the same arguments in the exponential function as the generating function of the binary annihilation (4.50). It solely differs from (4.50) by the additional prefactor $\left(\frac{\xi_0+1}{\xi+1}\right)^{\sigma/\lambda}$. We calculate the probability $P_n(t)$ by means of the contour integral with a saddle point approximation. The saddle point condition (4.64) combined with the solution of the approximated classical equation of motion (4.55) gives the dependence

$$\xi_0 = -\frac{\sigma}{\lambda n_0} + \sqrt{\left(1 + \frac{\sigma}{\lambda n_0}\right)^2 - \frac{n^2}{n_0^2}\frac{1-\xi_s^2}{\xi_s^2}} . \tag{4.92}$$

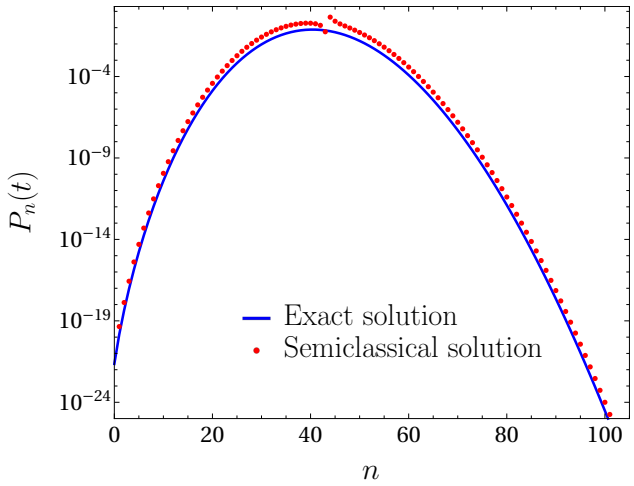

Figure 4.3.: Probability density distribution for the binary and single annihilation, see equation (4.81), at $t = 2$ on a logarithmic scale. Parameters are chosen as $n_0 = 300$, $\lambda = 0.01$ and $\sigma = 0.05$.

Recombining this equation with (4.55) yields an equation for ξ_s which can be solved numerically. Finally the probability reads

$$P_n(t) = \frac{\xi_0^{n_0}}{\sqrt{2\pi}} \left(\frac{1+\xi_0}{1+\xi_s}\right)^{\sigma/\lambda} \left(\frac{1-\xi_s^2}{1-\xi_0^2}\right)^{1/4} \left|\frac{1-\xi_s^2}{n-\langle n\rangle \xi_s^2}\right|^{1/2} \times \exp\left(-\frac{n^2}{2}\lambda t \frac{1-\xi_s^2}{\xi_s^2} - n\ln\xi_s\right) . \tag{4.93}$$

We notice that the probability has the same form as the probability for the binary annihilation. The differences are the additional prefactor and the value for ξ_s at the saddle point. The additional prefactor contributes only little to the value of (4.93) compared with the exponential. Furthermore, the value of the saddle point does not vary significantly from that of the binary annihilation. Hence, the probability $P_n(t)$ for the single and binary annihilation does not vary considerable from that for the pure binary annihilation. This means that the binary annihilation dominates the single annihilation considerably. In figure 4.3 we compare the approximation with the exact probabilities. We find some structure of the approximated probability near the maximum of the distribution. This is due to the prefactor which approaches zero in the denominator. Usually, in the saddle point approximation we consider the exponent only and do not consider the prefactor. If we do so, we would have to adapt an artificial prefactor in such a way that the normalization condition is

still fulfilled. In that case the structure would vanish. Overall the approximation coincides over many orders of magnitude well with the exact solution.

4.3.4. Third order reaction

We now study a reaction which combines the single and binary annihilation from the last example with the trimolecular annihilation. One may argue that trimolecular reactions do not occur as elementary events. There is, however, one instance where a trimolecular reaction can be used as an approximation to a multireaction sequence with a total of four reactant particles. For more details see [262].

The master equation for the combined reaction reads

$$\begin{aligned}\frac{d}{dt}P_n(t) = \mu\binom{n+3}{3}P_{n+3}(t) + \lambda\binom{n+2}{2}P_{n+2}(t) \\ + \sigma(n+1)P_{n+1}(t) - \left(\mu\binom{n}{3} + \lambda\binom{n}{2} + \sigma n\right)P_n(t)\ . \end{aligned} \tag{4.94}$$

We introduce the rate constant μ for the trimolecular reaction, which we assume to be of order λ^3. The rate constant σ of the single annihilation is of order λ. The corresponding "Schrödinger equation" is

$$\begin{aligned} i\lambda\frac{\partial}{\partial it}G(\xi,t) &= \lambda\sigma(1-\xi)\frac{\partial}{\partial\xi}G(\xi,t) + \frac{\lambda^2}{2}(1-\xi^2)\frac{\partial^2}{\partial\xi^2}G(\xi,t) \\ &\quad + \frac{\lambda\mu}{6}(1-\xi^3)\frac{\partial^3}{\partial\xi^3}G(\xi,t) \\ &= i\sigma(1-\xi)\hat{\pi}G(\xi,t) - \frac{1}{2}(1-\xi^2)\hat{\pi}^2G(\xi,t) \\ &\quad - i\frac{\mu}{6\lambda^2}(1-\xi^3)\hat{\pi}^3G(\xi,t)\ , \end{aligned} \tag{4.95}$$

with the momentum operator

$$\hat{\pi} = -i\lambda\frac{\partial}{\partial\xi}\ . \tag{4.96}$$

Applying the separation ansatz $G(\xi,t) = \psi(t)\varphi(\xi)$ yields to the result (4.16) for the time dependent part. The stationary "Schrödinger equation" can be written as

$$\begin{aligned} E\varphi(\xi) &= \lambda\sigma(1-\xi)\frac{\partial}{\partial\xi}\varphi(\xi) + \frac{\lambda^2}{2}(1-\xi^2)\frac{\partial^2}{\partial\xi^2}\varphi(\xi) \\ &\quad + \frac{\lambda\mu}{6}(1-\xi^3)\frac{\partial^3}{\partial\xi^3}\varphi(\xi)\ . \end{aligned} \tag{4.97}$$

We insert the ansatz $\varphi(\xi) = A(\xi)\exp(iS(\xi)/\lambda)$ to solve this equation. We sort for the real and imaginary parts and drop all terms of order λ^2 and above which gives

$$E = -\frac{1}{2}(1-\xi^2)\left(S'\right)^2 \tag{4.98}$$

$$0 = \sigma(1-\xi)AS' + \frac{\lambda}{2}(1-\xi^2)\left(2A'S' + AS''\right) - \frac{\mu}{6\lambda^2}(1-\xi^3)\left(S'\right)^3 A\,. \tag{4.99}$$

For convenience of the reader, we dropped the arguments of $A(\xi)$ and $S(\xi)$. Once again we remark the scaling behavior $\sigma \sim \lambda$ and $\mu \sim \lambda^3$. Interestingly, we find equation (4.98) which we also found in the last example and also for the binary annihilation. Its solution is given in equation (4.49). Furthermore, each single term of equation (4.99) is of order λ. This means that we formally can cancel the small parameter λ and so its order of magnitude does not appear in both equations. With $S'(\xi)$ from (4.98) we can solve equation (4.99) and find

$$A(\xi) = A_0(\xi_0)\exp\left(\frac{\mu E}{6\lambda^3}\frac{1}{1+\xi}\right)(\xi-1)^{(\lambda+\mu/\lambda^2 E)/4\lambda} \times (\xi+1)^{(3\lambda-12\sigma+\mu/\lambda^2 E)/12\lambda}\,. \tag{4.100}$$

With the initial condition $P_n(0) = \delta_{n,n_0}$ we are able to determine the constants. The probability now reads

$$P_n(t) = \frac{1}{2\pi i}\xi_0^{n_0}\exp\left(-\frac{\mu E}{6\lambda^3}\frac{1}{1+\xi_0}\right)\oint d\xi\, g(\xi,E)\exp\left(f(\xi,E)\right) \tag{4.101}$$

with

$$g(\xi,E) = \frac{1}{\xi}\left(\frac{\xi-1}{\xi_0-1}\right)^{(\lambda+\mu/\lambda^2 E)/4\lambda} \times \left(\frac{\xi+1}{\xi_0+1}\right)^{(3\lambda-12\sigma+\mu/\lambda^2 E)/12\lambda} \tag{4.102}$$

$$f(\xi,E) = \frac{\mu E}{6\lambda^3}\frac{1}{1+\xi} - \frac{\sqrt{2E}}{\lambda}(\arccos\xi - \arccos\xi_0) + \frac{Et}{\lambda} - n\ln\xi\,. \tag{4.103}$$

To make progress we specify the energy

$$E = i\sigma(1-\xi)\pi - \frac{1}{2}(1-\xi^2)\pi^2 - i\frac{\mu}{6\lambda^2}(1-\xi^3)\pi^3 \tag{4.104}$$

in terms of ξ. Therefore we have to solve the equations of motion

$$\frac{d\xi}{dit} = i\sigma(1-\xi) - (1-\xi^2)\pi - i\frac{\mu}{2\lambda^2}(1-\xi^3)\pi^2 \tag{4.105}$$

$$\frac{d\pi}{dit} = i\sigma\pi - \xi\pi^2 - i\frac{\mu}{2\lambda^2}\xi^2\pi^3 \ , \tag{4.106}$$

by inserting the solution of the energy for π into equation (4.106) which gives

$$\frac{\partial\xi}{\partial it} = \tau(\xi,E) \ . \tag{4.107}$$

The resulting equation cannot be solved analytically. Hence, we have to solve this equation by evaluating the integral (4.27) numerically. However, this can only be done if we know the functional coherence of ξ and ξ_0, which is obtained by the saddle point approximation, i.e., $f'(\xi_s,E) = 0$. We find

$$\begin{aligned} f'(\xi,E) = \frac{\mu E'}{6\lambda^3}\frac{1}{1+\xi} - \frac{\mu E}{6\lambda^3}\frac{1}{(1+\xi)^2} - \frac{\sqrt{2E'}}{\lambda}(\arccos\xi - \arccos\xi_0) \\ + \frac{\sqrt{2E}}{\lambda}\frac{1}{\sqrt{1-\xi^2}} + \frac{t}{\lambda}E' - \frac{n}{\xi} \end{aligned} \tag{4.108}$$

with E' from equation (4.33). Again, this equation has to be solved numerically. A value for ξ_s can be obtained by solving equation (4.36). This procedure requires the numerical solution of two equations combined with a numerical integration.

We remark that there are three possible solutions for π when solving equation (4.104). This is relevant for the numerical analysis as we find

$$\xi_s < 1 \quad \text{for} \quad n < \langle n\rangle \tag{4.109}$$

and

$$\xi_s > 1 \quad \text{for} \quad n > \langle n\rangle \tag{4.110}$$

where $\langle n\rangle$ is the average particle number. Thus, by performing the numerical analysis we have to use different solutions for π when we calculate the values for ξ_s. This is depending on the value of n being above or below $\langle n\rangle$. The mean field solution $\bar{\xi} = 1$ gives us the dynamics of the average particle number

$$\frac{d\bar{\pi}}{dit} = i\sigma\bar{\pi} - \bar{\pi}^2 - i\frac{\mu}{2\lambda^2}\bar{\pi}^3 \tag{4.111}$$

with

$$\bar{\pi} = -i\lambda\langle n\rangle \ . \tag{4.112}$$

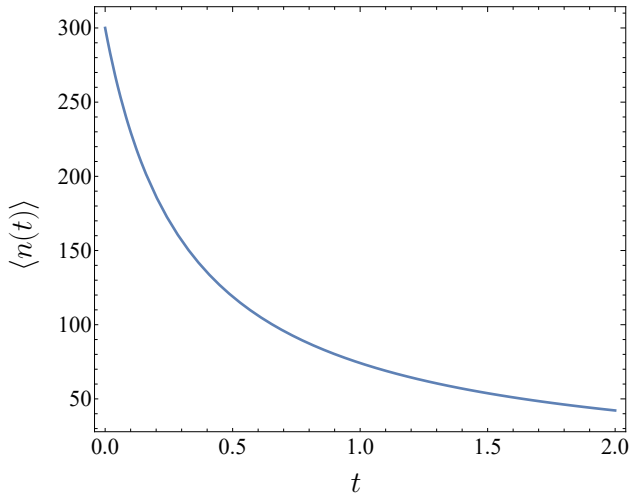

Figure 4.4.: Dependence of the average particle number on the time t. Parameters are chosen as $n_0 = 300$, $\lambda = 0.01$, $\sigma = \lambda$ and $\mu = \lambda^3$.

We show the average particle number $\langle n(t)\rangle$ in figure 4.4. We specify the parameters $\lambda = 0.01$, $\sigma = \lambda$, $\mu = \lambda^3$ and $n_0 = 300$. The average particle number at $t = 1$ is $\langle n(1)\rangle \approx 74.15$. Hence, the transition from $\xi_s < 1$ to $\xi_s > 1$ arises when $n \geq 75$ for $t = 1$ if we only consider integer particle numbers.

Having found the values for ξ_s we can now perform the saddle point approximation which gives us

$$P_n(t) = \frac{1}{2\pi}\xi_0^{n_0} \exp\left(-\frac{\mu E}{6\lambda^3}\frac{1}{1+\xi_0}\right) g(\xi_s, E_0) \times \frac{1}{\sqrt{|f''(\xi_s, E_0)|}} \exp\left(f(\xi_s, E_0)\right) \tag{4.113}$$

with the energy

$$E_0 = \lambda\sigma(1-\xi_0)n_0 + \frac{\lambda^2}{2}(1-\xi_0^2)n_0^2 + \frac{\lambda\mu}{6}(1-\xi_0^3)n_0^3 \tag{4.114}$$

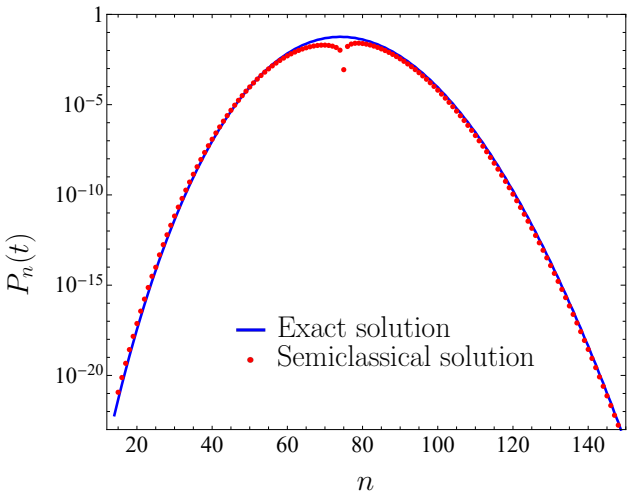

Figure 4.5.: Probability density distribution for the combined annihilation up to third order, see equation (4.94), at $t = 1$ on a logarithmic scale. Parameters are chosen as $n_0 = 300$, $\lambda = 0.01$, $\sigma = \lambda$ and $\mu = \lambda^3$.

and the second derivative

$$\begin{aligned} f''(\xi,E) = E'' &\left(\frac{\mu}{6\lambda^3}\frac{1}{1+\xi} - \frac{1}{\sqrt{2E}\lambda}(\arccos\xi - \arccos\xi_0) + \frac{t}{\lambda} \right) \\ + E' &\left(-\frac{\mu}{3\lambda^3}\frac{1}{(1+\xi)^2} + \frac{E'}{(2E)^{3/2}\lambda}(\arccos\xi - \arccos\xi_0) + \frac{2}{\sqrt{2E}\lambda}\frac{1}{\sqrt{1-\xi^2}} \right) \\ + &\frac{\mu E}{3\lambda^3}\frac{1}{(1+\xi)^3} + \frac{\sqrt{2E}}{\lambda}\frac{\xi}{(1-\xi^2)^{3/2}} + \frac{n}{\xi^2}\,, \end{aligned} \tag{4.115}$$

which is always real. In figure 4.5 we show the probability distribution $P_n(1)$ for the same parameter specification as in figure 4.4. Again we find a good agreement over many orders of magnitude between the semiclassical approximation and the exact solution, especially for the left tail of the distribution.

4.4. Conclusions

Extending the approach by Elgart and Kamenev, we put forward a model which is able to describe the probability of rare events in reaction-diffusion systems described by master equations. The systems consist of single-species particles with infinite-range interaction and we assume that spatial degrees of freedom are irrelevant. By means of a generating function we transform the master equation

into a time-dependent "Schrödinger equation" in imaginary time. As the master equation gives a probabilistic description of the system, so does the evolution equation for the generating function. In short, the master equation is equivalent to the time-dependent "Schrödinger equation" derived by means of the generating function. We separate the time-dependent part of the "Schrödinger equation" and the stationary part and thereby introduce a new constant which we will interpret as the energy or Hamilton function of the system. We apply a WKB approximation to solve the stationary part of the "Schrödinger equation", we identify a small parameter which is the analogue to Planck's constant $\hbar$. In order to find the rare event statistics we are interested in large deviations from a typical system behavior. A typical behavior can be calculated by the mean field approximation which allows us to calculate quantities such as the average particle number. Within the WKB approximation we can derive the classical equations of motion which determine the phase portrait of the system. The trajectories of the phase portrait are determined by the energy which is constant in the semiclassical description. These classical equations of motion need to be solved either analytically or numerically in order to find the solution for the generating function. Finally, the probability to find n particles at time t is calculated by Cauchy's integral formula on which we apply a saddle point approximation. At this point we make a transition from the semiclassical description in which the dynamics is determined by the phase portrait to a probabilistic description. Hence, when performing the saddle point approximation the energy does not remain constant and becomes a function of the phase space parameters. This dependence is determined by the classical equations of motion. We remark that the accuracy of the method breaks down in the vicinity of the average particle number and for small times when the condition $\langle n(t)\rangle \ll n_0$ is not satisfied.

We studied some systems. The single annihilation is exactly solvable. The binary annihilation process and the process which combines binary and single annihilation is analytically solved by means of the WKB approximation. For both systems we find good agreement over many orders of magnitude with the exact solution of the master equation. Finally, we analyzed a process that combines single, binary and triple annihilation. In general, the leading order of the stationary "Schrödinger equation" is obtained by the order of the highest annihilation process. The third order differential equation can be solved analytically when we require a certain scaling of its parameters and use the WKB approximation. However, the semiclassical equations of motion have to be solved numerically. Once more, in the tails of the distribution, we find a very good agreement with the exact solution over many orders of magnitude.

Rare events define the tail of the distribution. We are not interested in typical fluctuations near the maximum of the distribution where we find oscillations for

some examples. Nonetheless, the oscillations can easily be removed by dropping the prefactor of the distribution and replacing it with a normalization constant.

5. Summary and Outlook

Rare events can have significant influence on their environment or system. In this context they are referred to as extreme events. Such events are difficult to describe, especially when the constituents which form the system show correlated behavior or interact in a complex manner. Due to their ensuing consequences, it is of utmost importance to understand extreme events. An example of such an extreme event is the financial crisis 2007–2009 which had drastic influence on the world economy. It was triggered by the almost concurrent default of many small obligors who were not able to fully pay off their mortgages and housing loans. This is an economist's point of view as to why extreme events are important. There are many other fields where rare events are of great interest. Examples are epidemic disease spread or large fluctuations in the number of neutrons in a nuclear reactor, which causes an explosion.

In the first part of the thesis we focused on modeling financial markets and credit risk. Correlations between obligors are of central importance in credit risk estimation. If obligors are correlated by any kind of mutual dependencies they are, for example, most likely to be affected by bad news simultaneously. Thus, correlations increase the probability of default events to appear clustered. The influence of good news, however, is marginal because of the peculiar shape of the loss distribution of a credit portfolio which is usually asymmetric and has a heavy tail on the right-hand side, see figure 1.4. In addition, non-stationarity is a central aspect of financial markets. Particular attention was given to the non-stationarity of correlations.

We reviewed recent progress in modeling credit risk for correlated assets taking non-stationarity into account. We employed a new interpretation of the Wishart model for random correlation matrices to model non-stationary effects. We then used the Merton model for credit risk, in which default events and losses are derived from the asset values at maturity. To estimate the time development of the asset values, the stock prices are used. We accounted for the asset fluctuations by averaging over an ensemble of random matrices that models the truly existing set of measured correlation matrices. As a most welcome side effect, this approach drastically reduces the parameter dependence of the loss distribution, allowing us to obtain very explicit results which show quantitatively that the heavy tails prevail over diversification benefits even for small correlations. We calibrated the random

matrix model with market data and showed how it is capable of grasping different market situations. We showed the benefit of the random matrix approach in contrast to neglecting the fluctuations between the asset correlations by calculating the VaR. It is underestimated by up to 40% in the latter case. Furthermore, numerical simulations for two non-overlapping portfolios showed that concurrent large portfolio losses are more likely than concurrent small ones.

The numerical results revealed the necessity of incorporating the full dependence structure of joint risks and motivated new research on systemic credit risk. The full dependence structure is contained in the multivariate joint portfolio loss distribution. We analytically calculated this distribution for several cases. We showed that, for two non-overlapping credit portfolios, diversification does not work in a correlated market. Calculation of the portfolio loss correlations revealed that two creditors without any intersection are affected to similar losses simultaneously. This accounts not only for large portfolios with thousands of credit contracts, but also for small portfolios consisting of a few credit contracts only. We quantitatively modeled the reduction of risk if a credit portfolio invests in two on average uncorrelated markets rather than investing in merely one market. The former method yields a significantly lower tail risk also for very small portfolios than the latter method for very large portfolios. Furthermore, we included subordination levels, which were established in CDOs to protect the more senior tranches from high losses. We analytically corroborated the observation that an extreme loss of the subordinated creditor is likely to also yield a large loss of the senior creditor.

Current research in our group is based on the ensemble approach. It aims to further improve the agreement of the return distribution on empirical data. For further research, it is interesting to analyze avalanche and contagion effects. These effects are included only indirectly in our model, namely by calibrating to stock market states of crisis.

In the second part of this thesis we focused on rare event statistics in reacting systems. We considered systems of reacting particles and calculated the probabilities of finding them in states which largely deviate from typical behavior. We obtained the rare event statistics from the master equation, which describes the dynamics of the probability distribution of the particle number. We transformed the master equation by means of a generating function into a time-dependent "Schrödinger equation". Its solution is provided by a separation ansatz and an approximation for the stationary part which is of WKB type employing a small parameter. The solutions of the "classical" equations of motions and a saddle point approximation yield the proper generating function. Our approach extends a method put forward by Elgart and Kamenev (2004). We revisited the binary annihilation and showed by direct comparison that our extended method now outperforms the original method. We considered other examples analytically, such as the single annihilation and the

process which combines single and binary annihilation. Moreover, we calculated the rare event statistics for a system allowing for single, binary and triple annihilation, where the dynamics cannot be entirely analyzed in an analytical manner. For all examples mentioned, we find a good agreement in the region of validity of the approach, which is $1 \ll n \leq \langle n(t) \rangle$.

For future research, it is interesting to apply this approach to the migration of credit ratings. The migration can be described by a master equation. With the WKB approach one can calculate the probability for an extreme change in the current rating of a company. This could help to understand the intrinsic instabilities of the financial system.

A. Calculation of Moments

We define

$$\tau_{j,k}^{\iota,\lambda}(z,u) = \int_{-\infty}^{\hat{F}_k^{(\lambda)}} d\hat{V}_k \left(c^{(\iota)} - \frac{V_{k0}}{\hat{F}_k^{(\lambda)}} \exp\left(\sqrt{z}\hat{V}_k + \left(\mu_k - \frac{\rho_k^2}{2} \right) T \right) \right)^j \times \sqrt{\frac{N}{2\pi(1-c)T\rho_k^2}} \exp\left[\frac{N}{2(1-c)T\rho_k^2} \left(\hat{V}_k + \sqrt{cT}u\rho_k \right)^2 \right] , \quad \text{(A.1)}$$

where $\iota = S,J$ and $\lambda = S,J$, as well as $c^{(S)} = 1$ and $c^{(J)} = \frac{F_k}{F_k^{(J)}}$. Hence, we can write the moments

$$m_{j,k}^{(S)}(z,u) = \tau_{j,k}^{S,S}(z,u) \quad \text{(A.2)}$$

$$m_{j,k}^{(J)}(z,u) = \tau_{j,k}^{J,J}(z,u) - \tau_{j,k}^{J,S}(z,u) \, . \quad \text{(A.3)}$$

With the following definition

$$\Phi(x) = \frac{1}{2} + \frac{1}{2} \operatorname{erf}\left(\frac{x}{\sqrt{2}} \right) \quad \text{(A.4)}$$

and the error function

$$\operatorname{erf}(x) = \frac{2}{\sqrt{\pi}} \int_0^x dx e^{-x^2} \quad \text{(A.5)}$$

we can express the quantities $\tau_{j,k}^{\iota,\lambda}(z,u)$ for $j = 0,1,2$

$$\begin{aligned}
\tau_{0,k}^{\iota,\lambda}(z,u) &= \sqrt{\frac{N}{2\pi(1-c)T\rho_k^2}} \int_{-\infty}^{\hat{F}_k^{(\lambda)}} d\hat{V}_k \exp\left[\frac{N}{2(1-c)T\rho_k^2}\left(\hat{V}_k + \sqrt{cT}u\rho_k\right)^2\right] \\
&= \Phi\left(\sqrt{\frac{N}{(1-c)T\rho_k^2}}\left(\hat{F}_k^{(\lambda)} + \sqrt{cT}u\rho_k\right)\right) \qquad \text{(A.6)} \\
\tau_{1,k}^{\iota,\lambda}(z,u) &= c^{(\iota)}\tau_{0,k}^{\iota,\lambda}(z,u) - \frac{V_{k0}}{F_k^{(\iota)}} \exp\left[\frac{z(1-c)T\rho_k^2}{2N} - \sqrt{zcT}u\rho_k + \left(\mu_k - \frac{\rho_k^2}{2}\right)T\right] \\
&\quad \times \Phi\left(\sqrt{\frac{N}{(1-c)T\rho_k^2}}\left(\hat{F}_k^{(\lambda)} + \sqrt{cT}u\rho_k\right) - \sqrt{\frac{z(1-c)T\rho_k^2}{N}}\right) \qquad \text{(A.7)} \\
\tau_{2,k}^{\iota,\lambda}(z,u) &= -{c^{(\iota)}}^2\tau_{0,k}^{\iota,\lambda}(z,u) + 2c^{(\iota)}\tau_{1,k}^{\iota,\lambda}(z,u) \\
&\quad + \frac{V_{k0}^2}{{F_k^{(\iota)}}^2} \exp\left[\frac{2z(1-c)T\rho_k^2}{N} - 2\sqrt{zcT}u\rho_k + 2\left(\mu_k - \frac{\rho_k^2}{2}\right)T\right] \\
&\quad \times \Phi\left(\sqrt{\frac{N}{(1-c)T\rho_k^2}}\left(\hat{F}_k^{(\lambda)} + \sqrt{cT}u\rho_k\right) - 2\sqrt{\frac{z(1-c)T\rho_k^2}{N}}\right) . \qquad \text{(A.8)}
\end{aligned}$$

List of Figures

1.1. Evolution of the Dow Jones Industrial Average from 1950 to 2019 on a logarithmic scale. 5

1.2. (a) Daily closing prices in USD, (b) daily returns and (c) volatility estimated over a $T = 60$ day horizon for the Microsoft and Goodyear stock. The time period is January 1992 to June 2019. 7

1.3. Correlation matrices for 481 stocks from S&P500 index for four consecutive quarters beginning with the third quarter of 2018. . . . 10

1.4. Schematic loss distribution with $\mathrm{VaR}_{0.95}$ and $\mathrm{ETL}_{0.95}$ for a credit portfolio. 16

2.1. Schematic visualization of the Merton model. A default occurs if the asset value at maturity $V_K(T_\mathrm{M})$ drops below the face value F_k. In the red sketched scenario, a default occurs only to the junior subordinated creditor while the senior creditor obtains no loss. . . 23

2.2. Aggregated distribution of normalized returns $\tilde{r}$ for fixed covariances from the S&P 500 dataset, $\Delta t = 1$ trading day and window length $T = 25$ trading days. The circles show a normal distribution, the scale is logarithmic. Taken from [191]. 30

2.3. Aggregated distribution of the rotated and scaled returns $\tilde{r}$ for $\Delta t = 1$ (**top**) and $\Delta t = 20$ (**bottom**) trading days on a logarithmic scale. The circles correspond to the aggregation of the distribution (2.22). Taken from [191]. 31

2.4. Aggregated distribution for the normalized monthly returns with the empirical covariance matrix on a logarithmic scale. The black line shows the empirical distribution; the red dotted line shows the theoretical results. The insets show the corresponding linear plots. **Top** left/right: S&P 500 (1992–2012)/(2002–2012); **bottom** left/right: NASDAQ (1992–2012)/(2002–2012). Taken from [192]. . 32

2.5. Aggregated distribution for the normalized monthly returns with the effective correlation matrix on a logarithmic scale. The black line shows the empirical distribution; the red dotted line shows the theoretical results. The insets show the corresponding linear plots. **Top** left/right: S&P 500 (1992–2012)/(2002–2012); **bottom** left/right: NASDAQ (1992–2012)/(2002–2012). The average correlation coefficients are $c = 0.26$, 0.35, 0.21 and 0.25, respectively. Taken from [192]. 35

2.6. Average portfolio loss distribution for different portfolio sizes of $K = 10$, $K = 100$ and the limiting case $K \to \infty$. At the **top**, the maturity time is one month; at the **bottom**, it is one year. The scale is logarithmic. 38

2.7. Average loss distribution for different parameters taken from Table 2.1 on a logarithmic scale. The dashed line corresponds to the global financial crisis 2008–2010; the solid line corresponds to the calm period 2002–2004. 40

2.8. Average portfolio loss distribution for a homogeneous market and different values of N on a logarithmic scale. The portfolio size is $K = 100$. 41

2.9. Underestimation of the VaR if fluctuating asset correlations are not taken into account. The empirical covariance matrix is used and compared for different values of N. The scale is linear. Taken from [192]. 43

2.10. Heterogeneous correlation matrix for 481 stocks from S&P 500 index in the period January 2018 to July 2019 illustrating a financial market. The two rimmed squares correspond to two non-overlapping credit portfolios. 44

2.11. Average loss copula histograms for homogeneous portfolios with vanishing average asset correlations $c = 0$. The asset values are multivariate log-normal ($N \to \infty$) in the top figure and multivariate heavy-tailed ($N_{\text{eff}} = 5$) in the bottom figure. The color bar indicates the local deviations from the corresponding Gaussian copula. Taken from [193]. 46

2.12. Average loss copula histograms for homogeneous portfolios with asset correlations $c = 0.3$. The asset values are multivariate log-normal ($N \to \infty$). The drifts are $\mu = 10^{-3}\,\text{day}^{-1}$ (**top**), $3 \times 10^{-4}\,\text{day}^{-1}$ (**middle**) and $-3 \times 10^{-3}\,\text{day}^{-1}$ (**bottom**). The color bar indicates the local deviations from the corresponding Gaussian copula. Taken from [193]. 48

2.13. Average loss copula histograms for two portfolios with heterogeneous volatilities drawn from a uniform distribution in the interval (0,0.25). The color bar indicates the local deviations from the corresponding Gaussian copula. Taken from [193]. 49

2.14. Time averaged loss copula histograms for two empirical copulas of size $K = 50$. The asset values are multivariate log-normal ($N \to \infty$). **Top**: Portfolio 1 is always drawn from S&P 500 and Portfolio 2 from Nikkei 225; **middle**: both portfolios are drawn from S&P 500; **bottom**: both portfolios are drawn from Nikkei 225. The color bar indicates the local deviations from the corresponding Gaussian copula. Taken from [193]. 50

3.1. Setup of the generalized model illustrating a financial market by means of its average effective correlation matrix. The two rimmed squares correspond to two partially overlapping portfolios. 68

3.2. Average loss distribution on a logarithmic scale for a different number of markets and market size. The markets are homogeneous and we choose a face value of $F_0 = 75$ and the initial asset value $V_0 = 100$. 73

3.3. Average loss distribution for two disjoint portfolios of same sizes on a logarithmic scale. We show different market sizes, $K = 10$ orange, $K = 20$ blue and $K = 100$ green. The parameters are $\mu = 0.17\,\text{year}^{-1}$, $\rho = 0.35\,\text{year}^{-1/2}$, $N = 6$, $c = 0.28$ and a maturity time of $T_\text{M} = 1\,\text{year}$. 75

3.4. Probability of zero portfolio loss depending on the portfolio size K for different drift parameters μ on a logarithmic scale. 75

3.5. Portfolio loss correlation on a linear scale depending on the asset correlation c. Both portfolios are homogeneous and have the same size. The market size K ranges from 2 (blue) over 4, 8, 10, 20, 30, 50, 100, 200 to 500 (green). The bisecting line is shown in black. . 76

3.6. Portfolio loss correlation on a linear scale depending on the market size K for different average asset correlations c. The credit portfolios are disjoint, homogeneous and have the same size. 77

3.7. Average loss distribution for portfolios of different sizes on a logarithmic scale. Portfolio one is of fixed size $R_1 = 10$ and the market size is $K = 30$ (orange), $K = 110$ (blue) and $K \to \infty$ (green). The parameters are $\mu = 0.17\,\text{year}^{-1}$, $\rho = 0.35\,\text{year}^{-1/2}$, $N = 6$, $c = 0.28$ and a maturity time of $T_\text{M} = 1\,\text{year}$. 78

3.8. Portfolio loss correlation as a function of asset correlation c on a linear scale. Portfolio one is of fixed size $R_1 = 10$ and the market size K ranges from 30 (blue) over 50, 100, 200 to 500 (green). The limiting curve $K \to \infty$ is shown as dashed red line and the bisecting line is shown in black. 79
3.9. Average portfolio loss distribution of a subordinated debt structure on a logarithmic scale. Both portfolios operate on the entire market. We show different market sizes $K = 10$ orange, $K = 200$ blue and $K \to \infty$ green. 80
3.10. Marginal distributions of senior and junior subordinated creditor on a logarithmic scale. The upper three lines belong to the junior subordinated creditor and the lower three lines to the senior creditor. 81

4.1. Probability density distribution for the binary annihilation, see equation (4.40), at $t = 0.5$ on a logarithmic scale. Parameters are chosen as $n_0 = 300$ and $\lambda = 0.01$. 96
4.2. Decadic logarithm of the ratio of the exact solution and the time-dependent WKB approximations. The solid line shows the new approximation (4.68), the circles show the original result. Parameters are chosen as $n_0 = 300$, $t = 1$ and $\lambda = 0.01$. 97
4.3. Probability density distribution for the binary and single annihilation, see equation (4.81), at $t = 2$ on a logarithmic scale. Parameters are chosen as $n_0 = 300$, $\lambda = 0.01$ and $\sigma = 0.05$. 101
4.4. Dependence of the average particle number on the time t. Parameters are chosen as $n_0 = 300$, $\lambda = 0.01$, $\sigma = \lambda$ and $\mu = \lambda^3$. 105
4.5. Probability density distribution for the combined annihilation up to third order, see equation (4.94), at $t = 1$ on a logarithmic scale. Parameters are chosen as $n_0 = 300$, $\lambda = 0.01$, $\sigma = \lambda$ and $\mu = \lambda^3$. . 106

List of Tables

1.1. An excerpt of the order book for the SAP stock on Xetra stock exchange on July 24, 2019. The spread size is 0.06 Euro. 4
1.2. GICS classifications. 9

2.1. Average parameters used for two different time horizons. The values are taken from [192]. 39

Bibliography

[1] A. Mühlbacher and T. Guhr. Credit risk meets random matrices: Coping with non-stationary asset correlations. *Risks*, 6(42), 2018.

[2] A. Mühlbacher and T. Guhr. Extreme portfolio loss correlations in credit risk. *Risks*, 6(72), 2018.

[3] A. Mühlbacher and T. Guhr. WKB-type-of approximation for rare event statistics in reacting systems. *arXiv:1902.05280v2*, 2019.

[4] R. N. Mantegna and H. E. Stanley. *An introduction to econophysics: Correlations and complexity in finance*. Cambridge Univ. Press, Cambridge, 2007.

[5] J. Voit. *The statistical mechanics of financial markets*. Springer, Berlin, 2001.

[6] K. Gangopadhyay. Interview with Eugene H. Stanley. *IIM Kozhikode Society & Management Review*, 2(2):73–78, 2013.

[7] A. Bunde, J. Kropp, and H.-J. Schellnhuber. *The science of disasters: Climate disruptions, heart attacks and market crashes*. Springer, Berlin, 2002.

[8] A. Chatterjee, S. Yarlagadda, and B. K. Chakrabarti. *Econophysics of wealth distributions: Econophys-Kolkata I*. Springer Science & Business Media, 2007.

[9] O. Peters. The time resolution of the St Petersburg paradox. *Philosophical Transactions of the Royal Society A*, 369(1956):4913–4931, 2011.

[10] O. Peters and M. Gell-Mann. Evaluating gambles using dynamics. *Chaos: An Interdisciplinary Journal of Nonlinear Science*, 26(2):023103, 2016.

[11] D. Kahneman. *Thinking, fast and slow*. Lane, London, 2011.

[12] L. Bachelier. Théorie de la spéculation. *Annales scientifiques de l'École normale supérieure*, 3(3):21–86, 1900.

[13] A. Einstein. Über die von der molekularkinetischen Theorie der Wärme geforderte Bewegung von in ruhenden Flüssigkeiten suspendierten Teilchen. *Annalen der Physik*, 322(8):549–560, 1905.

[14] B. Mandelbrot. *The fractal geometry of nature*. Freemann, New York, 1988.

[15] B. Mandelbrot. The variation of certain speculative prices. *The Journal of Business*, 36, 1963.

[16] R. Friedrich, J. Peinke, and C. Renner. How to quantify deterministic and random influences on the statistics of the foreign exchange market. *Phys. Rev. Lett.*, 84(22):5224–5227, 2000.

[17] J. Peinke, F Böttcher, and S. Barth. Anomalous statistics in turbulence, financial markets and other complex systems. *Annalen der Physik*, 13:450–460, 2004.

[18] R. N. Mantegna and H. E. Stanley. Stock market dynamics and turbulence: Parallel analysis of fluctuation phenomena. *Physica A*, 239(1):255–266, 1997.

[19] R. Mantegna and H. E. Stanley. Turbulence and financial markets. *Nature*, 383:587–588, 1996.

[20] D. Sornette and A. Johansen. Large financial crashes. *Physica A*, 245(3):411–422, 1997.

[21] T. Kaizoji, S. Bornholdt, and Y. Fujiwara. Dynamics of price and trading volume in a spin model of stock markets with heterogeneous agents. *Physica A*, 316(1):441–452, 2002.

[22] S. Bornholdt. Expectation bubbles in a spin model of markets: Intermittency from frustration across scales. *International Journal of Modern Physics C*, 12(05):667–674, 2001.

[23] D. Chowdhury and D. Stauffer. A generalized spin model of financial markets. *The European Physical Journal B*, 8(3):477–482, 1999.

[24] J. C. Hull. *Options, futures, and other derivatives*. Pearson, Harlow, England, ninth edition, 2018.

[25] M. Wojtowicz. CDOs and the financial crisis: Credit ratings and fair premia. *Journal of Banking & Finance*, 39:1–13, 2014.

[26] F. Abergel, M. Anane, A. Chakraborti, A. Jedidi, and I. M. Toke. *Limit order books*. Cambridge University Press, 2016.

[27] M. Theissen, S. M. Krause, and T. Guhr. Regularities and irregularities in order flow data. *The European Physical Journal B*, 90(11):218, 2017.

[28] E. F. Fama and K. R. French. Long-horizon returns. *The Review of Asset Pricing Studies*, 8(2):232–252, 2018.

[29] W. C. Mitchell. *The making and using of index numbers*. US Government Printing Office Washington DC, 1938.

[30] M. Olivier. *Les Nombres indices de la variation des prix*. PhD thesis, Paris, 1926.

[31] F. C. Mills. *The Behavior of Prices*. National Bureau of Economic Research, Inc, 1927.

[32] P. K. Clark. A subordinated stochastic process model with finite variance for speculative prices. *Econometrica*, 41(1):135–155, 1973.

[33] D. Sornette. Multiplicative processes and power laws. *Phys. Rev. E*, 57(4):4811–4813, 1998.

[34] T. Lux and M. Marchesi. Scaling and criticality in a stochastic multi-agent model of a financial market. *Nature*, 397:498–500, 1998.

[35] R. N. Mantegna and H. E. Stanley. Scaling behavior in the dynamics of an economic index. *Nature*, 376:46–49, 1995.

[36] D. Challet, A. Chessa, M. Marsili, and Y C. Zhang. From minority games to real markets. *Quantitative Finance*, 1:168–176, 2000.

[37] X. Gabaix, P. Gopikrishnan, V. Plerou, and H. E. Stanley. A theory of power-law distributions in financial market fluctuations. *Nature*, 423:267–70, 2003.

[38] J. D. Farmer and F. Lillo. On the origin of power-law tails in price fluctuations. *Quantitative Finance*, 4(1):7–11, 2004.

[39] V. Plerou, P. Gopikrishnan, X. Gabaix, and H. E. Stanley. On the origin of power-law fluctuations in stock prices. *Quantitative Finance*, 4:11–15, 2004.

[40] P. Gopikrishnan, V. Plerou, L. A. N. Amaral, M. Meyer, and H. E. Stanley. Scaling of the distribution of fluctuations of financial market indices. *Phys. Rev. E*, 60:5305–16, 1999.

[41] R. D. F. Harris and C. C. Küçüközmen. The empirical distribution of UK and US stock returns. *Journal of Business Finance & Accounting*, 28(5-6):715–740, 2001.

[42] L. A. N. Amaral, V. Plerou, P. Gopikrishnan, M. Meyer, and H. E. Stanley. The distribution of returns of stock prices. *International Journal of Theoretical and Applied Finance*, 3:365–369, 2000.

[43] V. Plerou, P. Gopikrishnan, L. A. N. Amaral, M. Meyer, and H. E. Stanley. Scaling of the distribution of price fluctuations of individual companies. *Phys. Rev. E*, 60:6519–29, 1999.

[44] C. C. Ying. Stock market prices and volumes of sales. *Econometrica*, 34(3):676–685, 1966.

[45] T. W. Epps and M. L. Epps. The stochastic dependence of security price changes and transaction volumes: Implications for the mixture-of-distributions hypothesis. *Econometrica*, 44(2):305–21, 1976.

[46] P. C. Jain and G.-H. Joh. The dependence between hourly prices and trading volume. *Journal of Financial and Quantitative Analysis*, 23(3):269–283, 1988.

[47] R. J. Rogalski. The dependence of prices and volume. *The Review of Economics and Statistics*:268–274, 1978.

[48] J. M. Karpoff. The relation between price changes and trading volume: A survey. *The Journal of Financial and Quantitative Analysis*, 22(1):109–126, 1987.

[49] J. D. Farmer, L. Gillemot, F. Lillo, S. Mike, and A. Sen. What really causes large price changes? *Quantitative Finance*, 4(4):383–397, 2004.

[50] P. Weber and B. Rosenow. Large stock price changes: Volume or liquidity? *Quantitative Finance*, 6(1):7–14, 2006.

[51] T. A. Schmitt, R. Schäfer, M. C. Münnix, and T. Guhr. Microscopic understanding of heavy-tailed return distributions in an agent-based model. *Europhys. Letters*, 100(3):38005, 2012.

[52] R. Cont and J.-P. Bouchaud. Herd behavior and aggregate fluctuations in financial markets. *Macroeconomic Dynamics*, 4(2):170–196, 2000.

[53] F. Black. Studies of stock price volatility changes. In *Proceedings of the 1976 Meetings of the American Statistical Association, Business and Economics Statistics Section*, pages 177–181, 1976.

[54] G. W. Schwert. Why does stock market volatility change over time? *The Journal of Finance*, 44(5):1115–1153, 1989.

[55] Z. Ding, C. Granger, and R. Engle. A long memory property of stock market returns and a new model. *Journal of Empirical Finance*, 1(1):83–106, 1993.

[56] C. Granger and Z. Ding. Some properties of absolute return: An alternative measure of risk. *Annales d'Économie et de Statistique*, 40:67–91, 1995.

[57] R. Cont. Empirical properties of asset returns: Stylized facts and statistical issues. *Quantitative Finance*, 1(2):223–236, 2001.

[58] R. Cont. *Volatility clustering in financial markets: Empirical facts and agent-based models*. In *Long Memory in Economics*. Springer, Berlin, 2007, pages 289–309.

[59] F. H. Knight. *Risk, uncertainty and profit*. Boston: Houghton Mifflin, 1921.

[60] G. A. Holton. Defining risk. *Financial Analysts Journal*, 60(6):19–25, 2004.

[61] R. T. Rockafellar, S. Uryasev, and M. Zabarankin. Generalized deviations in risk analysis. *Finance and Stochastics*, 10(1):51–74, 2006.

[62] S. T. Rachev, S. Stoyanov, and F. J. Fabozzi. *Advanced Stochastic Models, Risk Assessment, and Portfolio Optimization: The Ideal Risk, Uncertainty, and Performance Measures*. The Frank J. Fabozzi series. Wiley, Hoboken (NJ), 2008.

[63] M. C. Münnix, T. Shimada, R. Schäfer, F. Leyvraz, T. H. Seligman, T. Guhr, and H. E. Stanley. Identifying states of a financial market. *Scientific reports*, 2(644), 2012.

[64] L. Laloux, P. Cizeau, J.-P. Bouchaud, and M. Potters. Noise dressing of financial correlation matrices. *Phys. Rev. Letters*, 83:1467, 1999.

[65] P. Gopikrishnan, B. Rosenow, V. Plerou, and H. E. Stanley. Quantifying and interpreting collective behavior in financial markets. *Phys. Rev. E*, 64(3):035106, 2001.

[66] L. Giada and M. Marsili. Data clustering and noise undressing of correlation matrices. *Phys. Rev. E*, 63(6):061101, 2001.

[67] L. Giada and M. Marsili. Algorithms of maximum likelihood data clustering with applications. *Physica A*, 315:650–664, 2002.

[68] T. Guhr and B. Kälber. A new method to estimate the noise in financial correlation matrices. *J. Phys. A*, 36(12):3009, 2003.

[69] A. Sklar. Fonctions de répartition án dimensions et leurs marges. *Publ. Inst. Statist. Univ. Paris*, 8:229–231, 1959.

[70] A. Sklar. Random variables, joint distribution functions, and copulas. *Kybernetika*, 9:449–460, 1973.

[71] J. V. Rosenberg and T. Schuermann. A general approach to integrated risk management with skewed, fat-tailed risks. *Journal of Financial Economics*, 79(3):569–614, 2006.

[72] V. Fernandez. Copula-based measures of dependence structure in assets returns. *Physica A*, 387(14):3615–3628, 2008.

[73] Y. Malevergne and D. Sornette. Testing the gaussian copula hypothesis for financial assets dependence. *Quantitative Finance*, 3:231–250, 2001.

[74] E. Kole, K. Koedijk, and M. Verbeek. Selecting copulas for risk management. *Journal of Banking & Finance*, 31(8):2405–2423, 2007.

[75] D. Brigo, A. Pallavicini, and R. Torresetti. *Credit Models and the Crisis: A Journey into CDOs, Copulas, Correlations and Dynamic Models*. John Wiley & Sons, 2010.

[76] U. Cherubini. *Copula methods in finance*. John Wiley & Sons, Hoboken, NJ, 2004.

[77] J. C. Hull and A. D. White. Valuing credit derivatives using an implied copula approach. *The Journal of Derivatives*, 14(2):8–28, 2006.

[78] M. Hofert and M. Scherer. CDO pricing with nested Archimedean copulas. *Quantitative Finance*, 11(5):775–787, 2011.

[79] A. Di Clemente and C. Romano. Measuring and optimizing portfolio credit risk: A copula-based approach*. *Economic Notes*, 33(3):325–357, 2004.

[80] C. Genest, M. Gendron, and M. Bourdeau-Brien. The advent of copulas in finance. *The European Journal of Finance*, 15(7-8):609–618, 2009.

[81] A. J. Patton. A review of copula models for economic time series. *Journal of Multivariate Analysis*, 110:4–18, 2012.

[82] D. Chetalova, M. Wollschläger, and R. Schäfer. Dependence structure of market states. *J. Stat. Mech.*, 2015(8):P08012, 2015.

[83] M. Wollschläger and R. Schäfer. Impact of nonstationarity on estimating and modeling empirical copulas of daily stock returns. *Journal of Risk*, 19(1), 2016.

[84] S. Wang and T. Guhr. Local fluctuations of the signed traded volumes and the dependencies of demands: A copula analysis. *J. Stat. Mech.*, 2018(3):033407, 2018.

[85] R. B. Nelsen. *An introduction to copulas*. Springer Science & Business Media, 2007.

[86] M. F. M. Osborne. Brownian motion in the stock market. *Operations Research*, 7(2):145–173, 1959.

[87] F. Black and M. Scholes. The pricing of options and corporate liabilities. *Journal of Political Economy*, 81(3):637–654, 1973.

[88] R. C. Merton. Theory of rational option pricing. *The Bell Journal of Economics and Management Science*, 4(1):141–183, 1973.

[89] M. L. Mehta. *Random matrices*. Elsevier, Amsterdam, 3. ed. Edition, 2004.

[90] V. Plerou, P. Gopikrishnan, B. Rosenow, L. A. N. Amaral, and H. E. Stanley. Universal and nonuniversal properties of cross correlations in financial time series. *Phys. Rev. Letters*, 83(7):1471, 1999.

[91] V. Plerou, P. Gopikrishnan, B. Rosenow, L. A. N. Amaral, T. Guhr, and H. E. Stanley. Random matrix approach to cross correlations in financial data. *Phys. Rev. E*, 65(6):066126, 2002.

[92] M. Potters, J.-P. Bouchaud, and L. Laloux. Financial applications of random matrix theory: Old laces and new pieces. *Science & Finance*, 36:2767–2784, 2005.

[93] Z. Burda, A. Jarosz, M. A. Nowak, J. Jurkiewicz, G. Papp, and I. Zahed. Applying free random variables to random matrix analysis of financial data. Part I: The Gaussian case. *Quantitative Finance*, 11(7):1103–1124, 2011.

[94] S. Drozdz, J. Kwapień, and P Oswiecimka. Empirics versus rmt in financial cross-correlations. *Acta Physica Polonica B*, 38:4027–4039, 2007.

[95] J. Daly, M. Crane, and H. Ruskin. Random matrix theory filters in portfolio optimisation: A stability and risk assessment. *Physica A*, 387(16):4248–4260, 2008.

[96] L. Laloux, P. Cizeau, M. Potters, and J.-P. Bouchaud. Random matrix theory and financial correlations. *International Journal of Theoretical and Applied Finance*, 03(3):391–397, 2000.

[97] S. Pafka and I. Kondor. Estimated correlation matrices and portfolio optimization. *Physica A*, 343:623–634, 2004.

[98] S. Sharifi, M. Crane, A. Shamaie, and H. Ruskin. Random matrix theory for portfolio optimization: A stability approach. *Physica A*, 335(3):629–643, 2004.

[99] P. Jorion. *Value at risk : The new benchmark for managing financial risk.* McGraw-Hill, New York, NY, 3. ed. Edition, 2007.

[100] A. J. McNeil, R. Frey, and P. Embrechts. *Quantitative risk management: Concepts, techniques and tools.* Princeton University Press, 2015.

[101] K. A. Horcher. *Essentials of financial risk management.* Wiley, Hoboken, N.J., 2005.

[102] H. Markowitz. Portfolio selection. *The Journal of Finance*, 7(1):77–91, 1952.

[103] P. Embrechts, A. J. McNeil, and D. Straumann. *Correlation and dependence in risk management: Properties and pitfalls.* In *Risk Management: Value at Risk and Beyond.* Cambridge University Press, 2002, 176–223.

[104] J. Daníelsson, B. N. Jorgensen, G. Samorodnitsky, M. Sarma, and C. G. de Vries. Fat tails, VaR and subadditivity. *Journal of Econometrics*, 172(2):283–291, 2013.

[105] Basel Comittee on Banking Supervision. Basel II: International Convergence of Capital Measurement and Capital Standards: A Revised Framework, 2006.

[106] Basel Comittee on Banking Supervision. Basel III: A global regulatory framework for more resilient banks and banking systems, 2010.

[107] P. Artzner, F. Delbaen, J.-M. Eber, and D. Heath. Coherent measures of risk. *Mathematical Finance*, 9(3):203–228, 1999.

[108] C. Acerbi and D. Tasche. On the coherence of expected shortfall. *Journal of Banking & Finance*, 26(7):1487–1503, 2002.

[109] J. C. Hull. The credit crunch of 2007: What went wrong? Why? What lessons can be learned? *J. Credit Risk*, 5(2):3–18, 2009.

[110] B. Eichengreen, A. Mody, M. Nedeljkovic, and L. Sarno. How the subprime crisis went global: Evidence from bank credit default swap spreads. *Journal of International Money and Finance*, 31(5):1299–1318, 2012.

[111] M. Crouhy, R. Jarrow, and S. Turnbull. The subprime credit crisis of 2007. *Journal of Derivatives*, 16:81–110, 2008.

[112] E. Benmelech and J. Dlugosz. The alchemy of CDO credit ratings. *Journal of Monetary Economics*:617–634, 2009.

[113] D. Duffie and N. Gârleanu. Risk and valuation of collateralized debt obligations. *Financial Analysts Journal*, 57(1):41–59, 2001.

[114] F. A. Longstaff and A. Rajan. An empirical analysis of the pricing of collateralized debt obligations. *The Journal of Finance*, 63(2):529–563, 2008.

[115] T. R. Bielecki and M. Rutkowski. *Credit risk: Modeling, valuation and hedging*. Springer Science & Business Media, 2013.

[116] C. Bluhm, L. Overbeck, and C. Wagner. *Introduction to credit risk modeling*. Crc Press, 2016.

[117] M. Crouhy, D. Galai, and R. Mark. A comparative analysis of current credit risk models. *Journal of Banking & Finance*, 24(1-2):59–117, 2000.

[118] D. Duffie and K. J. Singleton. Modeling term structures of defaultable bonds. *The Review of Financial Studies*, 12(4):687, 1999.

[119] P. Glasserman and J. Ruiz-Mata. Computing the credit loss distribution in the Gaussian copula model: A comparison of methods. *J. Credit Risk*, 2(4):33–66, 2006.

[120] E. Heitfield, S. Burton, and S. Chomsisengphet. Systematic and idiosyncratic risk in syndicated loan portfolios. *J. Credit Risk*, 2(3):3–31, 2006.

[121] D. Lando. *Credit risk modeling: Theory and applications*. Princeton University Press, 2009.

[122] G. Mainik and P. Embrechts. Diversification in heavy-tailed portfolios: Properties and pitfalls. *Annals of Actuarial Science*, 7(1):26–45, 2013.

[123] N. K. Avkiran, C. Ringle, and R. K. Y. Low. Monitoring transmission of systemic risk: Application of partial least squares structural equation modeling in financial stress testing. *Journal of Risk*, 20(5):83–115, 2018.

[124] D. Egloff, M. Leippold, and P. Vanini. A simple model of credit contagion. *Journal of Banking & Finance*, 31(8):2475–2492, 2007.

[125] K. Giesecke and S. Weber. Cyclical correlations, credit contagion, and portfolio losses. *Journal of Banking & Finance*, 28(12):3009–3036, 2004.

[126] K. Giesecke and S. Weber. Credit contagion and aggregate losses. *Journal of Economic Dynamics and Control*, 30(5):741–767, 2006.

[127] J. P. L. Hatchett and R. Kühn. Credit contagion and credit risk. *Quantitative Finance*, 9(4):373–382, 2009.

[128] R. K. Y. Low, J. Alcock, R. Faff, and T. Brailsford. Canonical vine copulas in the context of modern portfolio management: Are they worth it? *Journal of Banking & Finance*, 37(8):3085–3099, 2013.

[129] R. K. Y. Low. Vine copulas: Modelling systemic risk and enhancing higher-moment portfolio optimisation. *Accounting & Finance*, 58(S1):423–463, 2018.

[130] P. J. Schönbucher. Factor models: Portfolio credit risks when defaults are correlated. *Journal of Risk Finance*, 3(1):45–56, 2001.

[131] P. Glasserman. Tail approximations for portfolio credit risk. *The Journal of Derivatives*, 12(2):24–42, 2004.

[132] R. Schäfer, M. Sjölin, A. Sundin, M. Wolanski, and T. Guhr. Credit risk - A structural model with jumps and correlations. *Physica A*, 383(2):533–569, 2007.

[133] A. F. Koivusalo and R. Schäfer. Calibration of structural and reduced-form recovery models. *J. Credit Risk*, 8(4):31–51, 2012.

[134] T. A. Schmitt, D. Chetalova, R. Schäfer, and T. Guhr. Credit risk and the instability of the financial system: An ensemble approach. *Europhys. Letters*, 105(3):38004, 2014.

[135] M. Bardoscia, S. Battiston, F. Caccioli, and G. Caldarelli. Pathways towards instability in financial networks. *Nature Communications*, 8:14416, 2017.

[136] J. E. Humphrey, K. L. Benson, R. K. Low, and W.-L. Lee. Is diversification always optimal? *Pacific-Basin Finance Journal*, 35:521–532, 2015.

[137] R. Ibragimov and J. Walden. The limits of diversification when losses may be large. *Journal of Banking & Finance*, 31(8):2551–2569, 2007.

[138] F. Corsi, S. Marmi, and F. Lillo. When micro prudence increases macro risk: The destabilizing effects of financial innovation, leverage, and diversification. *Operations Research*, 64(5):1073–1088, 2016.

[139] W. Wagner. Diversification at financial institutions and systemic crises. *Journal of Financial Intermediation*, 19(3):373–386, 2010.

[140] Y.-T. Hu, R. Kiesel, and W. Perraudin. The estimation of transition matrices for sovereign credit ratings. *Journal of Banking & Finance*, 26:1383–1406, 2002.

[141] D. Lando and T. M. Skødeberg. Analyzing rating transitions and rating drift with continuous observations. *Journal of Banking & Finance*, 26(2-3):423–444, 2002.

[142] C. Stefanescu, R. Tunaru, and S. Turnbull. The credit rating process and estimation of transition probabilities: A bayesian approach. *Journal of Empirical Finance*, 16:216–234, 2009.

[143] E. I. Altman. The importance and subtlety of credit rating migration. *Journal of Banking & Finance*, 22(10-11):1231–1247, 1998.

[144] A. Bangia, F. X. Diebold, A. Kronimus, C. Schagen, and T. Schuermann. Ratings migration and the business cycle, with application to credit portfolio stress testing. *Journal of Banking & Finance*, 26(2):445–474, 2002.

[145] H. Frydman and T. Schuermann. Credit rating dynamics and markov mixture models. *Journal of Banking & Finance*, 32:1062–1075, 2008.

[146] K. Giesecke. Credit risk modeling and valuation: An introduction. In D. Shimko, editor, *Credit Risk: Models and Management*, pages 487–526. Risk Books, 2nd edition, 2004.

[147] R. C. Merton. On the pricing of corporate debt: The risk structure of interest rates. *The Journal of finance*, 29(2):449–470, 1974.

[148] F. Black and J. C. Cox. Valuing corporate securities: Some effects of bond indenture provisions. *The Journal of Finance*, 31(2):351–367, 1976.

[149] Y. Katz and N. Shokhirev. Default Risk Modeling Beyond the First-Passage Approximation: Extended Black-Cox Model. *Phys. Rev. E*, 82:016116, 2010.

[150] A. Elizalde. *Credit risk models II: Structural models.* Documentos de Trabajo CEMFI, 2005.

[151] S. Chava, C. Stefanescu, and S. Turnbull. Modeling the loss distribution. *Management Science*, 57(7):1267–1287, 2011.

[152] J. C. Hull and A. D. White. Valuing credit default swaps I. *The Journal of Derivatives*, 8(1):29–40, 2000.

[153] R. A. Jarrow and S. M. Turnbull. Pricing derivatives on financial securities subject to credit risk. *The Journal of Finance*, 50(1):53–85, 1995.

[154] P. J. Schönbucher. *Credit derivatives pricing models: Models, pricing and implementation.* John Wiley & Sons, 2003.

[155] G. M. Gupton, C. C. Finger, and M. Bhatia. *Creditmetrics: Technical document*. JP Morgan & Co., 1997.

[156] P. Crosbie and J. Bohn. *Modeling default risk*. Moody's KMV Company, 2003.

[157] C. S. F. Boston. CreditRisk+: A credit risk management framework. Technical report, Credit Suisse First Boston, 1997.

[158] T. C. Wilson. Portfolio credit risk (I). *Risk Magazine*, 10:111–117, 1997.

[159] P. Embrechts, C. Klüppelberg, and T. Mikosch. *Modelling extremal events for insurance and finance*. Springer, Berlin, 1997.

[160] H. Haken. *Synergetics: An introduction*. Springer, Berlin, 3., rev. and enl. Edition, 1983.

[161] G. Haag. *Modelling with the Master Equation: Solution Methods and Applications in Social and Natural Sciences*. Springer International Publishing, Cham, 2017.

[162] A. Nordsieck, W. Lamb, and G. Uhlenbeck. On the theory of cosmic-ray showers I the furry model and the fluctuation problem. *Physica*, 7(4):344–360, 1940.

[163] T. Jahnke and W. Huisinga. Solving the chemical master equation for monomolecular reaction systems analytically. *J. Math. Bio.*, 54(1):1–26, 2007.

[164] D. A. McQuarrie. Kinetics of small systems I. *J. Chem. Phys.*, 38(2):433–436, 1963.

[165] D. A. McQuarrie, C. J. Jachimowski, and M. E. Russell. Kinetics of small systems II. *J. Chem. Phys.*, 40(10):2914–2921, 1964.

[166] I. J. Laurenzi. An analytical solution of the stochastic master equation for reversible bimolecular reaction kinetics. *J. Chem. Phys.*, 113(8):3315–3322, 2000.

[167] G Haag, W Weidlich, and P Alber. Approximation methods for stationary solutions of discrete master equations. *Zeitschrift für Physik B Condensed Matter*, 26(2):207–215, 1977.

[168] J. Schnakenberg. Network theory of microscopic and macroscopic behavior of master equation systems. *Reviews of Modern physics*, 48(4):571, 1976.

[169] A. M. Walczak, A. Mugler, and C. H. Wiggins. Analytic methods for modeling stochastic regulatory networks. In X. Liu and M. D. Betterton, editors, *Computational Modeling of Signaling Networks*, pages 273–322. Springer, 2012.

[170] G. Jenkinson and J. Goutsias. Numerical integration of the master equation in some models of stochastic epidemiology. *PLoS ONE*, 7(5), 2012.

[171] D. Schnoerr, G. Sanguinetti, and R. Grima. Approximation and inference methods for stochastic biochemical kinetics - A tutorial review. *J. Phys. A*, 50(9):093001, 2017.

[172] H. Li, Y. Cao, L. R. Petzold, and D. T. Gillespie. Algorithms and software for stochastic simulation of biochemical reacting systems. *Biotechnology Progress*, 24(1):56–61, 2008.

[173] J. Pahle. Biochemical simulations: Stochastic, approximate stochastic and hybrid approaches. *Briefings in Bioinformatics*, 10(1):53–64, 2009.

[174] D. T. Gillespie, A. Hellander, and L. R. Petzold. Perspective: Stochastic algorithms for chemical kinetics. *J. Chem. Phys.*, 138(17):170901, 2013.

[175] S. Mauch and M. Stalzer. Efficient formulations for exact stochastic simulation of chemical systems. *IEEE/ACM Trans. on Computational Biology and Bioinformatics*, 8(1):27–35, 2011.

[176] D. T. Gillespie. A general method for numerically simulating the stochastic time evolution of coupled chemical reactions. *J. Comput. Phys.*, 22(4):403–434, 1976.

[177] D. T. Gillespie. Exact stochastic simulation of coupled chemical reactions. *J. Phys. Chem.*, 81(25):2340–2361, 1977.

[178] D. T. Gillespie. Stochastic simulation of chemical kinetics. *Annu. Rev. Phys. Chem.*, 58(1):35–55, 2007.

[179] H Risken. Solutions of the fokker-planck equation in detailed balance. *Zeitschrift für Physik A Hadrons and Nuclei*, 251(3):231–243, 1972.

[180] H. Risken. *The Fokker-Planck Equation*, volume 2. Springer, Berlin, 1996.

[181] N. G. Van Kampen. *Stochastic Processes in Physics and Chemistry*. Elsevier, Amsterdam, third edition, 2007.

[182] G Haag. Transition factor method for discrete master equations; and application to chemical reactions. *Zeitschrift für Physik B Condensed Matter*, 29(2):153–159, 1978.

[183] R. Kubo, K. Matsuo, and K. Kitahara. Fluctuation and relaxation of macrovariables. *J. Stat. Phys.*, 9(1):51–96, 1973.

[184] H. Gang. Stationary solution of master equations in the large-system-size limit. *Phys. Rev. A*, 36(12):5782–5790, 1987.

[185] M. I. Dykman, E. Mori, J. Ross, and P. M. Hunt. Large fluctuations and optimal paths in chemical kinetics. *The Journal of Chemical Physics*, 100(8):5735–5750, 1994.

[186] V. Elgart and A. Kamenev. Rare event statistics in reaction-diffusion systems. *Phys. Rev. E*, 70(4):041106, 2004.

[187] D. J. Fenn, M. A. Porter, S. Williams, M. Mcdonald, N. F. Johnson, and N. S. Jones. Temporal evolution of financial market correlations. *Phys. Rev. E*, 84:026109, 2011.

[188] Y. Zhang, G. H. T. Lee, J. C. Wong, J. L. Kok, M. Prusty, and S. A. Cheong. Will the US economy recover in 2010? A minimal spanning tree study. *Physica A*, 390(11):2020–2050, 2011.

[189] D.-M. Song, M. Tumminello, W.-X. Zhou, and R. N. Mantegna. Evolution of worldwide stock markets, correlation structure, and correlation-based graphs. *Phys. Rev. E*, 84(2):026108, 2011.

[190] L. Sandoval and I. D. P. Franca. Correlation of financial markets in times of crisis. *Physica A*, 391(1):187–208, 2012.

[191] T. A. Schmitt, D. Chetalova, R. Schäfer, and T. Guhr. Non-stationarity in financial time series: Generic features and tail behavior. *Europhys. Letters*, 103(5):58003, 2013.

[192] T. A. Schmitt, D. Chetalova, R. Schäfer, and T. Guhr. Credit risk: Taking fluctuating asset correlations into account. *J. Credit Risk*, 11(3):73–94, 2015.

[193] J. Sicking, T. Guhr, and R. Schäfer. Concurrent credit portfolio losses. *PLOS ONE*, 13(2):1–20, 2018.

[194] D. Chetalova, T. A. Schmitt, R. Schäfer, and T. Guhr. Portfolio return distributions: Sample statistics with stochastic correlations. *International Journal of Theoretical and Applied Finance*, 18(02):1550012, 2015.

[195] M. C. Münnix, R. Schäfer, and T. Guhr. A random matrix approach to credit risk. *PLoS ONE*, 9(5):e98030, 2014.

[196] D. X. Li. On default correlation: A copula function approach. *The Journal of Fixed Income*, 9(4):43–54, 2000.

[197] D. Di Gangi, F. Lillo, and D. Pirino. Assessing systemic risk due to fire sales spillover through maximum entropy network reconstruction. *Journal of Economic Dynamics and Control*, 94:117–141, 2018.

[198] J.-C. Duan. Maximum likelihood estimation using price data of the derivative contract. *Mathematical Finance*, 4(2):155–167, 1994.

[199] Y. H. Eom, J. Helwege, and J.-Z. Huang. Structural models of corporate bond pricing: An empirical analysis. *The Review of Financial Studies*, 17(2):499–544, 2004.

[200] J. Wishart. The generalised product moment distribution in samples from a normal multivariate population. *Biometrika*, 20A:32–52, 1928.

[201] R. J. Muirhead. *Aspects of multivariate statistical theory*. Wiley, New York, 1982.

[202] J.-P. Bouchaud and M. Potters. *Theory of financial risk and derivative pricing: From statistical physics to risk management*. Cambridge University Press, 2003.

[203] M. Tumminello, T. Aste, T. Di Matteo, and R. N. Mantegna. A tool for filtering information in complex systems. *Proceedings of the National Academy of Sciences*, 102(30):10421–10426, 2005.

[204] J. Gao. Recurrence time statistics for chaotic systems and their applications. *Phys. Rev. Letters*, 83(16):3178, 1999.

[205] R. Hegger, H. Kantz, L. Matassini, and T. Schreiber. Coping with nonstationarity by overembedding. *Phys. Rev. Letters*, 84(18):4092, 2000.

[206] P. Bernaola-Galván, P. C. Ivanov, L. A. N. Amaral, and H. E. Stanley. Scale invariance in the nonstationarity of human heart rate. *Phys. Rev. Letters*, 87(16):168105, 2001.

[207] C. Rieke, K. Sternickel, R. G. Andrzejak, C. E. Elger, P. David, and K. Lehnertz. Measuring nonstationarity by analyzing the loss of recurrence in dynamical systems. *Phys. Rev. Letters*, 88(24):244102, 2002.

[208] R. K. Zia and P. A. Rikvold. Fluctuations and correlations in an individual-based model of biological coevolution. *J. Phys. A*, 37(19):5135, 2004.

[209] R. K. Zia and B. Schmittmann. A possible classification of nonequilibrium steady states. *J. Phys. A*, 39(24):L407, 2006.

[210] Financial data from Yahoo! Finance. Available online: `http://finance.yahoo.com`, 2017.

[211] F. Meudt, M. Theissen, R. Schäfer, and T. Guhr. Constructing analytically tractable ensembles of stochastic covariances with an application to financial data. *J. Stat. Mech.*, 2015(11):P11025, 2015.

[212] C. Gouriéroux and R. Sufana. Derivative Pricing with Multivariate Stochastic Volatility: Application to Credit Risk. Working Papers 2004-31, Center for Research in Economics and Statistics, 2004.

[213] C. Gouriéroux, J. Jasiak, and R. Sufana. The wishart autoregressive process of multivariate stochastic volatility. *Journal of Econometrics*, 150(2):167–181, 2009.

[214] K. Itô. Stochastic integral. *Proceedings of the Imperial Academy*, 20(8):519–524, 1944.

[215] M. J. Lighthill. *An introduction to Fourier analysis and generalised functions*. Cambridge University Press, 1958.

[216] S. Heise and R. Kühn. Derivatives and credit contagion in interconnected networks. *The European Physical Journal B*, 85(4):115, 2012.

[217] A. Lucas, P. Klaassen, P. Spreij, and S. Straetmans. An analytic approach to credit risk of large corporate bond and loan portfolios. *Journal of Banking & Finance*, 25(9):1635–1664, 2001.

[218] T. Preis, D. Kenett, H. E. Stanley, D. Helbing, and E. Ben-Jacob. Quantifying the behavior of stock correlations under market stress. *Scientific reports*, 2:752, 2012.

[219] X. An, Y. Deng, J. B. Nichols, and A. B. Sanders. What is subordination about? Credit risk and subordination levels in commercial mortgage-backed securities (CMBS). *The Journal of Real Estate Finance and Economics*, 51(2):231–253, 2015.

[220] G. Gorton and A. M. Santomero. Market discipline and bank subordinated debt: Note. *Journal of Money, Credit and Banking*, 22(1):119–128, 1990.

[221] T. Nitschke. *Ensemble-Ansatz zur Modellierung des Kreditrisikos im Falle im Mittel unkorrelierter Märkte*. Bachelor's thesis, University of Duisburg-Essen, 2014.

[222] W. N. Goetzmann, L. Li, and K. G. Rouwenhorst. Long-term global market correlations. *The Journal of Business*, 78(1):1–38, 2005.

[223] L. Cardelli, M. Kwiatkowska, and L. Laurenti. Stochastic analysis of chemical reaction networks using linear noise approximation. *Biosystems*, 149:26–33, 2016.

[224] M. S. Bartlett. *Stochastic Population Models in Ecology and Epidemiology*. Wiley, New York, 1960.

[225] L. J. Allen. *An Introduction to Stochastic Processes with Applications to Biology*. CRC Press, Hoboken, NJ, 2010.

[226] R. M. Nisbet and W. Gurney. *Modelling Fluctuating Populations*. Wiley, New York, 1982.

[227] I. Nåsell. *Extinction and Quasi-Stationarity in the Stochastic Logistic SIS Model*. Springer, Berlin, 2011.

[228] A. Altland, A. Fischer, J. Krug, and I. G. Szendro. Rare events in population genetics: Stochastic tunneling in a two-locus model with recombination. *Phys. Rev. Lett.*, 106(8):088101, 2011.

[229] H. Andersson and T. Britton. *Stochastic Epidemic Models and Their Statistical Analysis*, volume 151 of *Lecture Notes in Statistics*. Springer, New York, NY, 2000.

[230] L. J. Allen, F. Brauer, P. Van den Driessche, and J. Wu. *Mathematical Epidemiology*. Springer, Berlin, 2008.

[231] M. J. Keeling and J. V. Ross. On methods for studying stochastic disease dynamics. *J. R. Soc. Interface*, 5(19):171–181, 2008.

[232] A. J. Black and A. J. McKane. Stochasticity in staged models of epidemics: Quantifying the dynamics of whooping cough. *J. R. Soc. Interface*, 7(49):1219–1227, 2010.

[233] L. J. Allen. *Stochastic Population and Epidemic Models*, volume 1. Springer International Publishing, 2015.

[234] C. Gardiner. *Stochastic Methods*, volume 4. Springer, Berlin, 2009.

[235] X. Mao, G. Marion, and E. Renshaw. Environmental brownian noise suppresses explosions in population dynamics. *Stochastic Processes and Their Applications*, 97(1):95–110, 2002.

[236] E. Roberts, S. Be'er, C. Bohrer, R. Sharma, and M. Assaf. Dynamics of simple gene-network motifs subject to extrinsic fluctuations. *Phys. Rev. E*, 92(6):062717, 2015.

[237] R. Lande. Risks of population extinction from demographic and environmental stochasticity and random catastrophes. *The American Naturalist*, 142(6):911–927, 1993.

[238] A. Kamenev, B. Meerson, and B. Shklovskii. How colored environmental noise affects population extinction. *Phys. Rev. Lett.*, 101(26):268103, 2008.

[239] D. T. Gillespie. A rigorous derivation of the chemical master equation. *Physica A*, 188(1-3):404–425, 1992.

[240] M. F. Weber and E. Frey. Master equations and the theory of stochastic path integrals. *Rep. Prog. Phys.*, 80(4):046601, 2017.

[241] C. Doering, K. Sargsyan, and L. Sander. Extinction times for birth-death processes: Exact results, continuum asymptotics, and the failure of the Fokker–Planck approximation. *Multiscale Modeling & Simulation*, 3(2):283–299, 2005.

[242] B. Gaveau, M. Moreau, and J. Toth. Decay of the metastable state in a chemical system: Different predictions between discrete and continuous models. *Letters in Mathematical Physics*, 37(3):285–292, 1996.

[243] L. D. Landau and E. M. Lifshitz. *Quantum Mechanics*, volume 3. Pergamon, Oxford, 1977.

[244] S. C. Miller and R. H. Good. A WKB-type approximation to the Schrödinger equation. *Phys. Rev.*, 91(1):174–179, 1953.

[245] A. Messiah. *Quantum Mechanics*. North-Holland Publ., Amsterdam, 1967.

[246] D. J. Griffiths and D. F. Schroeter. *Introduction to Quantum Mechanics*. Cambridge University Press, Cambridge, 3rd edition, 2018.

[247] C. M. Bender and S. A. Orszag. *Advanced Mathematical Methods for Scientists and Engineers I: Asymptotic Methods and Perturbation Theory*. Springer Science & Business Media, New York, 2013.

[248] M. Assaf and B. Meerson. Spectral formulation and WKB approximation for rare-event statistics in reaction systems. *Phys. Rev. E*, 74(4):041115, 2006.

[249] M. Assaf, B. Meerson, and P. V. Sasorov. Large fluctuations in stochastic population dynamics: Momentum-space calculations. *J. Stat. Mech.*, 2010(07):P07018, 2010.

[250] S. Be'er, M. Assaf, and B. Meerson. Colonization of a territory by a stochastic population under a strong allee effect and a low immigration pressure. *Phys. Rev. E*, 91(6):062126, 2015.

[251] S. Be'er and M. Assaf. Rare events in stochastic populations under bursty reproduction. *J. Stat. Mech.*, 2016(11):113501, 2016.

[252] C. S. Peters, M. Mangel, and R. Costantino. Stationary distribution of population size in tribolium. *Bull. Math. Bio.*, 51(5):625–638, 1989.

[253] M. Assaf and B. Meerson. WKB theory of large deviations in stochastic populations. *J. Phys. A*, 50(26):263001, 2017.

[254] O. Ovaskainen and B. Meerson. Stochastic models of population extinction. *Trends in Ecology & Evolution*, 25(11):643–652, 2010.

[255] P. C. Bressloff. Stochastic switching in biology: From genotype to phenotype. *J. Phys. A*, 50(13):133001, 2017.

[256] M. Assaf and B. Meerson. Spectral theory of metastability and extinction in a branching-annihilation reaction. *Phys. Rev. E*, 75(3):031122, 2007.

[257] M. Assaf and B. Meerson. Extinction of metastable stochastic populations. *Phys. Rev. E*, 81(2):021116, 2010.

[258] D. A. Kessler and N. M. Shnerb. Extinction rates for fluctuation-induced metastabilities: A real-space WKB approach. *J. Stat. Phys.*, 127(5):861–886, 2007.

[259] M. Assaf, A. Kamenev, and B. Meerson. Population extinction risk in the aftermath of a catastrophic event. *Phys. Rev. E*, 79(1):011127, 2009.

[260] C. Escudero and A. Kamenev. Switching rates of multistep reactions. *Phys. Rev. E*, 79(4):041149, 2009.

[261] C. L. Chang. *Introduction to Stochastic Processes in Biostatistics*. John Wiley And Sons, Inc; New York, 1968.

[262] D. T. Gillespie. *Markov processes: An introduction for physical scientists*. Academic Press, Boston, 1992.